

# **Synthesis Towards Nitrogenous Model Bitumen Archipelagos**

by

Devin James Reaugh

A thesis submitted in partial fulfillment of the requirements for the degree of

Master of Science

Department of Chemistry

University of Alberta

© Devin James Reaugh, 2015

## Abstract

The synthesis of functionalized quinolines is described herein. Utilizing condensation reactions, derivatized quinolines were prepared to serve as nitrogen-containing asphaltene *islands*. Basic halogenated phenylquinolines were synthesized *via* urea condensations. Highly substituted quinolines were prepared using a Brønsted acid-catalyzed Friedländer condensation. Benzophenone was used in combination with a variety of  $\alpha$ -methylene ketones. A novel adaptation for acetophenone was developed.

Individual islands were connected to alkyl tethers by *reductive cross-electrophile coupling*. Bromoarenes were coupled to  $\alpha$ -bromo- $\omega$ -chloroalkanes to install tethers with terminal chlorides. A cobalt-manganese catalyst-reductant system was first explored, and a second nickel-zinc system was refined for tether installation. Introductory experiments towards the use of these  $\omega$ -chloro tethered islands in the synthesis of bis-functionalized ketones was briefly explored using Collman's Reagent.

## Dedication

*For all those who are told “no”, without consideration or empathy.*

## **Acknowledgements**

I would like to thank my supervisor Dr. Jeff Stryker for giving me the opportunity to work within his group. The enthusiasm and excitement that I have felt throughout the completion of my work is in no small part due to his encouragement and passion for chemistry.

My successes in the lab would not have been possible without the continual advice, assistance, and support of Dr. Robin Hamilton. I was extremely lucky to work alongside him during my research.

To the many, many other Stryker Group members I've met during my degree, you all have my heartfelt thanks. The comradeship I found within this group has been invaluable to me throughout my degree.

Last, but certainly not least, I'd like to thank my close friends and family outside the department. Despite my overly long education, I've had consistent and sincere support from each of them. They all helped keep me grounded, and stood as a reminder of all that we work for.

## Table of Contents

1	Bitumen, Asphaltenes and the Issues of Heavy Crude Oil .....	1
1.1	Introduction.....	1
1.2	Asphaltenes.....	1
1.2.1	Asphaltene content in bitumen and issues arising therefrom.....	1
1.2.2	Asphaltene composition and proposed structure .....	3
1.2.3	Theoretical macrostructure of archipelago asphaltene aggregates .....	6
1.2.4	Model asphaltene mimics – generation one nitrogenous archipelagos.....	7
1.3	Model asphaltene mimics – generation two .....	10
2	Synthesis of Quinoline Islands for use as Archipelago Cores.....	13
2.1	Introduction.....	13
2.2	Synthesis of simple halophenylquinolines.....	15
2.2.1	Literature synthesis: the Hua haloacetophenone domino reaction .....	15
2.2.2	Optimization of the Hua domino reaction .....	17
2.2.3	Limitations in substrate scope .....	20
2.3	Synthesis of Complex Halophenylquinolines .....	22
2.3.1	Historical background: the Friedländer reaction.....	22
2.3.2	An ideal adaptation: the Wu-Friedländer haloquinoline synthesis.....	24
2.3.3	Optimization for 2-aminobenzophenone .....	24
2.3.4	Mechanistic considerations .....	28
2.3.5	Proof of concept: chloroacridine synthesis.....	30
2.3.6	The issue of 2-aminoacetophenone .....	31
2.3.7	Backup routes to 7-bromo-9-methyl-1,2,3,4-tetrahydroacridine.....	32
2.3.7.1	Route 1: Condensation via alternative halogenation.....	32
2.3.7.2	Route 2: Condensation via Lewis Acid catalysis .....	33
2.3.8	Modified conditions for Wu-Friedländer condensation of 2-aminoacetophenone.....	34
2.3.8.1	First modification: salt dissolution.....	34
2.3.8.2	Second modification: alternative solvent .....	35
2.3.8.3	Final modification: competitive salt formation.....	37
2.4	Conclusions.....	38
3	Organometallic Routes to Model Archipelagos .....	40
3.1	Introduction.....	40

3.2	Reductive cross-coupling of bromoarenes and haloalkanes: the cobalt-manganese system .....	44
3.2.1	Literature reaction: the Gosmini cobalt-manganese system .....	44
3.2.2	Intended adaptations .....	46
3.2.3	Initial evaluation of the cobalt-manganese REC system .....	47
3.2.4	Metal studies .....	48
3.3	Chloroalkylated island synthesis: $\alpha$ -bromo- $\omega$ -chloroalkane coupling .....	50
3.4	Reductive cross-coupling of haloarenes and bromoalkanes: the nickel-zinc system .....	52
3.4.1	Literature cross-coupling: the Weix nickel-zinc system .....	52
3.4.2	Initial evaluation of the nickel-zinc REC system .....	52
3.4.3	Optimization of the nickel-zinc REC reaction .....	54
3.4.4	Mechanism of the nickel-zinc REC reaction .....	57
3.4.5	Application of the nickel-zinc system to nitrogenous asphaltene mimics .....	58
3.5	Synthesis of Nitrogenous Archipelago Cores .....	60
3.5.1	Introduction .....	60
3.5.2	Dialkylketones by carbonylation – Collman’s Reagent .....	61
3.5.3	Towards the synthesis of symmetrical ketones – simple archipelago synthesis .....	62
3.6	Conclusions .....	64
4	Concluding Remarks .....	65
5	Experimental Section .....	66
5.1	General Procedure .....	66
5.2	Instrumental Analyses .....	66
5.3	Chemical Materials Used .....	67
5.4	Synthetic Procedures .....	68
5.4.1	General procedure for the condensation of ortho-haloacetophenones ...	68
5.4.2	General procedure for TBAT-catalyzed Wu-Friedländer condensations.	70
5.4.3	Additional syntheses of 7-bromo-9-methyl-1,2,3,4-tetrahydroacridine	<b>104</b>
		80
5.4.4	General procedure for cobalt-manganese REC reactions .....	82
5.4.5	General procedure for nickel-zinc REC reactions .....	83

## List of Abbreviations

dtbipy	4,4'-bis( <i>tert</i> -butyl)-2,2'-bipyridine
dmbipy	4,4'-bismethyl-2,2'-bipyridine
bipy	2,2'-bipyridine
DBT	dibenzothiophene
DCM	dichloromethane
DMA	dimethylacetamide
DME	1,2-dimethoxyethane
DMF	N,N-dimethylformamide
DMPU	N,N-dimethylpropyleneurea
DMSO	dimethyl sulfoxide
dppe	bis-(diphenylphosphino)ethane
EtOH	ethanol
<sup>i</sup> PrOH	isopropanol
LDA	lithium diisopropylamide
MeCN	acetonitrile
MeOH	methanol
NBS	N-bromosuccinimide
NMP	N-methylpyrrolidinone
SOCl <sub>2</sub>	thionyl chloride
TBAB	tetra- <i>n</i> -butylammonium bromide
TBAT	tetra- <i>n</i> -butylammonium tribromide
THF	tetrahydrofuran
TLC	thin-layer chromatography

## List of Tables

<i>Title</i>	<i>Page</i>
Table 1.1 Major elemental composition of Athabaskan bitumen and asphaltenes	3
Table 1.2 Comparative carbon-hydrogen ratios of asphaltenes and their models	10
Table 2.1 Redesign of the Hua domino reaction	19
Table 2.2 Comparative atomic ratios of asphaltene and two model systems	20
Table 2.3 2-aminobenzophenone bromination conversion over time	25
Table 2.4 TBAT recovery and regeneration	26
Table 2.5 Comparative atomic ratios of representative types of second-generation Wu-Friedländer phenylhaloquinoline model asphaltene islands	27
Table 2.6 2-aminoacetophenone bromination conversion over time	32
Table 2.7 5-bromo-2-aminoacetophenone water solubility data	35
Table 2.8 Amine screening for 2-aminoacetophenone	37
Table 3.1 First-round screening of the cobalt-manganese REC system	47
Table 3.2 Variations of the reductive metal in the cobalt-manganese REC	48
Table 3.3 Optimization of the nickel-zinc REC catalyst for 4-chloro-1-phenylbutane	55

## List of Figures

<i>Title</i>	<i>Page</i>
Figure 1.1 Bitumen	1
Figure 1.2 Bitumen and its constituents	2
Figure 1.3 Asphaltene	3
Figure 1.4 Basic heteroatomic structures found within asphaltene	4
Figure 1.5 Theoretical examples of the archipelago and continental asphaltene models	5
Figure 1.6 Overview of theoretical asphaltene intramolecular asphaltene aggregation. Reprinted with permission from ACS	6
Figure 1.7 Fenniri first-generation nitrogenous archipelago model	7
Figure 1.8 Tykwinski first-generation nitrogenous archipelago model	8
Figure 1.9 Tykwinski first-generation porphyrin-based archipelago model	9
Figure 2.1 Quinoline	13
Figure 2.2 Ephedrine	14
Figure 2.3 Quinine	14
Figure 3.1 Expected REC reaction side products	49
Figure 3.2 Commercially available $\alpha$ -bromo- $\omega$ -chloroalkanes	50
Figure 3.3 Alternative bipyridine-based ligands 4,4'-dimethyl-2,2'-bipyridine <b>168</b> and 4,4'-di-tert-butyl-2,2'-bipyridine <b>169</b>	55
Figure 3.4 GC-MS analysis of the nickel-zinc REC product distribution as a function of conditions (Table <b>3.3</b> )	56
Figure 3.5 Nitrogenous asphaltene mimic chain-extension products	59
Figure 3.6 Iron carbonyl complexes	62

## List of Schemes

<i>Title</i>	<i>Page</i>
Scheme 1.1 Synthesis of the Fenniri first-generation nitrogenous archipelago model	8
Scheme 1.2 Synthesis of Tykwinski's first-generation nitrogenous archipelago model	9
Scheme 1.3 A general outline of second-generation model nitrogenous asphaltene targets	10
Scheme 1.4 Second-generation model nitrogenous asphaltene islands by Heidt and Wang	10
Scheme 2.1 Proposed retrosynthesis of 2-(2-chlorophenyl)-4-methylquinoline 27	16
Scheme 2.2 Mechanism of 2-(2-chlorophenyl)-4-methylquinoline 27 formation	16
Scheme 2.3 Mechanism of urea decomposition	18
Scheme 2.4 Retrosynthetic scheme I: ring modification	21
Scheme 2.5 Retrosynthetic scheme II: chain extension	21
Scheme 2.6 Literature synthesis of 1-(2-bromophenyl)propan-1-one	22
Scheme 2.7 Fisher's flavaniline synthesis	23
Scheme 2.8 Results of the Wu-Friedländer literature conditions	25
Scheme 2.9 Isolated Wu-Friedländer products	27
Scheme 2.10 Proposed Wu-Friedländer mechanism	29
Scheme 2.11 Modified Wu-Friedländer synthesis using TBATCl	30
Scheme 2.12 Two-island archipelago retrosynthesis	31
Scheme 2.13 Wu-Friedländer synthesis as applied to 2-aminoacetophenone	32
Scheme 2.14 Synthesis of 7-bromo-9-methyl-1,2,3,4-tetrahydroacridine via 2-aminoacetophenone hydrogen chloride salt	33
Scheme 2.15 Lewis acid catalyzed synthesis of 7-bromo-9-methyl-1,2,3,4-tetrahydroacridine	34
Scheme 2.16 Wu-Friedländer solvent modification trial	37
Scheme 3.1 Retrosynthesis of tethered islands by the Wu-Friedländer reaction	40
Scheme 3.2 Retrosynthesis of the first-generation Tykwinski archipelago	40

<i>Title</i>	<i>Page</i>
Scheme 3.3 A general retrosynthetic plan for archipelago construction	40
Scheme 3.4 Traditional vs. reductive coupling	41
Scheme 3.5 Retrosynthetic plan for archipelago synthesis 1: REC and alternate tether attachment	43
Scheme 3.6 Retrosynthetic plan for archipelago synthesis 2: dual REC tether attachment	44
Scheme 3.7 General mechanism for the Gosmini alkyl-aryl cross-coupling	45
Scheme 3.8 Proposed reaction scheme for one-pot, two-island tethering	46
Scheme 3.9 Potential side products of the nickel-zinc REC system	53
Scheme 3.10 Initial analysis of the nickel-zinc REC system	54
Scheme 3.11 Proposed mechanism for the nickel-zinc REC system, as described by Weix and coworkers	58
Scheme 3.12 Retrosynthetic plan for the Friedlander synthesis of archipelago model asphaltenes	61
Scheme 3.13 Determination of the purity of Collman's Reagent; synthesis of nonenal	62
Scheme 3.14 Generic symmetrical ketone synthesis	63
Scheme 3.15 Synthesis of bis-tethered symmetrical ketones	63

# 1 Bitumen, Asphaltenes and the Issues of Heavy Crude Oil

## 1.1 Introduction

By far, the majority of Canada's fossil fuel reserves reside in bituminous oil sands, unconventional petroleum deposits located in northern Alberta and Saskatchewan. The Wabiskaw-McMurray deposits, commonly referred to as Athabasca oil sands, contain one of the largest reserves of oil sands in the world.<sup>1</sup> Bitumen, a highly viscous and high-density solid crude oil, constitutes the most problematic fraction of material typically found within the oil sands. Athabaskan bitumen makes up approximately 169.3 billion barrels or 99.1% of all *established* oil sand reserves;<sup>2</sup> that is, oil sand deposits that can be extracted and processed using current technology.

As conventional oil well production continues to decline, efficient processing of oil sands has become increasingly necessary. New advances in refining and upgrading technology are needed to improve bitumen processing, addressing the ever-growing global demand for fossil fuels, the increasing complexity and costs of extraction and upgrading, and the ever more stringent regulatory and environmental requirements. Before such advances and sustainability issues can be achieved, however, we require a deeper, *molecular-level* understanding of the chemical nature of bitumen and its constituents.

## 1.2 Asphaltenes

### 1.2.1 Asphaltene content in bitumen and issues arising therefrom

Athabaskan oil sands are comprised of a mixture of fine sandstone and quartz sands, water, silt, clay, and petroleum bitumen,<sup>3</sup> the latter shown below in Figure 1.1.



**Figure 1.1** Bitumen<sup>4</sup>

Bitumen is itself a mixture of innumerable structurally-distinct components that have neither discrete nor homologous composition, making it difficult to characterize or classify these components. Current convention,<sup>3,5</sup> following precedents set in early compositional investigations,<sup>6,7</sup> instead divides bitumen into two main constituents by general solubility characteristics.

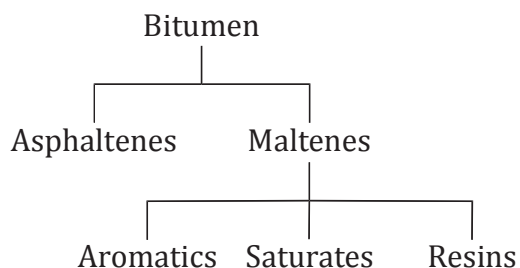


**Figure 1.2** Bitumen and its constituents

*Maltenes* are relatively low molecular weight compounds comprised of aromatic and heteroaromatic rings, saturated alkyl chains, and paraffinic resins. The resultant mixture of these compounds is soluble in both aromatic hydrocarbons and aliphatic solvents. This favourable solubility leads to more facile processing, demanding less rigorous conditions and, as such, improved processing technologies are not required at this time. Thus maltenes will not be discussed further within this work.

*Asphaltenes* (Figure 1.3), so-named by Boussingault due to their similarities to construction asphalt,<sup>7</sup> are relatively high molecular weight alkylated polycyclic aromatic compounds with entrained heteroatoms and trace metals. An individual asphaltene compound will contain some or all of the functionality contained in the maltenes within a singular, interconnected framework, held together by both covalent bonds and non-covalent associations. These compounds, though soluble in aromatic solvents such as toluene and benzene, are insoluble in aliphatic solvents such as *n*-hexane and *n*-heptane.



**Figure 1.3** Asphaltenes<sup>8</sup>

Chemical characterization of the asphaltenes has been ongoing since their initial classification in 1837,<sup>6</sup> but some of the first succinct research was published by Marccuson in 1919,<sup>9</sup> wherein direct comparisons were made between petroleum asphaltene and coke resins from coal.

Athabaskan bitumen typically contains between fourteen and eighteen percent asphaltenes by weight.<sup>5</sup> While not the principal constituents, it is the asphaltenic compounds that cause serious issues during transport, processing and upgrading of oil sands,<sup>1,2,5,10</sup> due in part to their low overall solubility and high melting point.

Deposition of solid asphaltenes within pipelines creates an increased need for maintenance, decreasing throughput on an already strained and overused petroleum transportation system.<sup>11</sup> Further downstream, during upgrading and refining operations, asphaltenes that precipitate from the feedstock stream accumulate on vessel interiors,<sup>12</sup> inhibiting proper separation and increasing the frequency of processing facility turnaround. Worse yet, asphaltenes deposit on catalyst pore surfaces<sup>13</sup> which leads to catalyst deactivation by fouling. Due to these continual deposition processes, asphaltenes have an increasingly deteriorative effect on oilfield processes. Before new technologies can be developed to better handle asphaltenes and other heavy crude products, which will constitute an ever-increasing portion of feedstock into upgrading and refining operations, a deeper understanding of their molecular composition is required.

### *1.2.2 Asphaltene composition and proposed structure*

The most prevalent elements that comprise Athabaskan bitumen and asphaltenes are outlined below (Table 1.1).<sup>5,14</sup>

**Table 1.1** Major elemental composition of Athabasca bitumen and asphaltenes

	Carbon	Hydrogen	Sulfur	Oxygen	Nitrogen
<b>Bitumen</b>	84.0	10.2	4.6	2.0	0.7
<b>Asphaltene</b>	81.3	7.9	7.5	2.8	1.1

Note: values shown are averages generated from elemental analysis of many bitumen samples, and are expressed as a percentage.

Additionally, both nickel and vanadium are present between 50 and 200 ppm concentrations within bitumen residues.

When these percentages are viewed in terms of the individual atomic masses, the ratio of sulfur to oxygen to nitrogen is approximately 4 : 3 : 1, and the carbon to hydrogen ratio is approximately 1 : 1.2. The majority of the sulfur content is entrained within *refractory sulfur compounds*, sulfurous polycyclic aromatic scaffolds containing thiophene **1**, with a lesser amount presenting as alkylsulfides **2**.<sup>5</sup> Nitrogen is found entrained within more variable polyaromatic structures such as acridines **3**, quinolines **4**, isoquinolines **5**, and carbazoles **6**.<sup>5</sup> The remainder of the heteroatom content is made up by oxygen, which, though present as esters, ketones, and furans **7** in minor amounts, is primarily found in *naphthenic acids* **8**, largely aliphatic molecules with long-chain alkyl carboxylic acids.<sup>5</sup> Vanadium and nickel are mainly found entrained within porphyrin-like structures **9**.<sup>5</sup>

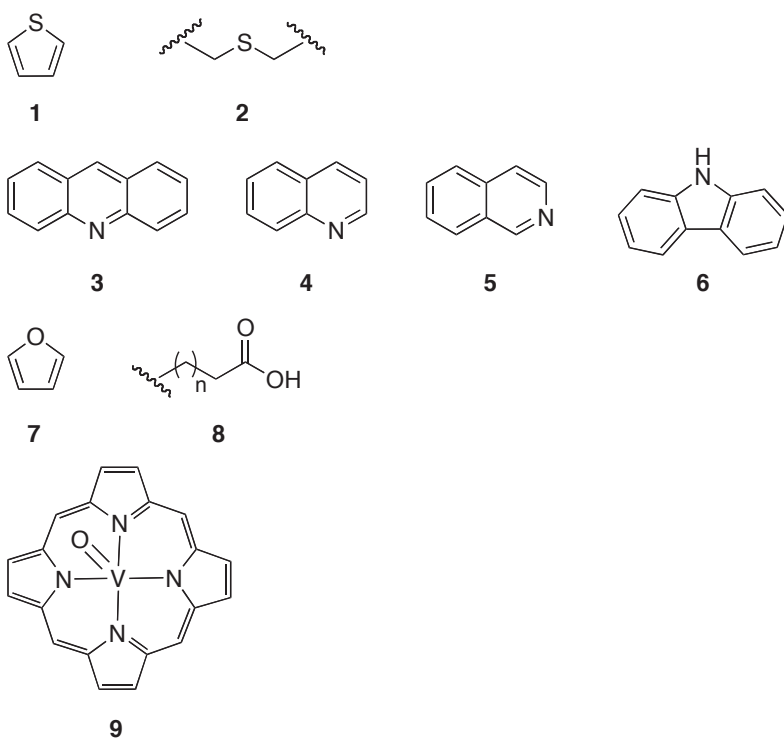


**Figure 1.4** Basic heteroatomic structures found within asphaltene

While average bulk atomic composition of the asphaltenes is readily discerned, no such finite determination of specific structural composition has been established. It is generally agreed that most asphaltenes fall in a mass range of 300-2000 amu,<sup>15</sup> although investigations of this range remain far from definitive.<sup>16</sup> Though the major structural motifs discussed above have been identified—polycyclic aromatic cores with alkyl chain substitutions<sup>17</sup>—the organization of these and other functional groups remains under heated debate.

Two contrasting theories of asphaltene structure have been developed: often termed *continental* and *archipelago* (Figure 1.5).<sup>18</sup> Continents display one large polycyclic aromatic core with ancillary alkyl decoration and functionality, while archipelagos contain several smaller polycyclic asphaltene *islands* interconnected by saturated alkyl bridges, further decorated with short alkyl side chains. A detailed review of compounds synthesized for investigation of both theoretical models is forthcoming.<sup>19</sup>

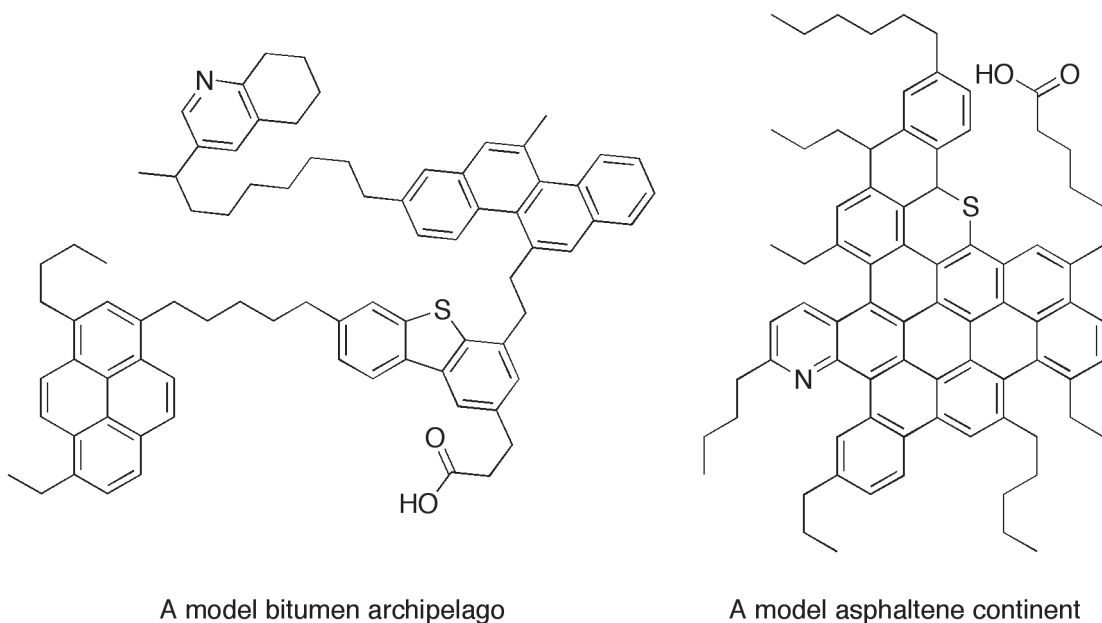


**Figure 1.5** Theoretical examples of the archipelago and continental asphaltene models

Analyses conducted on model compounds of both types has involved a wide range of available methodologies and has produced enormous amounts of data.<sup>5,14</sup> Despite these investigations, none, together or apart, provide definitive evidence of which model is the correct representation of the general asphaltenes.<sup>18</sup> Growing evidence, which contains several strong examples of mass balance and the use of

multiple experimental analyses, has been presented in favour of the archipelago model, although the truth almost certainly lies in some combination of both.<sup>21</sup> As such, our efforts, presented in this thesis, were focused on the synthesis of model asphaltene archipelagos and will not deal with model asphaltene continents.

### 1.2.3 Theoretical macrostructure of archipelago asphaltene aggregates

Strong self-association of discrete asphaltene compounds, referred to as *aggregation*, is thought to be the key to asphaltene insolubility.<sup>22</sup> It is this intermolecular aggregation that drives precipitation and flocculation of asphaltenes from solution,<sup>19</sup> beginning the deposition process. Due to the highly variable nature of asphaltenes, many factors doubtlessly contribute to this association, including aromatic  $\pi$ - $\pi$  stacking, acid-base and hydrogen bonding interactions, van der Waals interactions, as well as other interactions. Each of the interactions are depicted at the molecular level in a hypothetical asphaltene model proposed by Gray, Stryker and Tykwinski,<sup>23</sup> reproduced below.

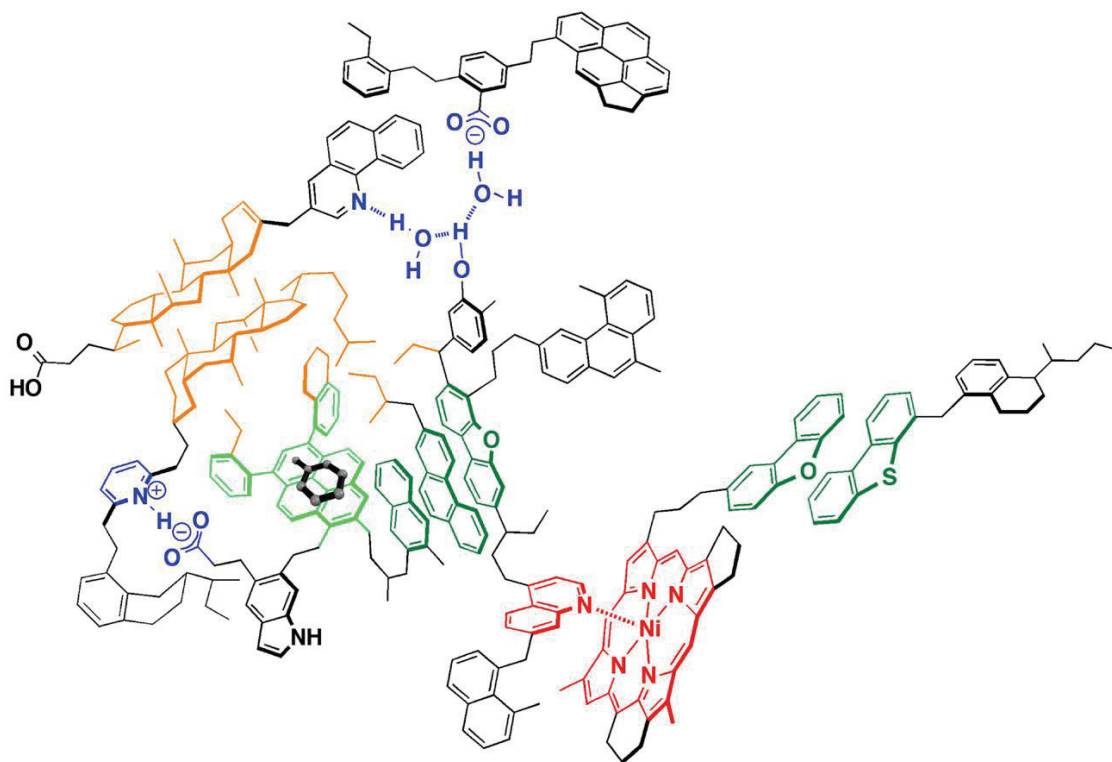


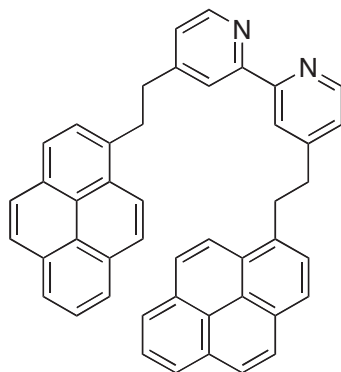
**Figure 1.6** Overview of theoretical asphaltene intramolecular aggregation.<sup>23</sup>

Hydrogen bonding, as shown above in blue (ion pairing also pictured in blue), may be achieved *via* interactions between heteroatoms and water entrained within the overall asphaltene matrix, either through direct, ionic interactions or through associations with lone-pairs. Interactions between water and asphaltenes are well documented<sup>24</sup>, with examples of strong association both at water-solvent interfaces<sup>25</sup> and when water is only present in trace amounts<sup>26</sup>.

Our synthetic targets were thus determined to be heteroaromatic model compounds, in hopes of shedding light on one of the principal mechanisms driving asphaltene aggregation – hydrogen bonding – at the molecular level.

#### 1.2.4 Model asphaltene mimics – generation one nitrogenous archipelagos

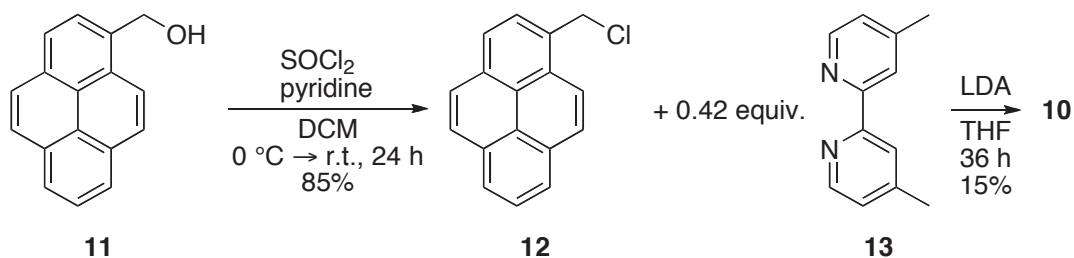
Nitrogen has been suggested as a likely hydrogen-bonding heteroatom within asphaltenes, and has previously been targeted for model asphaltene synthesis. First-generation nitrogenous model asphaltenes were reported by the groups of Fenniri<sup>27</sup> and Tykwinski.<sup>28</sup> These compounds were comprised of a bipyridine core with ethylpyrene pendants.



10

**Figure 1.7** Fenniri first-generation nitrogenous archipelago model

The Fenniri archipelago was obtained by treatment of 4,4'-dimethyl-1,1'-bipyridine **13** with LDA and a slight excess of (1-chloroethyl)pyrene **12**, as shown in Scheme 1.1. While facile, the yield of this synthesis is low and is restricted to the use of methylated, nitrogenous aromatic substrates and benzylic electrophiles.



**Scheme 1.1** Synthesis of the Fenniri first-generation nitrogenous archipelago model

A wider series of asphaltene archipelagoes was next synthesized by the Tykwinski group, using a more efficient approach (Figure 1.8). By using Sonogashira alkynyl coupling reactions, the substrate scope was expanded to include brominated pyridine derivatives and ethynyl aromatic partners.

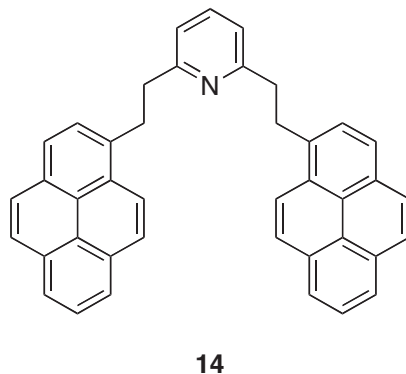
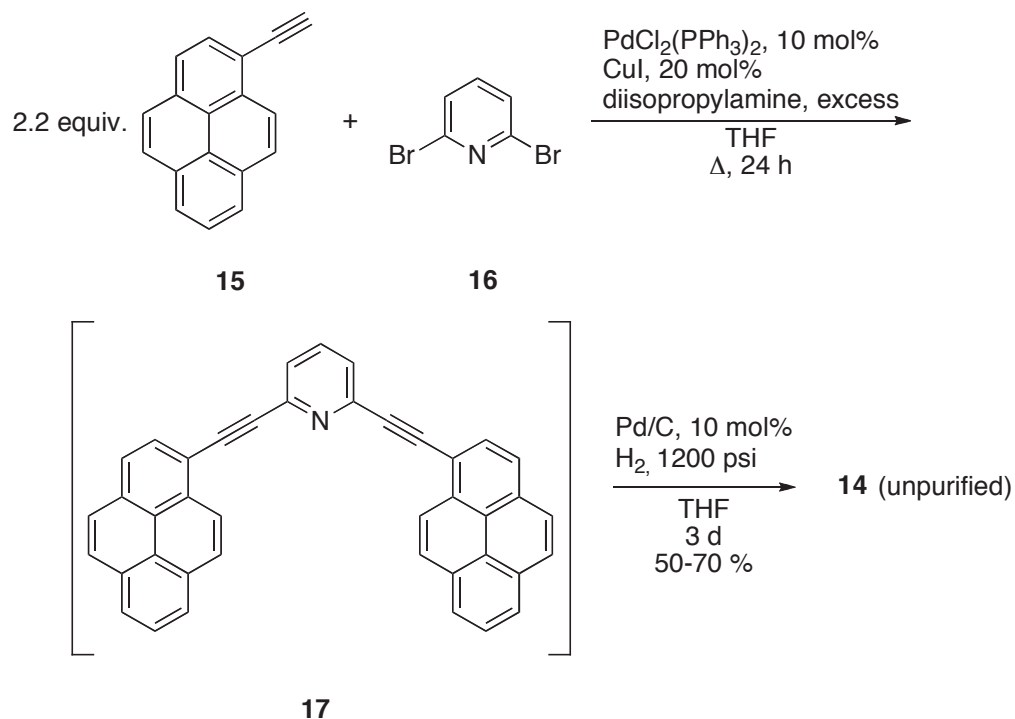


**Figure 1.8** Tykwinski first-generation nitrogenous archipelago model

Following the coupling of 2,6-dibromopyridine **16** and reduction of the intermediate diethynyl archipelago **17**, the final two-carbon bridged bis(2,6-(1-pyrenylethyl)pyridine was obtained in reasonable yields.

Despite increasing model archipelago diversity to include central islands containing thiophene, benzene, and biphenyl, the Sonogashira coupling suffered from competitive homocoupling of the ethynyl component and the final palladium-catalyzed hydrogenation was plagued by over-reduction of the pyrenes and catalyst poisoning. Alkynylation/reduction thus produces three-island archipelagoes only bearing two-carbon tethers, in small quantities, contaminated by inseparable impurities.



**Scheme 1.2** Synthesis of Tykwinski's first-generation nitrogenous archipelago model

Further work by Schulze and Tykwinski<sup>29</sup> produced a small suite of porphyrin-based archipelago model compounds. One example is shown in Figure 1.9. These porphyrin-containing models were synthesized using standard porphyrin synthesis,<sup>30</sup> condensing an aromatic aldehyde **19**, here substituted with the first generation ethylpyrene linkage, with bis-pyrrole **20**.

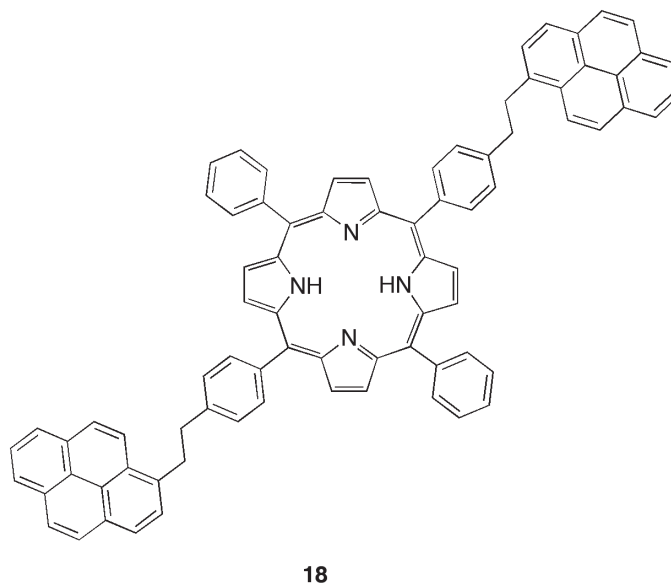
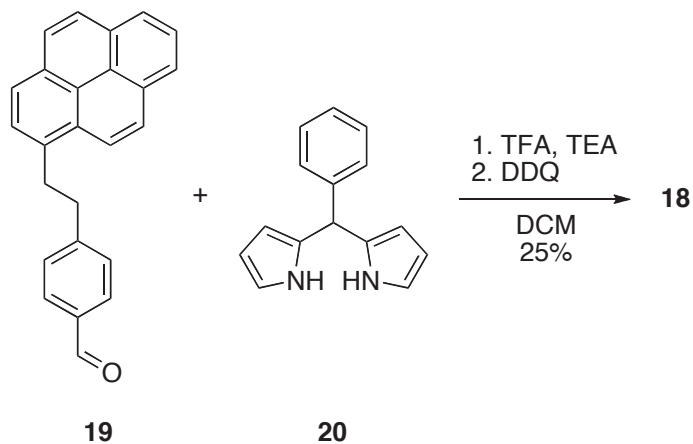


**Figure 1.9** Tykwinski first-generation porphyrin-based archipelago model

Though producing the desired porphyrin product (in high yield for a porphyrin preparation), this synthesis also gives several byproducts, greatly reducing isolated yields of purified material.

**Eq. 1.1**



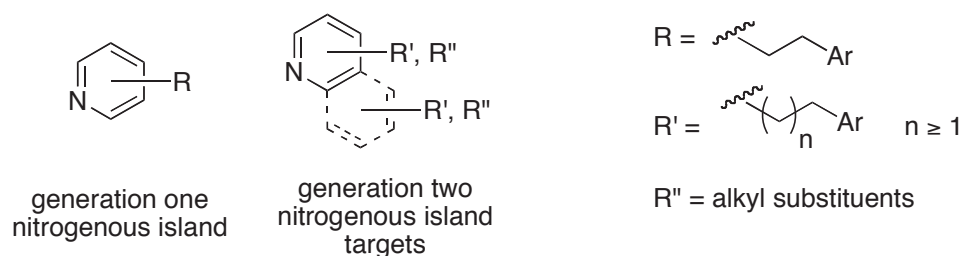
**1.3 Model asphaltene mimics – generation two**

The first generation compounds discussed above allowed for preliminary investigations to begin, but it was our goal to obtain asphaltene mimics in larger scale, in higher purity, and that display higher orders of diversity. Specifically, we desired compounds that adhere more closely to asphaltene carbon-hydrogen ratios, 1 : 1.2, as determined by Strauss<sup>5</sup> authentic asphaltenes. Each of the first-generation examples displays a higher ratio of carbon to hydrogen, owing to their largely polyaromatic nature, short two-carbon tethers, and lack of short alkyl substituents.

**Table 1.2** Comparative carbon-hydrogen ratios of asphaltenes and their models

Asphaltene	Atomic Composition		Ratio
	Carbon	Hydrogen	
<b>Athabasca Asphaltenes</b>	<b>81.3</b>	<b>7.9</b>	<b>1 : 1.2</b>
Fenniri Model Archipelago	90.1	5.5	1.3 : 1
Tykwinski Model Archipelago	91.9	5.5	1.4 : 1
Tykwinski Porphyrin-based Model Archipelago	89.7	5.2	1.4 : 1

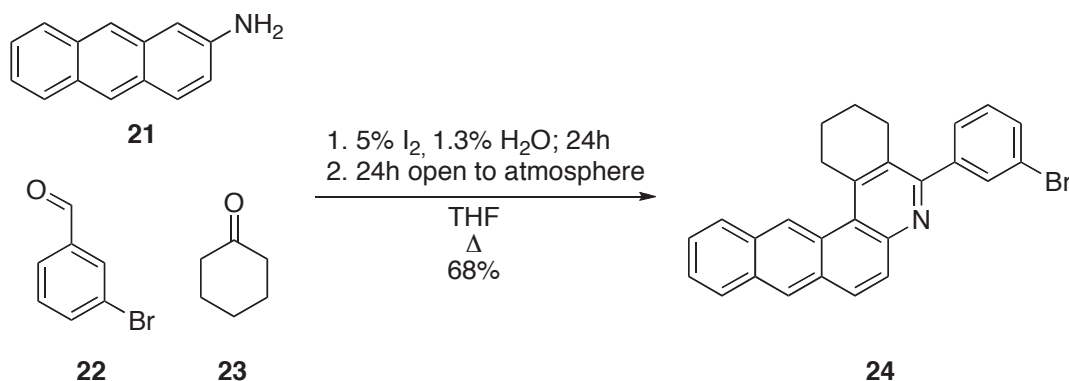
Our goals for second-generation compound synthesis, outlined in Scheme 1.3, were twofold: (1) to develop general syntheses allowing for highly diverse, nitrogenous, polyaromatic islands bearing increased alkyl substitution, and (2) to develop methodology for linking islands together using *saturated* alkyl chains of variable lengths.



**Scheme 1.3** A general outline of second-generation model nitrogenous asphaltene targets

Thus we were determined to expand our targets to involve quinolines and acridines, along with higher polycyclic aromatic systems bearing basic nitrogens. At the same time, we were committed to improving upon generation one methodology to assemble such structures into the final archipelago model compounds.

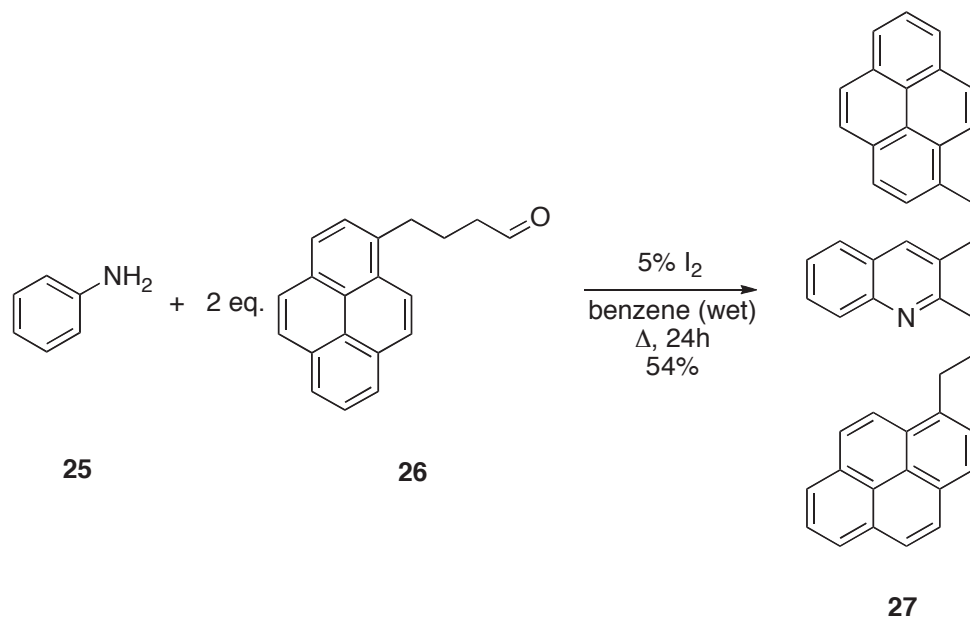
Concurrent to this work, efforts by Heidt and Wang<sup>31</sup> in the Stryker group refined a multicomponent reaction (MCR) procedure to produce benzo- and naphthoquinoline islands, which has been further refined by both Tykwinski and Stryker groups.<sup>32</sup>



**Scheme 1.4** Second-generation model nitrogenous asphaltene islands by Heidt and Wang

A large group of compounds have thus been synthesized using this catalytic MCR condensation, which involves an aromatic amine **21**, an aromatic aldehyde **22**, and an enolizable ketone **23**. The procedure, which generates catalytic amounts of hydroiodic acid *in situ*, accommodates a wide variety of ketones, from 2-butanone to 3-cholestanone, as well as any aromatic aldehyde, an expansion of substrate scope which greatly increases alkyl substitution and thus improves the carbon-hydrogen ratios of the individual islands. A similar iodine-catalyzed system for incorporating two aliphatic aldehydes was introduced by Tomlin<sup>33</sup> and optimized by Scott<sup>34</sup> to provide a one-pot route to quinoline archipelagos.

Eq. 1.2



Tomlin demonstrated that two equivalents of aldehyde **26** condensed with aromatic amine **25** using iodine as precatalyst in wet benzene; the reaction affords tethers of two different lengths in the resulting unsymmetrical archipelago product **27**. These compounds were the first models synthesized by either group that display alkyl tethers of more than two carbons, and the first to display differing tether lengths within the same archipelago. A full series of related archipelago compounds has now been completed, using different conditions (hydroiodic acid in place of iodine, alcohol solvents, and O<sub>2</sub> sparge) and returning even higher yields.<sup>34</sup>

The above examples, along with the syntheses that will be detailed within this thesis, constitute the second-generation of synthetic nitrogenous asphaltene model compounds to emerge from our collaborative efforts with Gray and Tykwinski. These efforts have been made specifically, targeting nitrogenous mimics, in hopes of elucidating any connection between overall aggregation and asphaltene intermolecular hydrogen bonding.

While these compounds offer routes towards viable archipelagoes, the amount of diversity that can be eked from such syntheses is inevitably limited by the individual reaction conditions. It was our wish to have additional, robust methodology in place to allow for a wider range of asphaltene mimics. The following chapters illustrate specific, targeted syntheses designed for the preparation of diverse alkylated nitrogenous aromatic islands (Chapter 2), and our efforts to establish general methodology to connect these islands by carbon tethers of at least two carbons (Chapter 3).

## 2 Synthesis of Quinoline Islands for use as Archipelago Cores

### 2.1 Introduction

Quinoline **28** is a benzo[b]pyridine formally derived from naphthalene, differing by the replacement of one of the  $\alpha$ -CH groups with nitrogen.<sup>35</sup> The IUPAC numbering scheme is identical to that of naphthalene, beginning at the  $\alpha$ -position, in this case nitrogen, and moving away from the point of ring fusion.

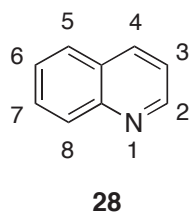
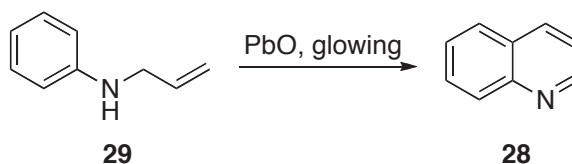


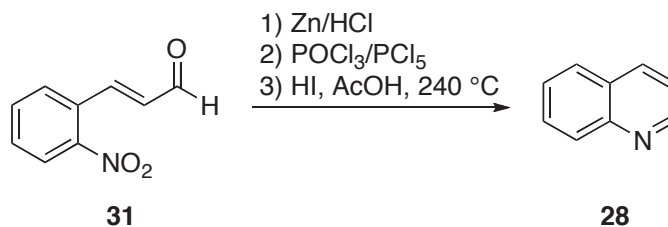
**Figure 2.1** Quinoline

Runge first extracted quinoline from basic coal tar distillates in 1834, revealing it to be one of the major nitrogenous, polyaromatic components of heavy oil.<sup>36</sup> Dewar commented briefly in 1871 that the structure of quinoline might be related to pyridine in the same fashion that naphthalene is related to benzene.<sup>37</sup> The structural definition, however, was not confirmed until 1879 when both Koenigs, using allylaniline, **29** (Eq. 2.1),<sup>38</sup> and Baeyer, using 2-nitrocinnamaldehyde, **31** (Eq. 2.2),<sup>39</sup> independently synthesized and characterized quinoline.

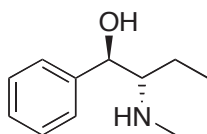
#### Equation 2.1



#### Equation 2.2



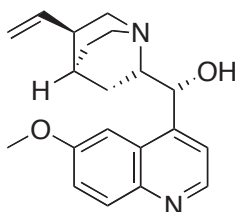
Quinoline is one of aromatic scaffolds found within *alkaloids*, a large family of extremely diverse, pharmacologically active, nitrogenous natural products whose use has been widespread throughout human history. One of the first recorded examples of alkaloid usage,<sup>40</sup> dating to about 2700 B.C., describes preparation of *má huáng* (麻黄), an ancient Chinese drug containing the simple alkaloid ephedrine **32**.



**32**

**Figure 2.2** Ephedrine

The nineteenth century saw the isolation of many such compounds, including quinine **33**, from which quinoline derives its name.<sup>41</sup> Quinine, the first antimalarial that saw worldwide usage, is a prime example of the enormous importance of alkaloids in the treatment of disease.



**33**

**Figure 2.3** Quinine

With the discovery of the pharmacological importance of these compounds, considerable efforts were put towards their total synthesis.<sup>41</sup> The development of synthetic routes involving these compounds exploded around the turn of the twentieth century, resulting in a wide variety of reactions leading to quinoline and quinoline-based compounds.

With a range of methodologies available, we found ourselves in a position to pick methods that best suited to the synthesis of quinoline asphaltene compounds. For our purposes, the best route must satisfy three basic conditions: 1) the overall synthesis

must employ as few steps as possible, as we intend to generate only one piece of an archipelago structure and do so in multigram quantities; 2) the synthesis must tolerate a wide range of substrates to afford a similarly wide range of substituted and functionalized quinolines, and 3) the resultant quinoline must have a handle for further reactions leading towards the final archipelago.

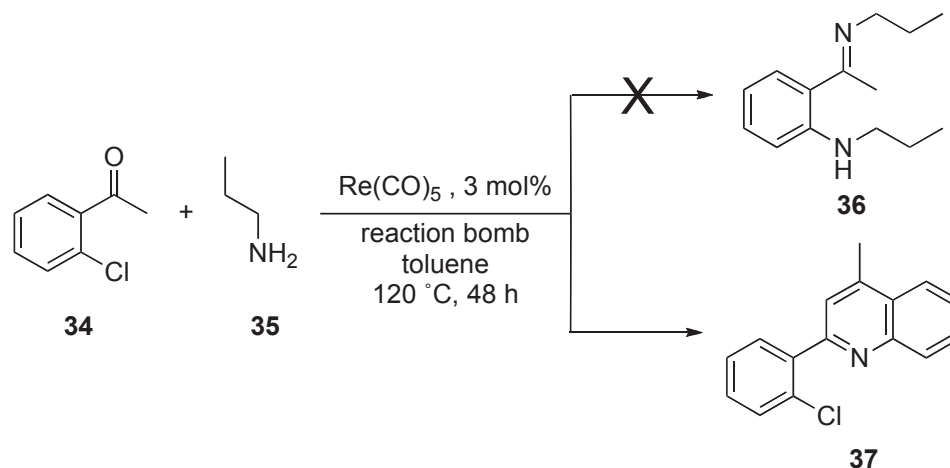
The following discussion outlines the identification and investigation of two such methodologies: the first a simple multicomponent reaction and the second, a superior two-step cascade, both of which incorporate the key characteristics mentioned above.

## 2.2 Synthesis of simple halophenylquinolines

### 2.2.1 Literature synthesis: the Hua haloacetophenone domino reaction

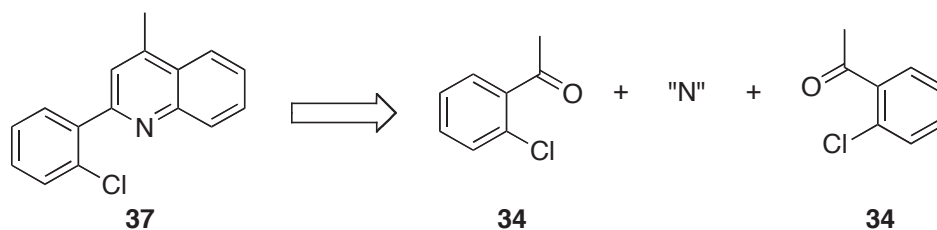
Hua and coworkers observed a serendipitous reaction while attempting to develop a rhenium-catalyzed N-arylation reaction, which provided instead a concise and novel route to simple halophenylquinolines (Eq. 2.3).<sup>42</sup> The reaction of *ortho*-chloroacetophenone **34** and a primary amine at high temperature and pressure furnished the unexpected chlorophenylquinoline **37** rather than the intended (propylimino)alkylaniline **36**.

#### Equation 2.3

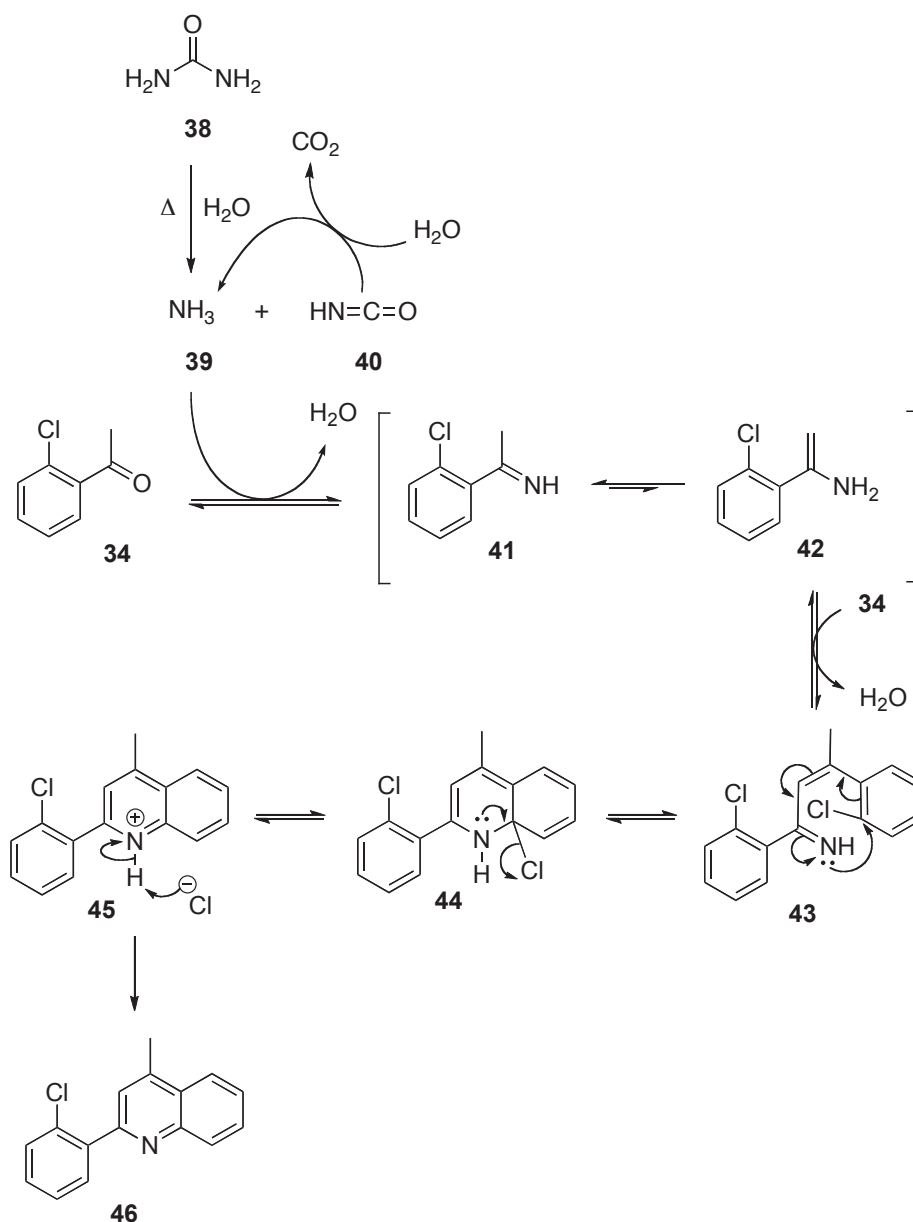


It was postulated that this quinoline product resulted from a self-condensation between two equivalents of 2'-chloroacetophenone **34** and the inclusion of a singular nitrogen atom from propylamine **35** (Scheme 2.1). The authors suggest the active nitrogen species is ammonia, produced *via* hydrolysis and/or thermal decomposition of

the amine, but no investigation into the exact mechanism was undertaken. With intent to optimize the reaction, and, very likely, reduce the overall reaction cost, the nitrogen source was changed to urea (Scheme 2.2).



**Scheme 2.1** Proposed retrosynthesis of 2-(2-chlorophenyl)-4-methylquinoline 27

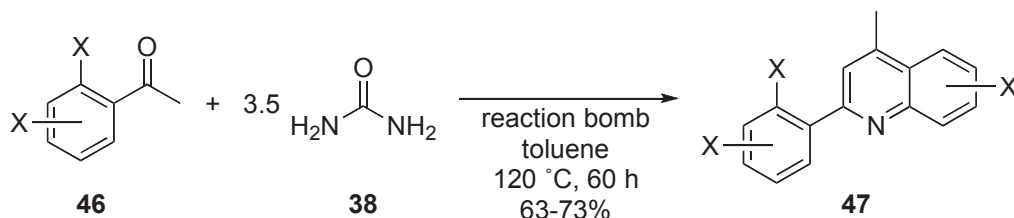


**Scheme 2.2** Mechanism of 2-(2-chlorophenyl)-4-methylquinoline 27 formation

For brevity, the condensation of the enamine **42** with the second equivalent of 2'-chloroacetophenone **34**, and the subsequent dehydration of the imineol intermediate (not pictured), has been omitted. While the authors propose step-wise formation of the  $\alpha$ -chloro amine **44**, it is also possible that this intermediate is formed *via* a 6- $\pi$  electrocyclization.

When reagents and solvents were used as purchased, trace amounts of water were present, providing a means to initiate decomposition of urea **38**. Subsequent production of ammonia or other active nitrogenous species is effected by water generated during the two condensations required to form the product. Using a limited series of bromo- and chloroacetophenones **46**, Hua demonstrated the synthesis of halogenated phenylquinolines **47** in moderate yield (Eq. **2.4**).

#### Equation 2.4



X = Br, Cl

#### 2.2.2 Optimization of the Hua domino reaction

The work of Hua *et al.* displayed promise as a potential reaction for the synthesis of quinoline-based asphaltenes. Taken at face value, the reaction meets two of our three conditions: the reaction is one-pot and, by nature of the substrates used, delivers one or more halogen handles and, as a bonus, installs a short chain alkyl substituent on the heteroaromatic ring. Substrate scope, the last condition, remained for us to explore, but altogether the reaction was promising enough to begin work.

Our attempts to replicate the reaction under the reported conditions met with low yields. After several lackluster results, extremely low yields that were obtained by following the literature procedure exactly as written, we elected to redesign the reaction from the ground up. Under literature conditions, after the reaction was complete, an unidentified solid compacted so heavily on the interior of the reaction vessel that it was nearly impossible to remove, either by hot water dissolution or ultrasonication,



Entry	Reaction vessel	Solvent	Temperature (°C)	Yield (%)
1	sealed flask	toluene	150	56
2	open flask	toluene	110	49
3 <sup>b</sup>	open flask	toluene	100	51
4	sealed flask	benzene	100	40
5	open flask	benzene	80	32
6	sealed flask	mesitylene	150	81
7	open flask	mesitylene	164	79
8 <sup>b</sup>	open flask	mesitylene	150	83
9 <sup>c</sup>	open flask	mesitylene	150	82
10 <sup>d</sup>	open flask	mesitylene	150	53
11 <sup>e</sup>	open flask	mesitylene	150	61

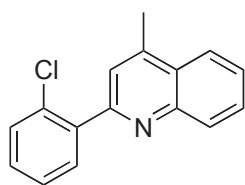
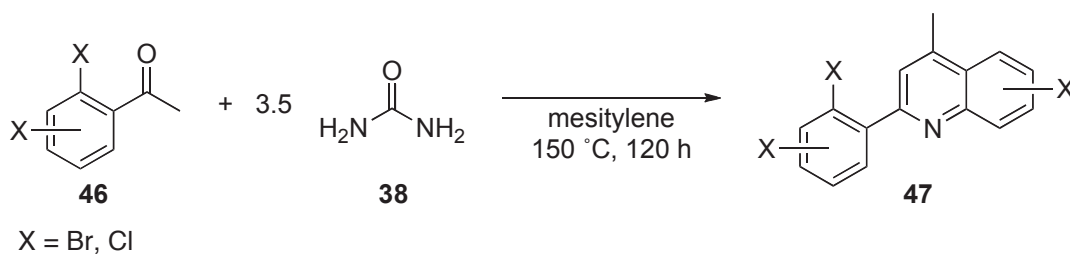
<sup>a</sup> Reaction conditions: *o*-bromoacetophenone (40 mmol), urea (140 mmol), solvent (10 mL) were added to a 25mL flask and heated just below reflux for 120 hours. <sup>b</sup> Standard condenser replaced with a dry-ice condenser. <sup>c</sup> 200 mmol urea used. <sup>d</sup> Reaction time decreased to 72 hours. <sup>e</sup> Reaction time decreased to 96 hours.

Increased temperature promotes the reaction, as seen in the increasing yield from benzene to toluene to mesitylene (Table 2.1). Little change in yield was observed when using an unsealed flask in place of a standard round bottom with a condenser. Reactions run using a dry ice condenser to trap released ammonia (Entries 3 and 8) displayed no appreciable increase in yield. The excess urea added appears to compensate for small loss(es) of reactive nitrogen intermediate(s) to the atmosphere; these results also suggest that ammonia may not be an intermediate in the reaction mechanism and that the formation of a urea-derived imine facilitates nitrogen inclusion.<sup>21</sup> It is also possible that ammonia generation is slow enough<sup>44</sup> that it is never present in high concentration and is captured efficiently, prior to loss to the atmosphere.

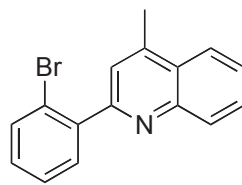
Using the optimized conditions (Entry 9), the Hua domino phenylquinoline synthesis becomes amenable to reproducibility and scale-up (Eq. 2.5).

The quinolone solubility was greatly reduced from that of the starting haloacetophenones, which allowed for purification by serial recrystallizations in hot alcohol and complete avoidance of chromatography. With the exception of the trichloromethylquinoline **56**, which could be obtained in acceptable purity by a single recrystallization, each of the monohaloquinoline products were purified by two or three successive recrystallizations. 2-(2-Chlorophenyl)-4-methylquinoline **37** was prepared on a 25-gram scale (relative to 2'-chloroacetophenone) and provided a yield of 88%.

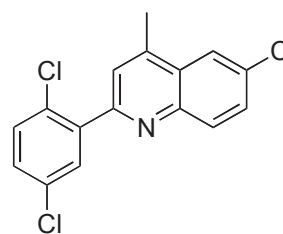
### Equation 2.5



**37**  
88%



**55**  
81%



**56**  
86%

This optimization allowed us to synthesize the suite of Hua phenylquinolines with a 10-15% increase in yields over the values reported, and without chromatographic purification.

#### 2.2.3 Limitations in substrate scope

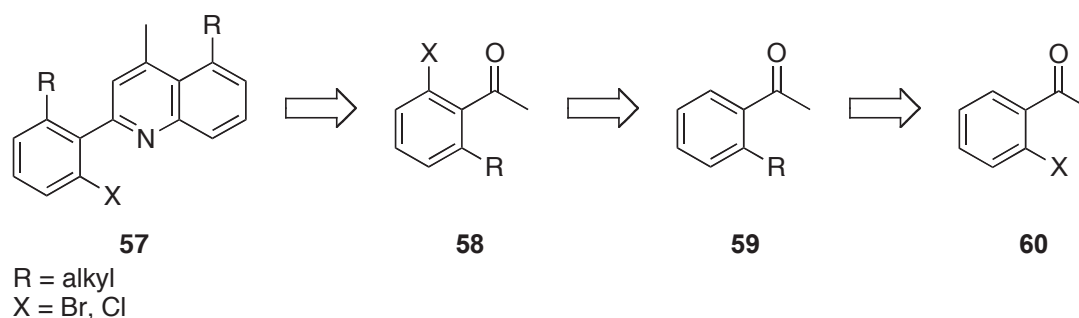
The facile nature of the Hua domino reaction was attractive, but viable as a general strategy for archipelago synthesis only if more complex haloacetophenones undergo the domino process, or if the phenylquinoline products themselves could be easily derivatized. One of the criteria used to determine if the model is an acceptable asphaltene mimic is its carbon-hydrogen ratio. Athabaskan asphaltenes display a carbon-hydrogen ratio of 1 : 1.3; the products shown above, with their halogen handles corrected to hydrogen, display a ratio high in carbon, 1.2 : 1, reminiscent of the first-generation nitrogenous archipelago models. To achieve the correct ratio, and to display the appropriate toluene solubility of asphaltenes, the above halophenylquinolines **37**, **55**, and **56** require saturated side chains.

**Table 2.2** Comparative atomic ratios of asphaltene and two model systems

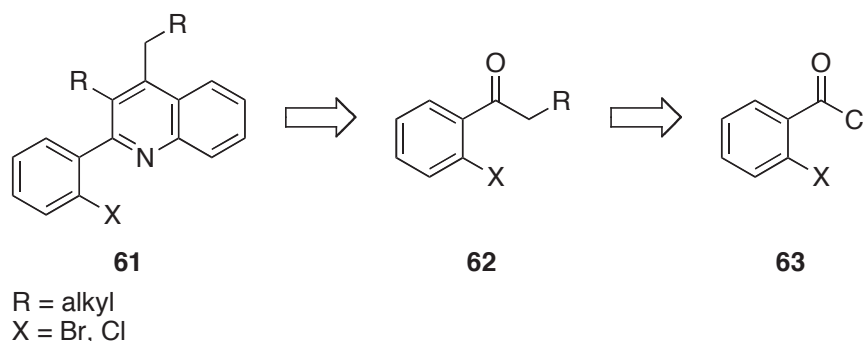
Asphaltene	Atomic Composition		Ratio
	Carbon	Hydrogen	
Athabasca Asphaltenes	81.3	7.9	1 : 1.2
Tykwinski Model Archipelago	91.9	5.5	1.4 : 1

Asphaltene	Atomic Composition		Ratio
	Carbon	Hydrogen	
2-(2-chlorophenyl)-4-methylquinoline <b>37</b>	75.7	4.8	1.3 : 1

Modification of the *o*-haloacetophenone to install additional, longer-chain alkyl groups was thus explored. Two strategies were available: (1) alkylation by cross-coupling, followed by re-halogenation on the aromatic ring, as shown in Scheme 2.4, and (2) extension of the acetyl alkyl chain, as shown in Scheme 2.5.



**Scheme 2.4** Retrosynthetic scheme I: ring modification

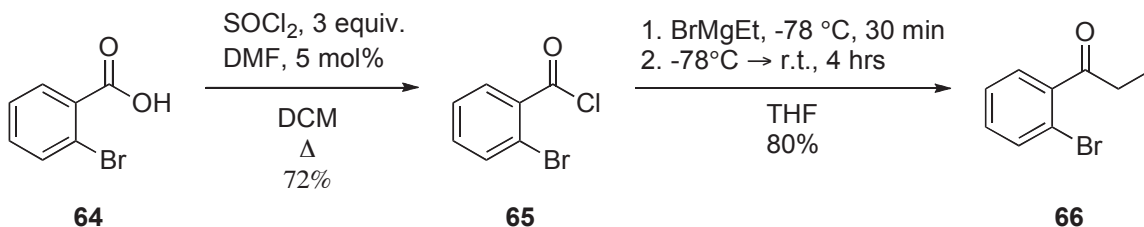


**Scheme 2.5** Retrosynthetic scheme II: chain extension

The latter appeared to be more realistic than the former. An attempt to use the bromide or chloride handles to install the side chain *via* cross-coupling would require subsequent regioselective re-halogenation *ortho* to the acyl group, a potentially difficult or multistep transformation. As such, no work following this strategy was attempted.

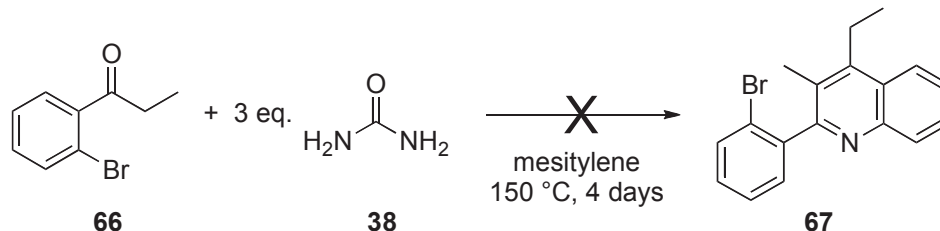
Starting material modification began with a single-carbon extension of the acyl side chain. Hua and coworkers reported that the cyclocondensation of 1-(2-chlorophenyl)pentan-2-one was unsuccessful,<sup>42</sup> so the first substrate synthesized to investigate the viability of extended side chains was 1-(2-bromophenyl)propan-1-one **66**,

which was prepared as shown (Scheme 2.6).<sup>45</sup> Unfortunately, similar to Hua's report, this acyl chain also disrupted the condensation and no cycloadduct was formed (Eq. 2.6).



**Scheme 2.6** Literature synthesis of 1-(2-bromophenyl)propan-1-one

### Equation 2.6



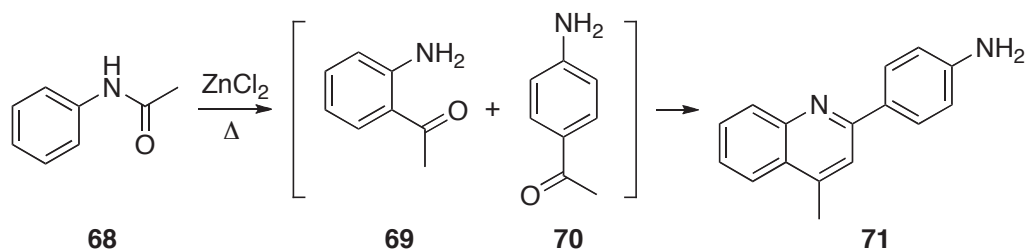
Hua and coworkers report that the addition of reactive functional groups (i.e. cyano groups) to the acyl chain also inhibited the condensation<sup>42</sup> and, as such, additional substrate variation was abandoned. It is possible that the extended chains, in addition to adding slight steric interference, reduced the rate of formation for one or more intermediates, prevented the condensation from occurring.

Thus although the Hua domino reaction offers an efficient pathway into simple halophenylquinolines, limited substrate scope precludes the possibility of using this methodology for the concise synthesis of an extended library of more highly derivatized nitrogenous asphaltene islands.

## 2.3 Synthesis of Complex Halophenylquinolines

### 2.3.1 Historical background: the Friedländer reaction

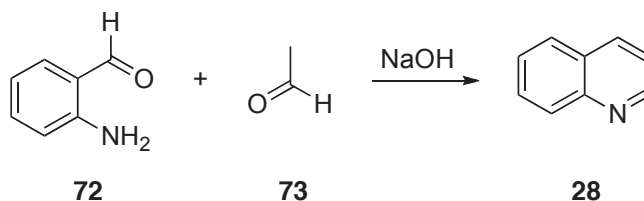
The Friedländer reaction is one of the oldest known methods for preparing substituted quinolines; Fisher is actually credited with the discovery, having performed a Friedländer reaction *in situ* during the synthesis of flavaniline **71** in 1882 (Scheme 2.7).<sup>46</sup>



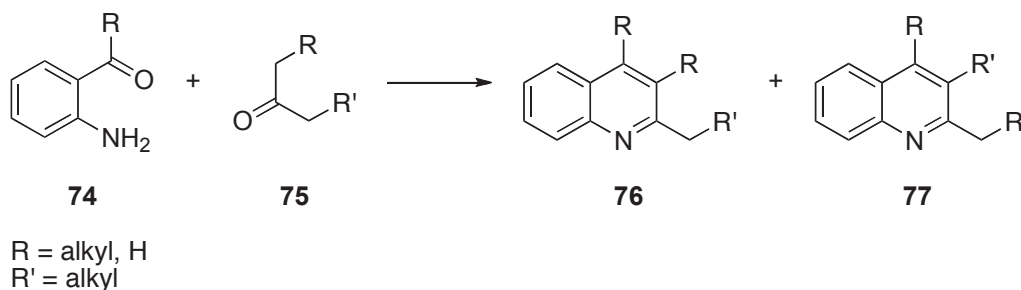
**Scheme 2.7** Fisher's flavaniline synthesis

Friedländer reported a direct, simplified version of the reaction that same year, combining *ortho*-aminobenzaldehyde **72** and acetaldehyde **73** in the presence of base to give quinoline itself (Eq. 2.7).<sup>47</sup> It is from this experiment that the synthesis was defined: a Friedländer reaction is the cyclocondensation of an *ortho*-carbonylaniline **74** with an  $\alpha$ -saturated ketone **75** to form a quinoline.

**Equation 2.7**



**Equation 2.8**



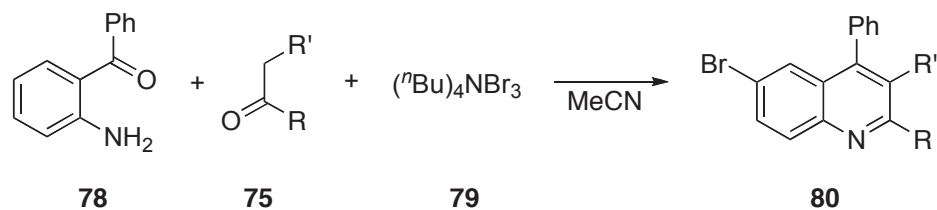
The Friedländer reaction is extremely robust; it is tolerant of different types of 1-amino-2-acyl compounds,<sup>48</sup> highly variable in the range of ketones,<sup>49</sup> promoted by an ever-growing span of catalysts,<sup>26</sup> and displaying high tolerance towards ancillary functional groups.<sup>49a,50</sup> As such, the reaction offered excellent potential for developing a

generalized synthesis of a broad range of functionally diverse nitrogenous asphaltene mimics.

### 2.3.2 An ideal adaptation: the Wu-Friedländer haloquinoline synthesis

Wu, *et al.* developed a regioselective Friedländer variant for the direct synthesis of halogenated quinolines using the *in-situ* generated Brønsted acid-catalyst obtained from electrophilic halogenation of the starting aniline (eq. **2.9**).<sup>51</sup> The initial halogenation uses commercial tetra-*n*-butylammonium tribromide **79** (TBAT) to brominate 2-aminobenzophenone **78** selectively and quantitatively, with the resultant hydrobromic acid utilized as the Friedländer catalyst for the subsequent reaction with carbonyl compound **75**. Using this multipurpose reagent, the authors synthesized a diverse selection of 5-bromo-3-phenylquinolines **80** and 7-bromo-9-phenyl acridines (see Scheme **2.9**) using a small selection of ketones.

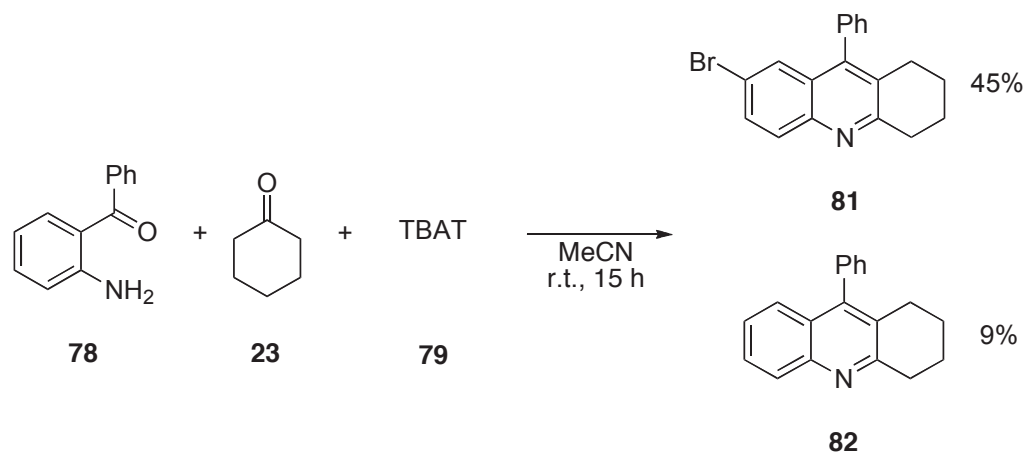
#### Equation 2.9



R, R' = alkyl groups

### 2.3.3 Optimization for 2-aminobenzophenone

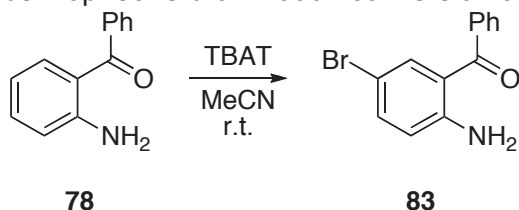
Initial attempts to replicate the work of Wu *et al.* met with minor operational issues. Though the original procedure does yield the desired products, it is far from optimized and use of the methodology as described cannot achieve the reported yields. When applied exactly as outlined, the reaction conditions fail to meet the published results. Yield is dramatically reduced and a side-product, identified as 9-phenyl-1,2,3,4-tetra-hydroacridine **82**, is produced to a significant extent (Scheme **2.8**).



**Scheme 2.8** Results of the Wu-Friedländer literature conditions

Investigation into the rate of bromination was accomplished using GC-MS analysis over time, in an attempt to determine the root cause of the non-brominated side product **82** (Table 2.3). This analysis showed that the bromination step is fast. Within five minutes, conversion to 2-amino-5-bromobenzophenone **83** was >98%. The side product **82** was thus avoided by allowing the aniline and TBAT to stir briefly prior to ketone addition.

**Table 2.3** 2-aminobenzophenone bromination conversion over time



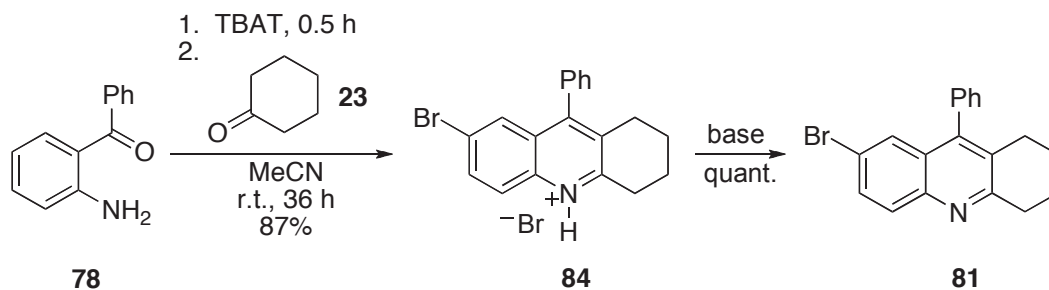
Time (min)	2-aminobenzophenone (A%)	Conversion (%)
~0	8.0	92%
5	2.0	98%
10	<0.1%	>99%

Reaction conditions: 2-aminobenzophenone (0.5 mmol), TBAT (0.5 mmol), and acetonitrile (5 mL) were added to a 10 mL round-bottomed flask equipped with a stirbar. GC-MS instrument method may be found in Section 5.2. A% is area normalization of the GC chromatogram.

Yield and purity was increased simply by using longer reaction times for the initial bromination (Eq. 2.10). Reaction mixtures were monitored *via* TLC until the ketone was consumed, after which the reaction mixture was initially allowed to stir an additional

12h. During this time, large amounts of precipitate formed, at differing times for different substrates. These solids were shown by  $^1\text{H}$  NMR spectroscopy and elemental analysis to be the HBr salts of their respective quinoline products. Crude reaction mixtures were placed under high vacuum to remove water and acetonitrile, allowing the pure aniline salt to be isolated by suction filtration.

### Equation 2.10



Additionally, the atom economy of the reaction was boosted through recovery of the tetra-*n*-butylammonium bromide side product, easily separable by basic aqueous washes of the crude mother liquor. Adapting a one-pot procedure used by Buchwald,<sup>52</sup> TBAB generated from the condensation reaction was brominated cleanly with elemental bromine to reform the tribromide. The recycled TBAT, once dried under high vacuum, was reused twice for the same reaction with little affect on the condensation yield (Table 2.4).

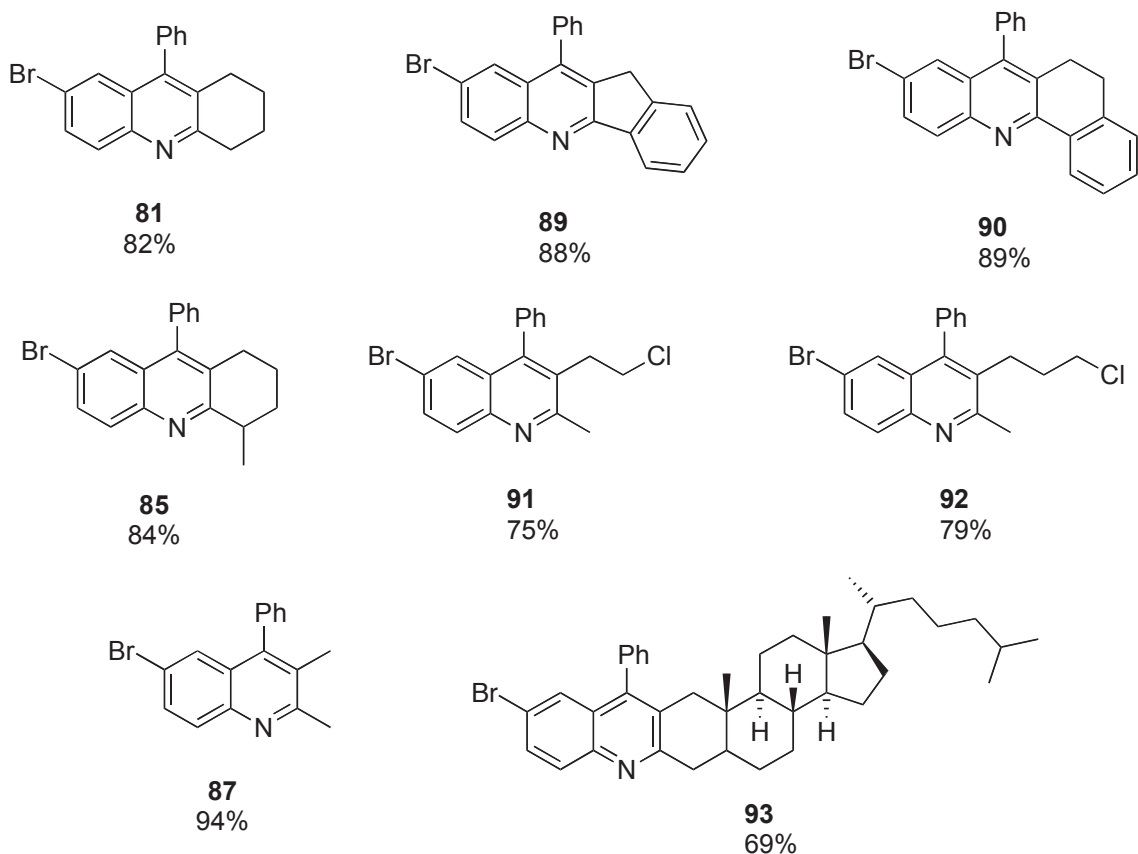
**Table 2.4** TBAT recovery and regeneration

Condensations	Condensation yield (%)	TBAB recovered (%)	Bromination yield (%)
1	87%	94%	99%
2	84%	96%	99%

Reaction conditions: Friedländer reaction was carried out according to Eq. 2.10, 1mmol scale. Following its completion, the remaining mother liquors were added to a separatory funnel and washed with 10% sodium hydroxide. Aqueous washes were combined, neutralized, and then back extracted with ethyl acetate. The recovered crude TBAB was purified according to literature procedures<sup>53</sup> prior to re-bromination.

Having reconfigured the reaction conditions, a wide range of structurally diverse 6-bromo-4-phenylquinolines and 7-bromo-9-phenyl acridines were synthesized in good to excellent yields (Scheme 2.9). Each of the cycloadducts displays a favourable carbon-hydrogen ratio, even with inclusion of the bromine handle (Table 2.5). The increased

differentiation of these islands alone, prior to their inclusion within an archipelago compound, are closer to that of natural asphaltenes than previous model quinolines.



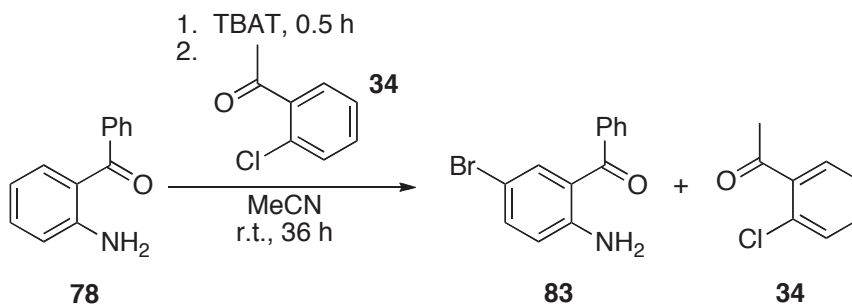
**Scheme 2.9** Isolated Wu-Friedländer products

**Table 2.5** Comparative atomic ratios of representative types of second-generation Wu-Friedländer phenylhaloquinoline model asphaltene islands

Asphaltene model compound	Atomic Composition		Ratio
	Carbon	Hydrogen	
<b>Athabasca asphaltenes</b>	<b>81.3</b>	<b>7.9</b>	<b>1 : 1.2</b>
Tykwinski model archipelago <b>14</b>	91.9	5.5	1.4 : 1
7-bromo-9-phenyl-1,2,3,4-tetrahydroacridine <b>81</b>	67.5	4.8	1.1 : 1
9-bromo-7-phenyl-5,6-dihydrobenzo[c]acridine <b>90</b>	71.5	4.2	1.3 : 1
6-bromo-3-(3-chloroethyl)-2-methyl-4-phenylquinoline <b>92</b>	60.9	4.6	1.1 : 1

Unfortunately, attempted reactions using acetophenones as the ketone component failed to produce the 1-phenylquinoline products. The reaction of 2-aminobenzophenone **78** and 2'-chloroacetophenone **34** (Eq. 2.11) for example, yielded only 5-bromo-2-aminobenzophenone **83** and the unaltered chloroacetophenone **34**.

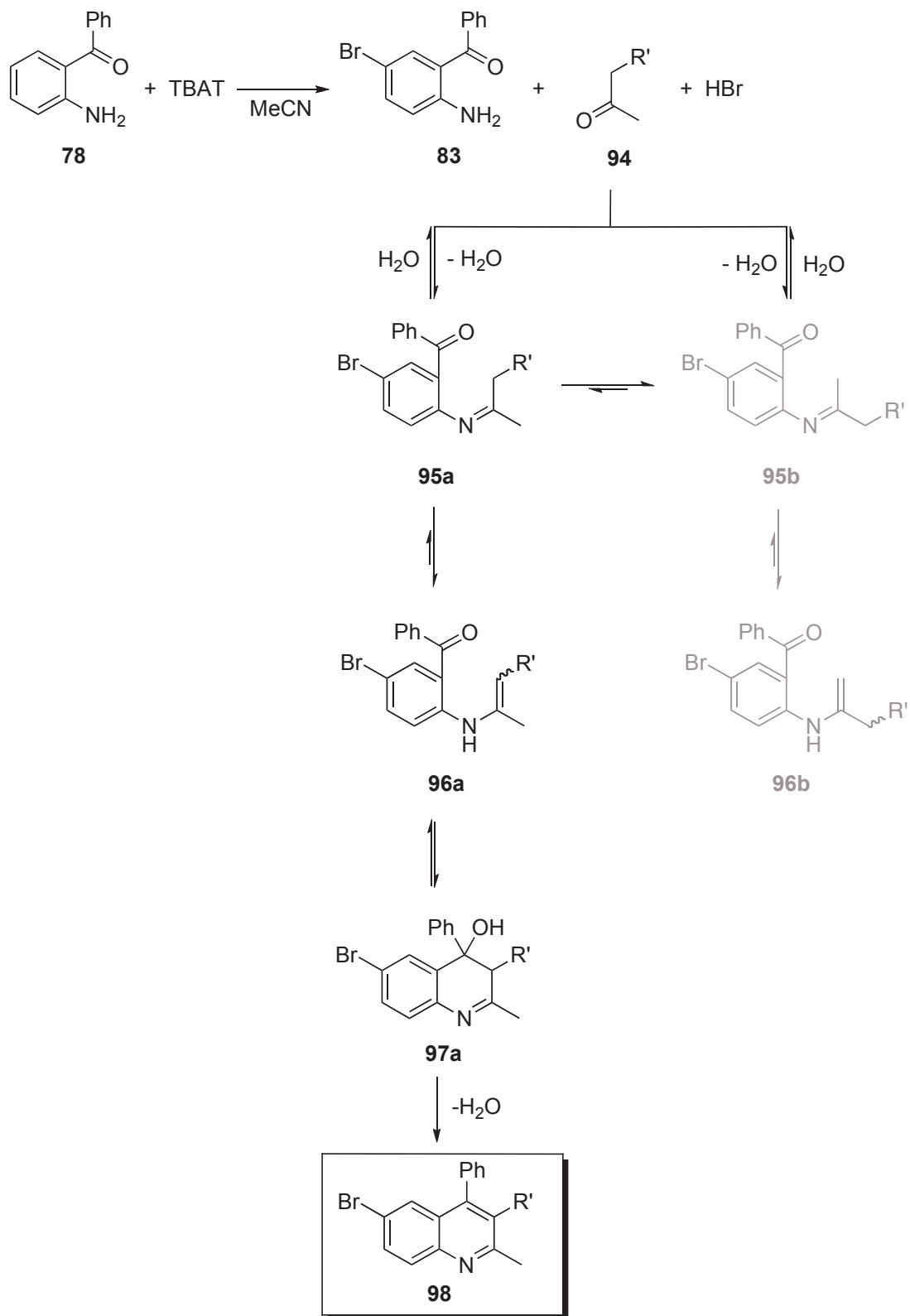
### Equation 2.11



Nonetheless, using this reaction, we were able to synthesize model nitrogenous asphaltene islands with highly variable alkyl side chains. While these derivatizations were localized on the quinolone A ring, we were able to provide compounds with both cyclic (**81**, **85**, and **86**) and acyclic alkyl segments (**87** and **88**) of variable length, two islands with tethered alkylchlorides (**91** and **92**) ideal for future cross-coupling reactions, two islands with segregated aromatic systems (**89** and **90**), and one island bearing a steroid-derived biomarker, **93**. Optimized reaction conditions were scaled up to 0.1 mol for several ketones (approximately 20g based on benzophenone) and achieved yields higher than 80% in almost every case.

#### 2.3.4 Mechanistic considerations

The mechanism of the Friedländer reaction has not been definitively established. While it is agreed that the mechanism proceeds *via* both an aldol condensation and the formation of an imine,<sup>54</sup> the order in which each occurs—indeed, even the rate-limiting step itself—cannot be generally classified. As Wu does not do so, we propose a general mechanism for the Wu-Friedländer (Scheme **2.10**). For the purposes of discussion, we define unsymmetrical ketone alkyl substituents by size, such that  $R' > R$ .



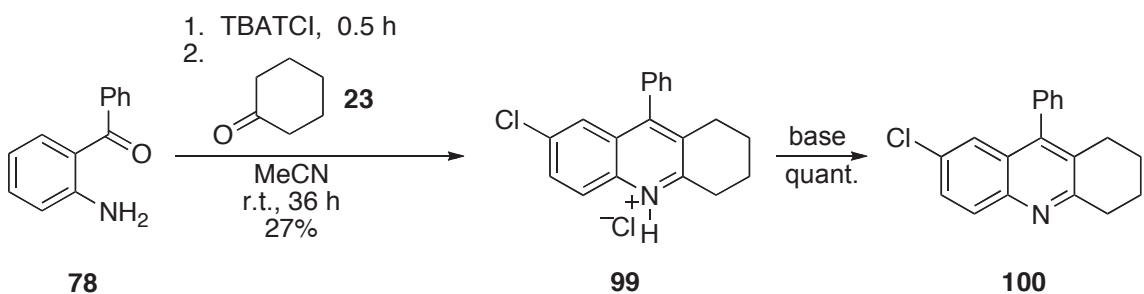
**Scheme 2.10** Proposed Wu-Friedländer mechanism

The initial bromination of 2-aminobenzophenone **78** (not illustrated) generates HBr, which catalyzes both Schiff base formation and the aldol condensation. With the reaction proceeding at room temperature under acidic conditions, it is reasonable to expect the reversible formation of the two possible Schiff bases **95a** and **95b** to occur under equilibrium conditions prior to the aldol condensation. The study performed by Wu and coworkers<sup>51</sup> does not describe the formation of quinoline products descendant of Pathway B (Scheme **2.10**), nor did we observe these regioisomers when the reaction was performed in our hands. Each compound synthesized by this method follows Pathway A.

The observed products result from the favoured (*E*) ketimine **95a**, which leads to the (*E*) enamine **96b**. This isomer is energetically less favourable due to steric interactions, particularly in cases where R is a methyl group, but is thermodynamically favoured. It may be assumed that the aldol condensation of the enamine **96b** is inhibited due to its reduced reactivity, disfavoring the formation of quinoline by Pathway B. We therefore obtain complete regioselectivity for the Friedländer reaction in this case.

### 2.3.5 Proof of concept: chloroacridine synthesis

Following the work done with the tribromide **79**, we attempted to use a tetra-*n*-butyltetrachloroiodate (TBATCl) to effect a similar reaction and generate chloride handles on the same quinoline and acridine compounds shown above (Scheme **2.11**). While not immediately advantageous, as the product presents a stronger carbon-halogen bond, chloride is a viable cross-coupling handle on nitrogen heteroaromatic scaffolds.<sup>55</sup> Although the yield was greatly reduced compared to our optimized TBAT conditions, the unoptimized reaction furnished pure chloroacridine and was not further pursued.

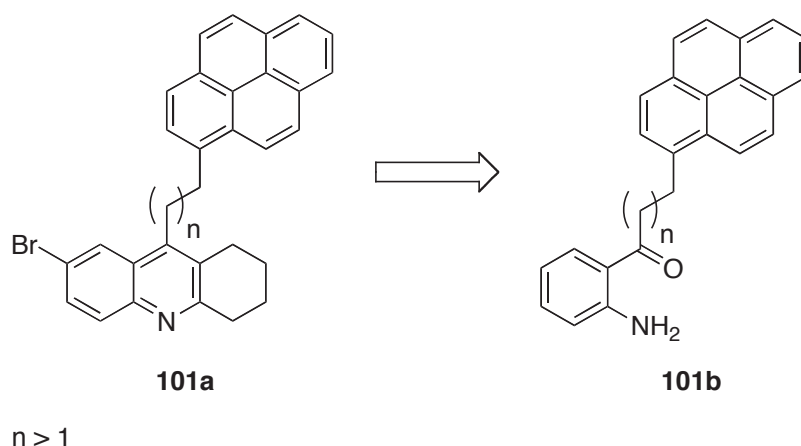


**Scheme 2.11** Modified Wu-Friedländer synthesis using TBATCl

### 2.3.6 The issue of 2-aminoacetophenone

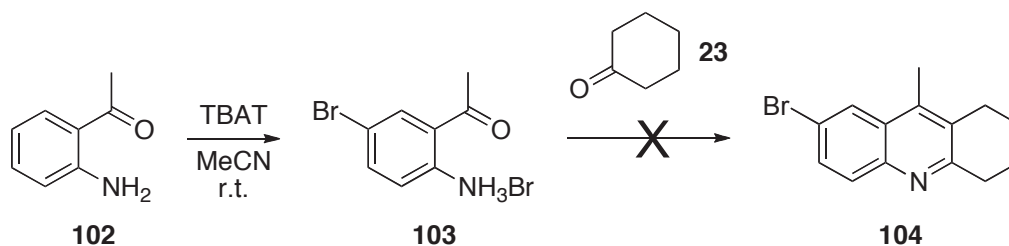
The most desirable starting material in terms of carbon-hydrogen ratios and, thereby, archipelago solubility, is 2'-aminoacetophenone **102**. There is little evidence for zero-carbon aromatic tethers within archipelago structures,<sup>5,14</sup> so rather than installing a phenyl substituent, it is preferable for each model compound to have short-chain alkyl substitution (the 4-position within the quinoline scaffold; the 9-position within the acridine scaffold) instead of the aryl group used exclusively in Section 2.3.3.

This particular compound is also desirable as a probe into substrate scope expansion. Should the reaction conditions prove viable for 2-aminoacetophenone **102**, it may be possible to form a two-island archipelago **101a**.



**Scheme 2.12** Two-island archipelago retrosynthesis

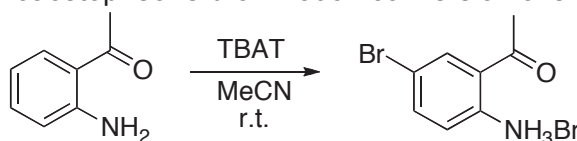
Reaction of 2-aminoacetophenone under the previously optimized TBAT conditions (Eq. **2.10**), however, produced no condensation product (Scheme **2.13**). Rather than the expected bromotetrahydroacridine **104** or its hydrogen bromide salt (not pictured), the 5-bromo-2-aminoacetophenone hydrogen bromide salt **103** precipitated completely, ending the reaction. This anilinium salt shows very poor solubility; it is insoluble in chloroform, dichloromethane, and THF at all temperatures, and shows extremely limited solubility in dioxane, DME, or DMF at reflux. At elevated temperatures, however, side reactions began to dominate and dioxane was degraded. This is likely due the acidic conditions in combination with the  $\text{Br}^-$  and  $\text{Br}_3^-$ , as halide ions are known to ring open cyclical etheral solvents in strongly acidic solutions.<sup>56</sup>



**Scheme 2.13** Wu-Friedländer synthesis as applied to 2-aminoacetophenone

GC-MS analysis of the bromination step showed it to be faster than that observed in the case of 2-aminobenzophenone (Table 2.6). Given the speed of the bromination and the rapid appearance of the aniline salt, we began exploring modifications to the synthesis to circumvent this issue.

**Table 2.6** 2-aminoacetophenone bromination conversion over time



	102	103	
Time (min)	2-aminoacetophenone (A%)	5-bromo-2-aminoacetophenone (A%)	Conversion (%)
~0	<0.05%	>99%	>99%
5	<0.05%	>99%	>99%
10	<0.05%	>99%	>99%

Reaction conditions: 2-aminoacetophenone (0.5mmol), TBAT (0.5mmol), and acetonitrile (5mL). GC-MS instrument method may be found in Section 5.2. A% is area normalization of the GC chromatogram.

### 2.3.7 Backup routes to 7-bromo-9-methyl-1,2,3,4-tetrahydroacridine

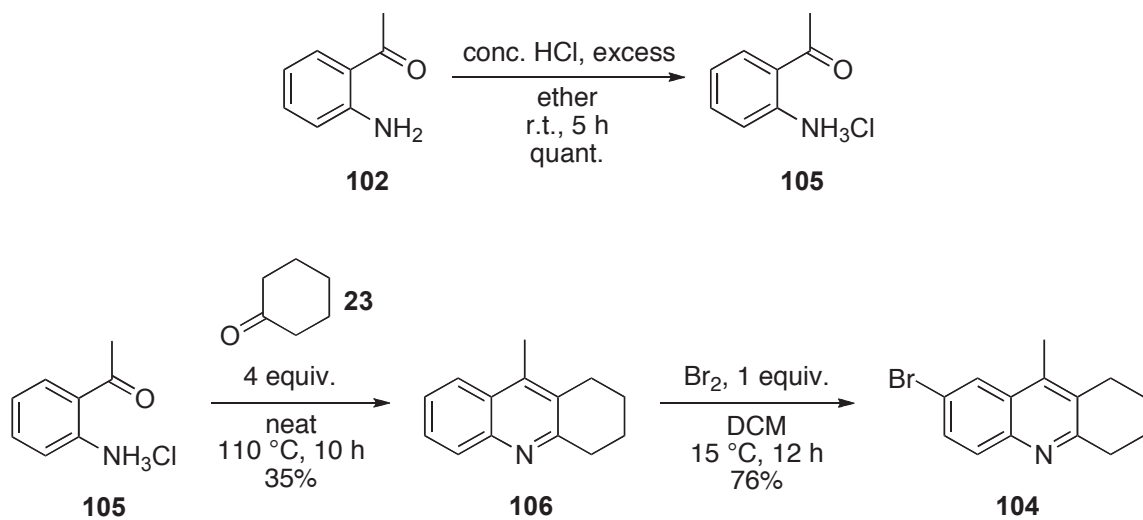
Concurrent to circumventing the issue of the 2-aminoacetophenone salt **103**, 7-bromo-9-methyl-1,2,3,4-tetrahydroacridine **104** was synthesized by two alternate means.

#### 2.3.7.1 Route 1: Condensation via alternative halogenation

The first alternative route involved the synthesis of the halogen-free acridine from the aniline hydrogen chloride salt **105**, produced *via* acidification of 2-aminoacetophenone **102** (Eq. 2.12). This salt was then added to an excess of

cyclohexanone **23** to produce 9-methyl-1,2,3,4-tetrahydroacridine **106**, which was cleanly brominated in the 7-position to generate the desired product **104** (Scheme 2.14). Given that the condensation step uses an undesirable excess of ketone, achieves a low yield, and is limited to ketones that are low melting and stable at high temperatures, a second alternative was explored.

### Equation 2.12

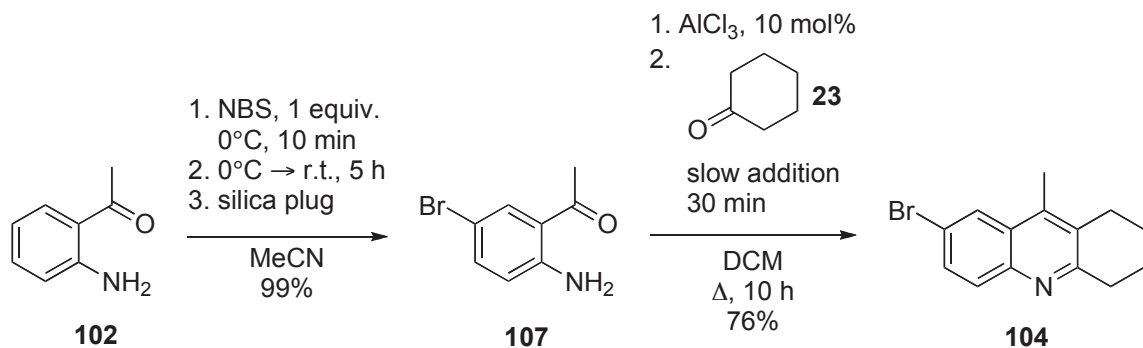


**Scheme 2.14** Synthesis of 7-bromo-9-methyl-1,2,3,4-tetrahydroacridine via 2-aminoacetophenone hydrogen chloride salt

#### 2.3.7.2 Route 2: Condensation via Lewis Acid catalysis

The literature is saturated<sup>54</sup> with independent examples describing catalytic systems that effect the Friedländer reaction. Thus encouraged, we effected the condensation of 5-bromo-2-aminoacetophenone **107** and cyclohexanone **23** using catalytic aluminum trichloride (Scheme 2.15).<sup>54</sup> This method proved superior to the anilinium salt condensation described above (Section 2.3.7.1)

With a viable synthetic route to 7-bromo-9-methyl-1,2,3,4-tetrahydroacridine **104** in reasonable yields, our focus then returned to modifying the original TBAT-mediated condensation.



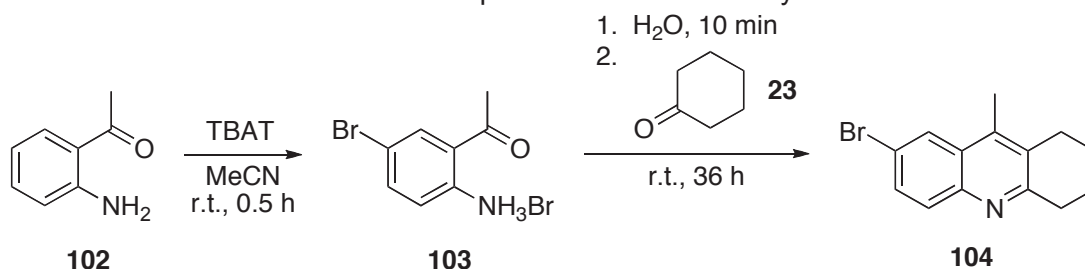
**Scheme 2.15** Lewis acid catalyzed synthesis of 7-bromo-9-methyl-1,2,3,4-tetrahydroacridine

### 2.3.8 Modified conditions for Wu-Friedländer condensation of 2-aminoacetophenone

With our expected product **104** in-hand, we returned to the original Wu-Friedländer reaction to continue optimization. To be complementary to the original conditions for 2-aminobenzophenoneone **78**, any modifications made to the TBAT-catalyzed Friedländer must maintain the moderate reaction conditions, ease of use, and broad substrate tolerance.

#### 2.3.8.1 First modification: salt dissolution

Observation of anilinium bromide salt **103** saw it slowly yellow upon exposure to air; organic washes of the exposed salt yielded a soluble, visible spot by TLC (UV), which was confirmed to be the *neutral* 1-(2-amino-5-bromophenyl)ethanone **107** by <sup>1</sup>H NMR spectroscopy. When water is added to the Wu-Friedländer reaction mixture (acetonitrile, TBAB, and 1-(2-amino-5-bromophenyl)ethanone hydrogen bromide **103**), the precipitated anilinium salt slowly dissolves. The minimum amount required to dissolve the salt completely at room temperature was found to be 0.68 mL water in 10.00 mL acetonitrile, with the reaction run on a 1 mmol scale. A short series of reactions was then attempted to probe the effect of water on the outcome of the Friedländer reaction (Table 2.7).

**Table 2.7** 5-bromo-2-aminoacetophenone water solubility data<sup>a</sup>

entry	Water (mg/mL)	Isolated yield (%)
1	0.68	9
2 <sup>b</sup>	0.68	11
3	0.35	14
4 <sup>b</sup>	0.35	15
5	0.10	27
6 <sup>b</sup>	0.10	30

<sup>a</sup>Reaction conditions: 2-aminoacetophenone (1mmol), TBAT (1mmol), and acetonitrile (10mL), 30min; water added, 10min; cyclohexanone added. <sup>b</sup>Following the addition of water, the reaction was warmed to 50 °C and maintained there for the duration of the reaction.

Although the addition of water promoted the dissolution of the anilinium salt **103** at room temperature, the condensation yield remained poor. When the amount of water added was reduced to 0.1 mg/mL (entry 5), the yield was increased substantially, but only to 30%. Reaction mixtures warmed to 50 °C (entries 2, 4, and 6) did not return a significant increase in yield over those run at room temperature. As such, this particular modification was abandoned.

### 2.3.8.2 Second modification: alternative solvent

Ionic liquids have been increasingly adapted for organic synthesis in the twenty-first century.<sup>57a</sup> Should a given ionic liquid display proper solubility, viscosity, and ease of recovery, it may be a viable option for large scale reactions, with the immediate aim the reduction of solvent waste. The use of such nonvolatile, reusable solvents is one of the central goals of the environmentally-centered *green chemistry* field. While it is true that obtaining the perfect combination of those ionic liquid traits for a specific reaction can be difficult, research in this area continues to provide new ionic liquids with an expanding range of properties.<sup>57b</sup>

Given the nature of the aminoacetophenone hydrogen bromide salt **103**, it was postulated that an ionic liquid might be used in place of acetonitrile to effect the condensation. Further, it was anticipated that, should this endeavour be successful, the same ionic liquid could be used in other cases where the ketone solubility prohibits the use of standard solvents.

One example of a Friedländer condensation between 2-aminoacetophenone **102** and cyclohexanone **23** in the presence of an ionic liquid has previously been reported.<sup>58</sup> The researchers used two quaternary nitrogen components, 1-*n*-butylimidazolium **108** and 1,3-di-*n*-butylimidazolium **110** (Figure 2.4) with several counter ions in their ionic solvent screening. In this case the ionic liquid employed was used as both solvent and as the Friedländer acid catalyst.

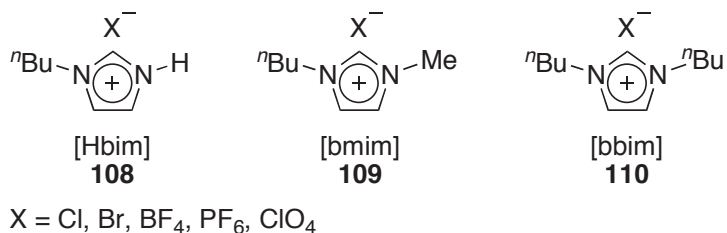
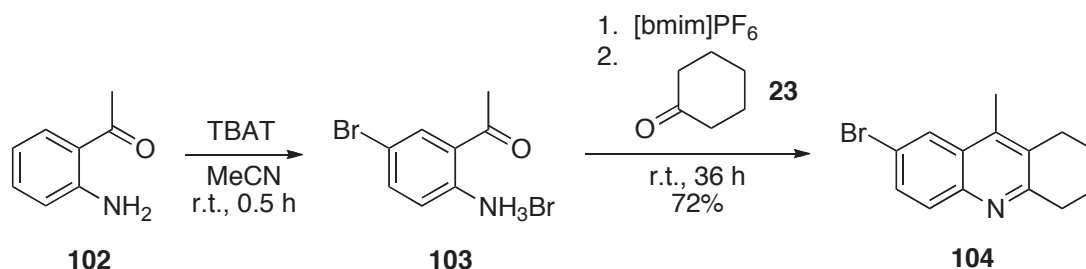


**Figure 2.4** Ionic liquids

A brief note on naming convention: imidazolium-based ionic liquids are given an acronym based on the first letter of each alkyl substituent and “im” for imidazole. Thus 1-*n*-butyl-3-methylimidazolium bromide is shortened to [bmim]Br.

Palimkar and coworkers showed that superior condensation yields were obtained using the [Hbim] system with a tetrafluoroborate or hexafluorophosphate counterion,<sup>58</sup> with both examples leading to yields of  $\geq 90\%$ . Wishing to expand upon this literature, we selected the non-acidic 1-*n*-butyl-3-methylimidazolium perfluoroborate, [bmim]PF<sub>6</sub>, for our screening. The initial reaction of 2-aminoacetophenone **102** and TBAT **79** was carried out under the previously optimized conditions (Eq. 2.10), allowing for the complete conversion of 2-aminoacetophenone **102** to the anilinium salt **103** before the addition of the ionic liquid (Scheme 2.16). After the reaction, the crude mixture was washed with hot diethyl ether and hot ethyl acetate to remove the product.



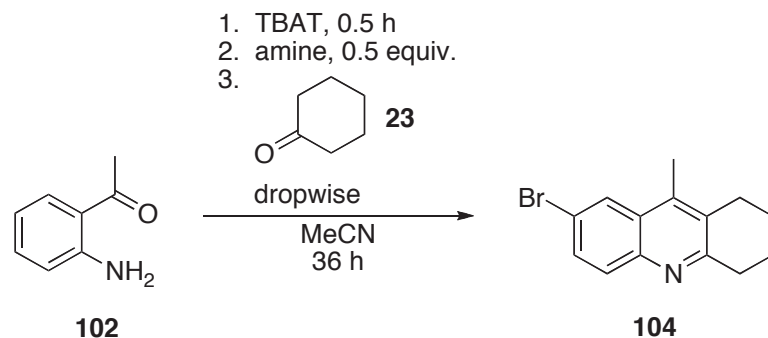
**Scheme 2.16** Wu-Friedländer solvent modification trial

### 2.3.8.3 Final modification: competitive salt formation

One additional study was undertaken: to determine if a catalytic amount of added amine could compete with the aniline substrate for HBr salt formation. A series of reasonably basic amines was selected, each of which effected the dissolution of the anilinium salt **103** and allowed the Friedländer condensation to proceed (Table **2.8**). Triethylamine (TEA) furnished 7-bromo-9-methylacridine **104** in the highest yield; following these results, a short series of stoichiometry trials was performed to optimize the reaction. Optimal triethylamine addition for the given conditions was determined to be 0.25 equivalents.

Given its increased ease-of-use, low-cost, and superior yield over the water dissolution (Table **2.7**) and alternative solvent (Scheme **2.16**) modifications, the TEA modification was determined to be the superior Wu-Friedländer synthesis adaptation for 2-aminoacetophenone (Eq. **2.13**).

**Table 2.8** Amine screening for 2-aminoacetophenone

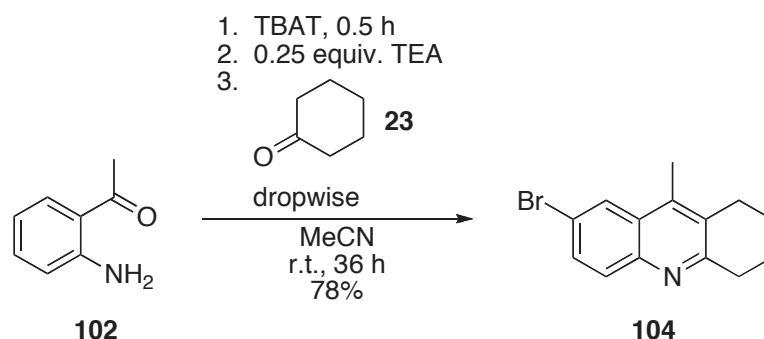


entry	amine	Equivalents	Yield (%)
1 <sup>a</sup>	pyridine	0.5	18
2 <sup>b</sup>	pyridine	0.5	21

entry	amine	Equivalents	Yield (%)
3 <sup>a</sup>	diisopropylamine	0.5	25
4 <sup>b</sup>	diisopropylamine	0.5	26
5 <sup>a</sup>	triethylamine	0.5	42
6 <sup>b</sup>	triethylamine	0.5	45
7 <sup>a</sup>	triethylamine	1.0	6
8 <sup>a</sup>	triethylamine	0.75	27
9 <sup>a</sup>	triethylamine	0.25	78
10 <sup>a</sup>	triethylamine	0.10	36

Reaction conditions: <sup>a</sup> 2-aminoacetophenone (1mmol), TBAT (1mmol), and acetonitrile (10mL), 30 min prior to amine and ketone addition. <sup>b</sup> Following the addition of amine, and prior to the addition of the ketone, the reaction was warmed to 50 °C and maintained there for the duration of the reaction.

### Equation 2.13



## 2.4 Conclusions

Two separate “one-pot” halophenylquinoline syntheses have been sufficiently optimized to provide gram-scale quantities of nitrogenous, polyaromatic islands for incorporation into archipelago model asphaltene compounds. Both of these syntheses meet the first and third goals of this project, as outlined in the beginning of this chapter; both achieve the desired haloquinoline islands in relatively simple one-pot procedures (Goal 1) at large scale without the necessity of chromatographic purification. Both syntheses also furnished nitrogenous islands with halogen handles for future cross-coupling (Goal 3). Only the Wu-Friedländer synthesis, however, demonstrated the required substrate tolerance (Goal 2) to provide the required variety in aliphatic substitution to achieve lower carbon-hydrogen ratios and improve asphaltene model solubility.

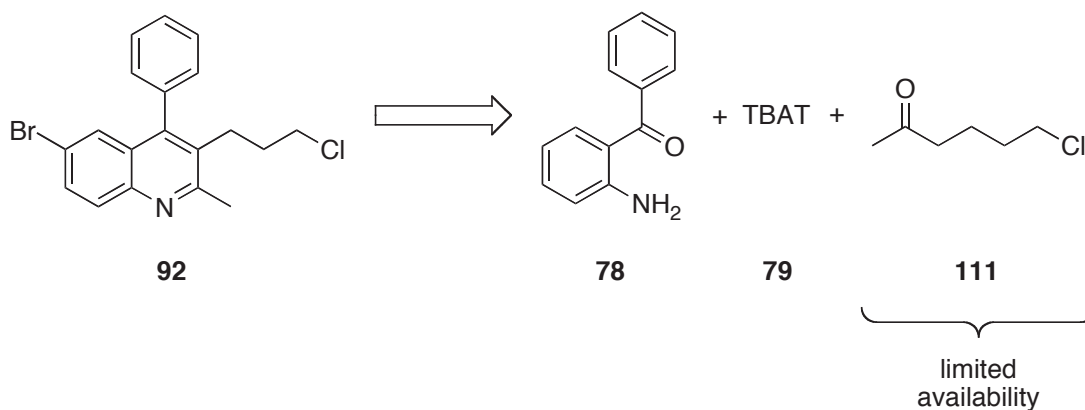
The Wu-Friedländer synthesis was further translated to a (slightly) new chlorination reagent and *in-situ* catalyst generator, TBATCl, and successfully adapted for the difficult, yet superior, asphaltene substrate, 2-aminoacetophenone, which may lead to a viable two-island archipelago synthesis.

Further derivatization and work towards the synthesis of full archipelagos will be discussed in the following chapter.

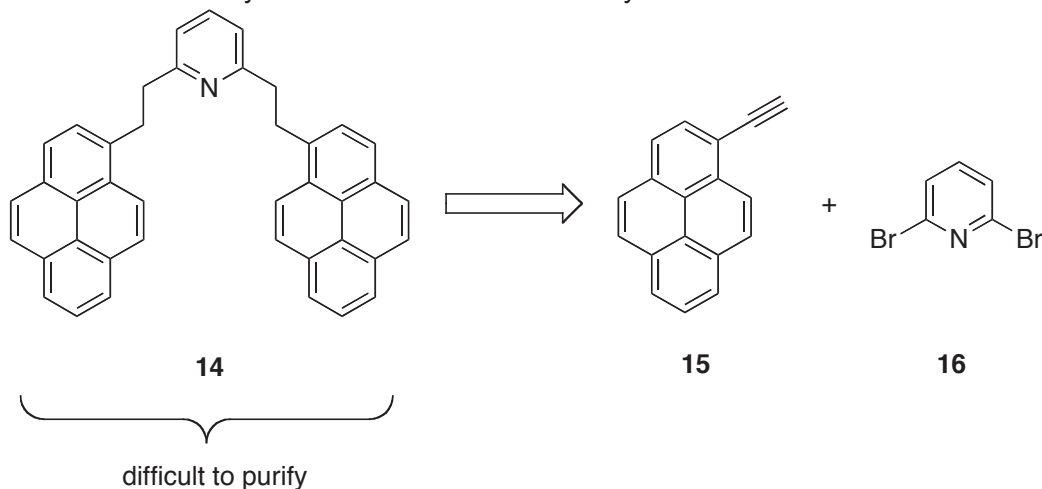
### 3 Organometallic Routes to Model Archipelagos

#### 3.1 Introduction

Installation of saturated alkyl tethers between islands remains a difficult challenge in archipelago synthesis. While we have provided examples whereby one or more tethers can be installed during the Wu-Friedländer synthesis (e.g. **92**, Scheme 3.1), such compounds rely on bifunctional reagents, here 6-chloro-hexan-2-one **111**. Only this  $\omega$ -chloromethylketone and 5-chloro-2-pentanone (not pictured) are commercially available. The first-generation nitrogenous archipelagos developed by Tykwinski, et al. (Scheme 3.2), were synthesized using Sonogashira coupling reactions to install two-carbon alkynyl tethers and, while this broadens the range of substrates to include halogenated aromatic compounds, the nonselective hydrogenation made this synthesis unsatisfactory as a general method for archipelago construction.

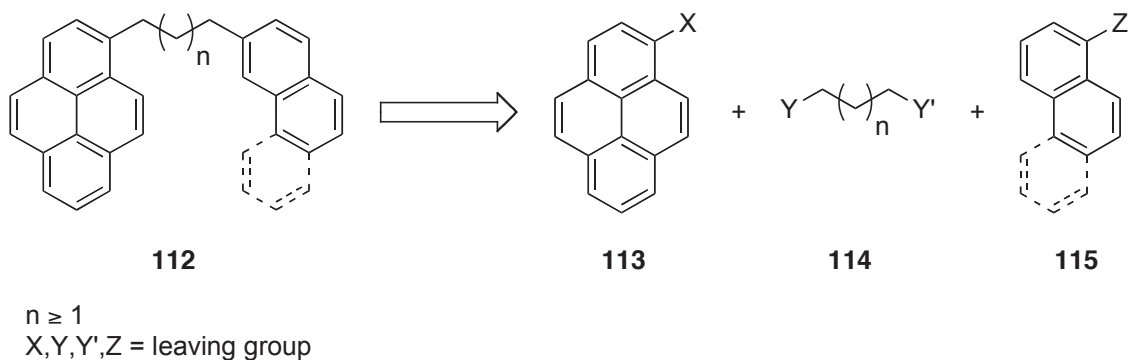


**Scheme 3.1** Retrosynthesis of tethered islands by the Wu-Friedländer reaction



**Scheme 3.2** Retrosynthesis of the first-generation Tykwinski archipelago

To expand the scope of archipelago synthesis, we found it necessary to develop a robust stepwise method for archipelago construction. Such a method should, as with our previous syntheses, tolerate a wide range of substrates. The ideal situation would involve a tether with *orthogonal* reactivity at each end, allowing for specific coupling to each island (Scheme 3.3). With the hope of finding methodology that is widely applicable, we explored other avenues within the cross-coupling literature.



**Scheme 3.3** A general retrosynthetic plan for archipelago construction

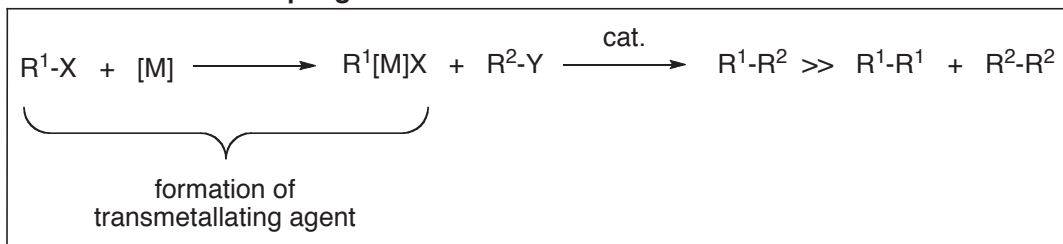
Catalytic cross-coupling has become one of the most powerful and widely used means of creating carbon-carbon bonds. While this area has long been dominated by palladium<sup>59</sup> and nickel catalysts,<sup>60</sup> new advances continue to push the elemental boundaries of this area of catalysis. Additional first-row transition metals, including several *base metals*, are now common cross-coupling catalysts, with iron<sup>61</sup> and cobalt<sup>62</sup> playing increasingly prominent roles.

Among recent advances in first-row catalysis, significant work has been focused on the creation of viable *reductive cross-electrophile coupling* (REC) reactions, whereby the two electrophilic carbons are coupled directly, without the use of an intervening transmetallating agent.<sup>63</sup> Such reactions use a reducing reagent, often inexpensive metal powders, to reduce the primary catalytic metal to the oxidation states required for the coupling reaction to proceed.

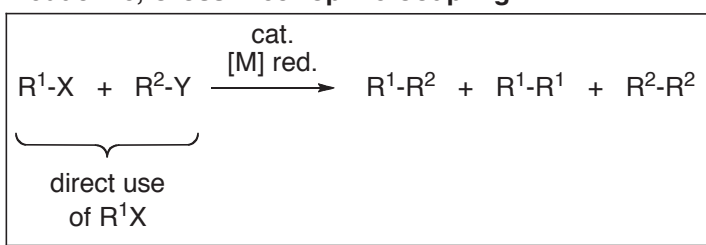
The main advantage of the REC method is the direct coupling of two carbon electrophiles *as-is* (Scheme 3.4), without further modification of the intended reactive carbon or protection of competitively reactive ancillary functional groups. This potentially allows for a massive expansion in reaction scope, including high tolerance for functional groups such as ketones, nitriles, and esters, that are often incompatible with standard

organometallic cross-coupling processes due to the inherently high reactivity of transmetallating agents.

#### Traditional Cross Coupling



#### Reductive, Cross-Electrophile Coupling

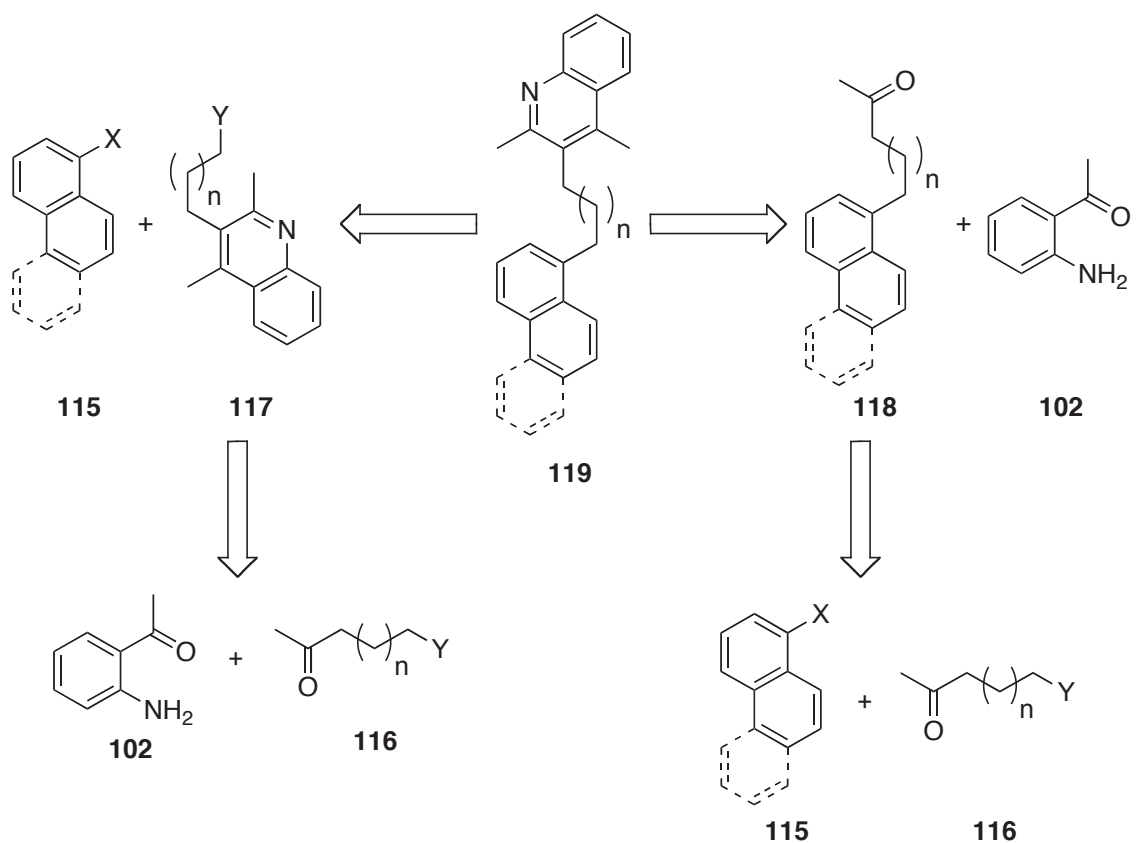


R, R' = alkyl or aryl  
X, Y = leaving groups

#### Scheme 3.4 Traditional vs. reductive coupling

Issues can arise regarding the specificity of these reactions, however. The core tenet of traditional coupling reactions is that the reagents are truly *crossed*; that is, their reactivity is precisely opposite, one reagent bearing an electrophilic carbon, the other a nucleophilic carbon. REC reactions lose this advantage through the use of two electrophilic reagents and, as such, require significant method development to avoid side product formation due to competitive homo-coupling.

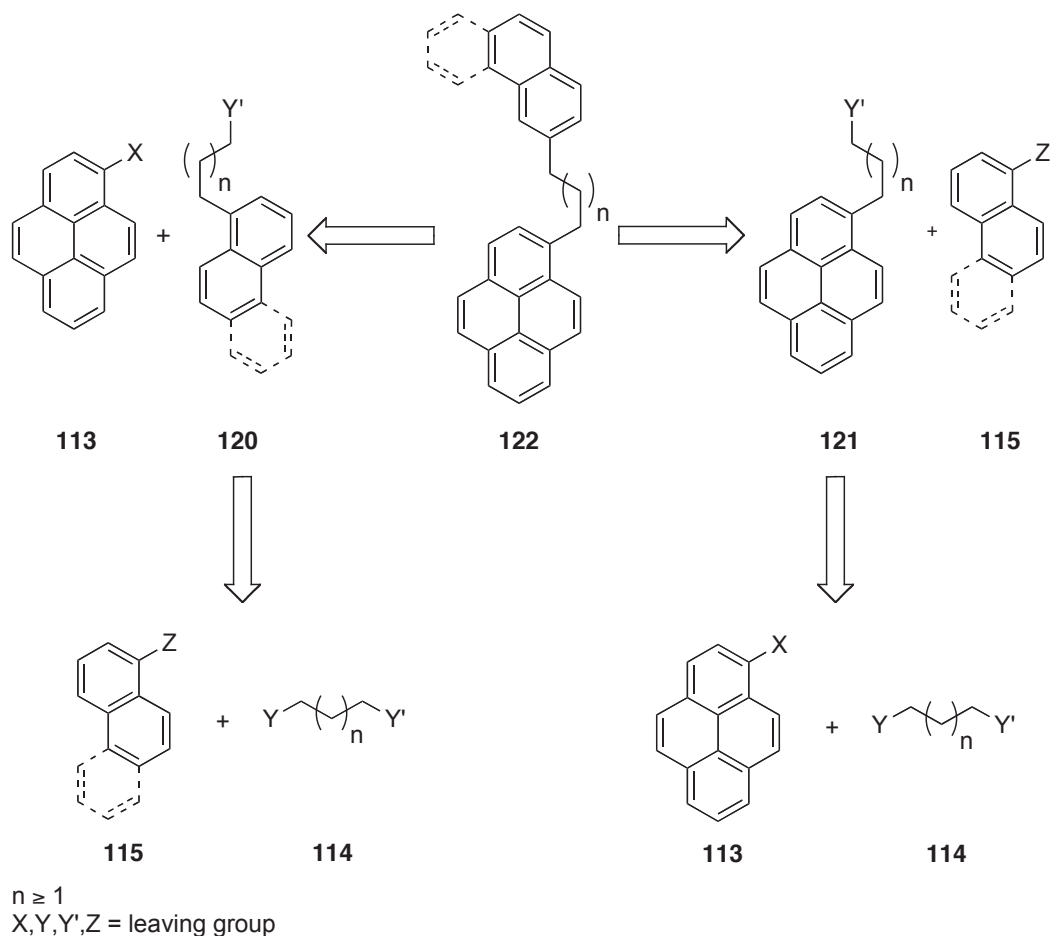
Despite this drawback, such reactions remain attractive for archipelago synthesis. Besides the expanded substrate tolerance inherent to the mild conditions, we envisioned REC methods to allow for, at minimum, the coupling of a halogenated island to a halogenated tether. One of two pathways could be used: in the first (Scheme 3.5), a “heterogeneously” bifunctional tether **116**, bearing two distinct but related terminal functionalities, is coupled to the first island *via* a REC reaction, then to a second island by a separate method. The second pathway (Scheme 3.6) involves a two-step REC procedure, utilizing the differing reactivity of a “homogeneously” bifunctional tether **114**, where Y and Y' are, for example, different leaving groups.



$n \geq 1$   
 $X, Y =$  leaving group

**Scheme 3.5** Retrosynthetic plan for archipelago synthesis 1: REC and alternate tether attachment

In the idealized case, the two-step REC coupling shown in Scheme 3.6 could be performed using the same catalytic system in a one-pot method. In this chapter are discussed several first-row transition metal-catalyzed methods exemplifying each of the above pathways, allowing for step-wise construction of variable-length alkyl tethers joining polycyclic aromatic islands.



**Scheme 3.6** Retrosynthetic plan for archipelago synthesis 2: dual REC tether attachment

### 3.2 Reductive cross-coupling of bromoarenes and haloalkanes: the cobalt-manganese system

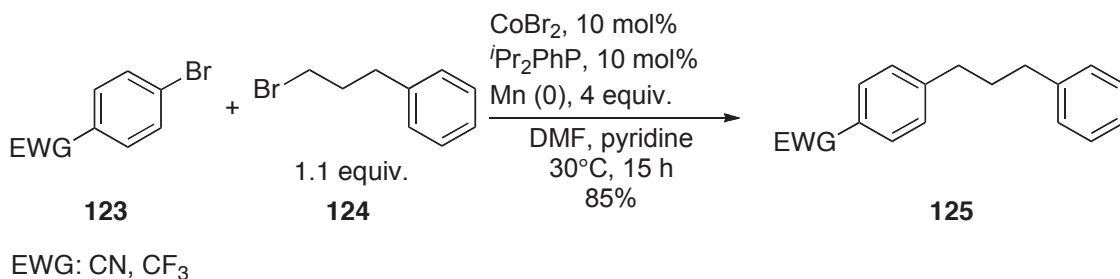
#### 3.2.1 Literature reaction: the Gosmini cobalt-manganese system

Following their success in cobalt-catalyzed biaryl cross-coupling,<sup>64</sup> Gosmini and Amatore redesigned their system for cross-coupling between alkyl bromides **124** and aryl bromides **123** (Eq. **3.1**), and for coupling aryl bromides and benzylic chlorides **126** (Eq. **3.2**) using cobalt(II) bromide as catalyst and manganese(0) as the stoichiometric reductant.<sup>65</sup>

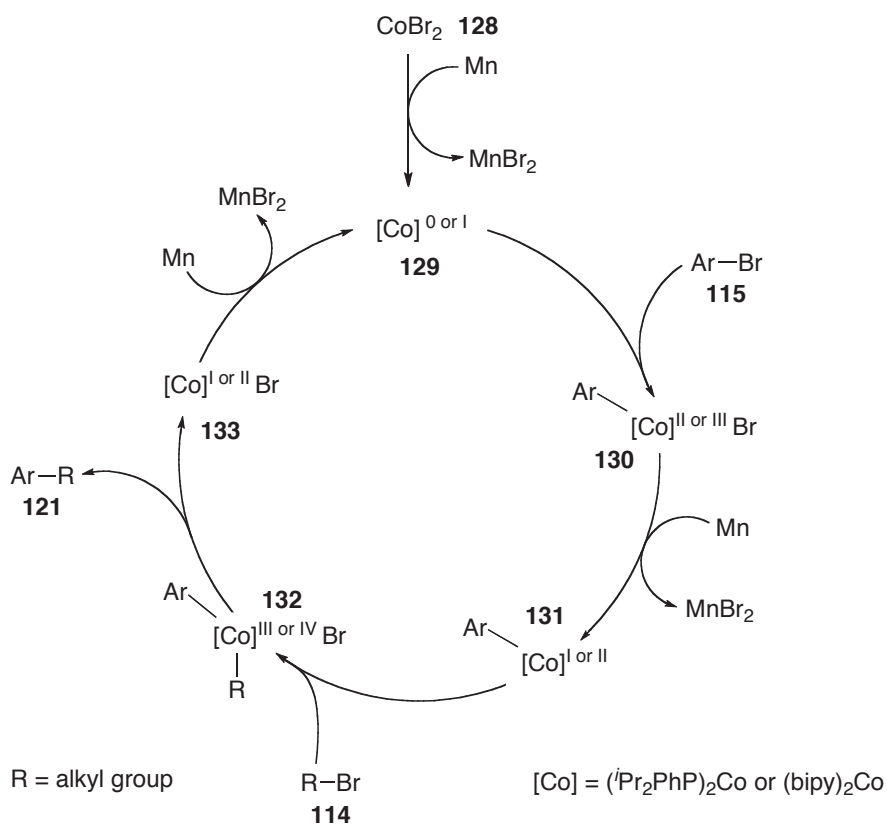
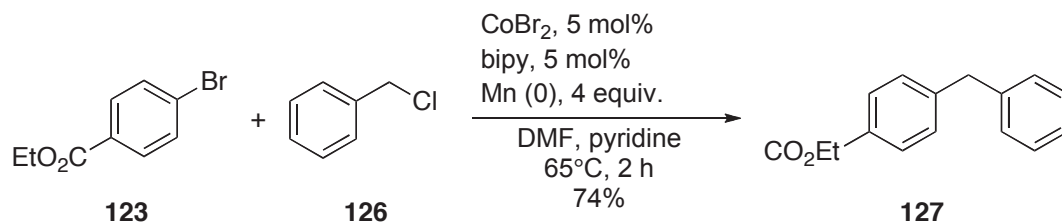
This provides a tempting method for archipelago synthesis, with the potential to successfully couple the archipelago analogues of the brominated island **115** and a brominated tether **114** (Scheme **3.6**). Of additional importance is the nature of the reducing agent, here manganese powder, which is used to maintain the low oxidation

state of the metal catalyst, as illustrated in the generalized catalytic cycle proposed by Gosmini and Amatore (Scheme 3.7). With little mechanistic investigation, the authors propose only a very general mechanism to describe the REC cycle.

**Equation 3.1**



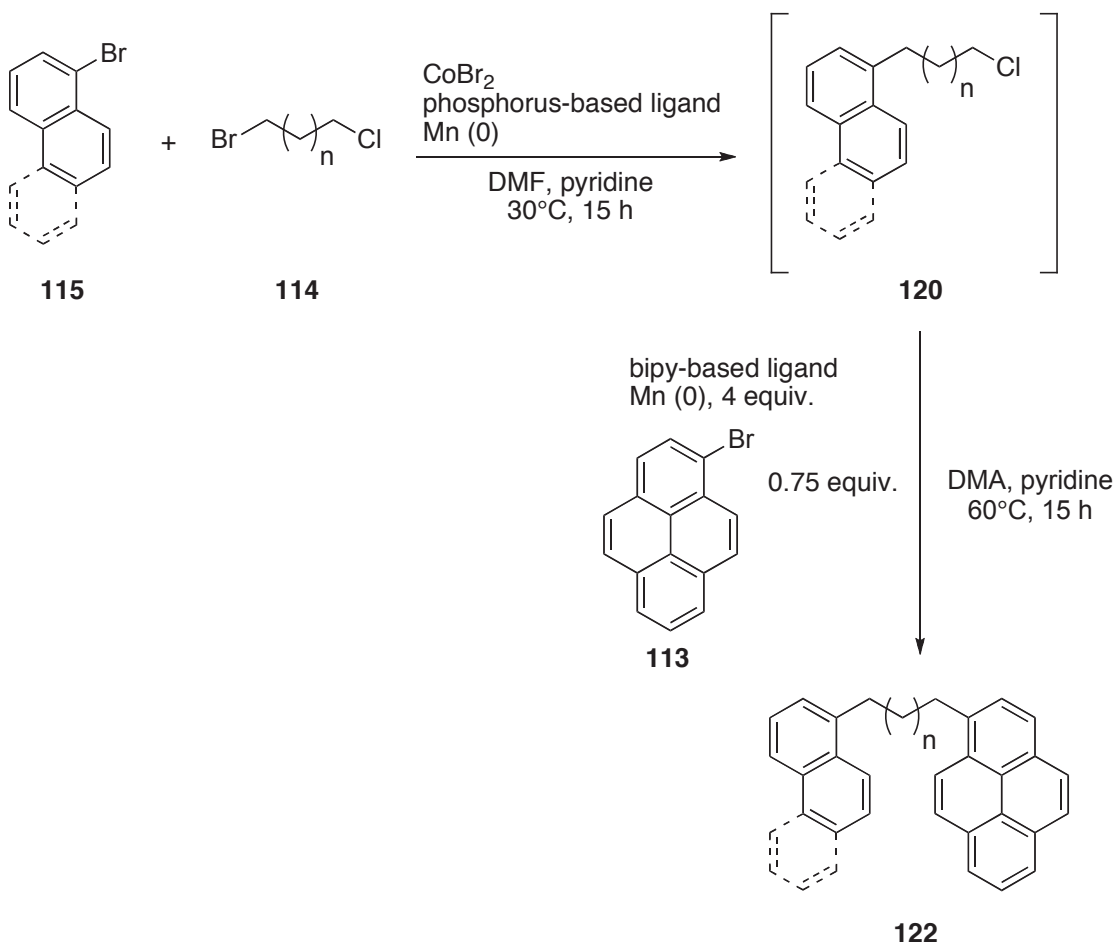
**Equation 3.2**



**Scheme 3.7** General mechanism for the Gosmini alkyl-aryl cross-coupling

### 3.2.2 Intended adaptations

Our interest in the REC system outlined by Gosmini and Amatore was specifically related to the chloride coupling (Eq. 3.2) and the difference in reaction conditions between coupling of alkyl bromides and chlorides. As the benzylic chloride example required a higher reaction temperature and 2,2'-bipyridine, rather than phosphine as the ligand, we proposed that it may be possible to execute two sequential REC reactions in the same pot (Scheme 3.3). The first aryl bromide–alkyl bromide coupling (**114** and **115**) could be achieved at low temperature in the presence of a phosphorus ligand, then a second island, bipy (or a superior ligand), and additional manganese powder would be added to the same flask, the temperature increased, and the intermediate aryl-tethered alkyl chloride **120** would couple to the second aryl bromide **137**. Used thus, the cobalt–manganese system would perform sequential REC reactions to install tethers of variable length between two model asphaltene islands.

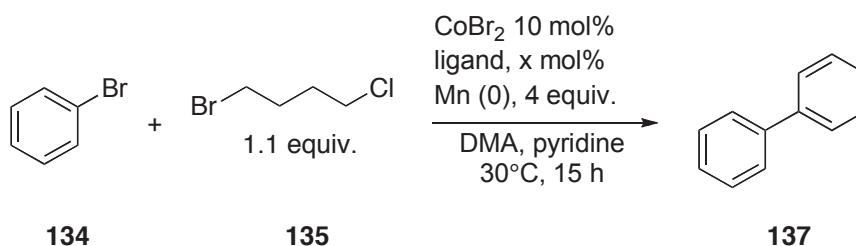


**Scheme 3.8** Proposed reaction scheme for one-pot, two-island tethering

### 3.2.3 Initial evaluation of the cobalt-manganese REC system

Bromobenzene **134** and 1-bromo-4-chlorobutane **135** were selected as model substrates, and DMA as the reaction solvent, the latter used to evaluate an alternative to DMF should higher temperatures be required for the additional chloride coupling. Pure ( $\geq 99.9\%$  trace metals basis) manganese powder was used as the reductant (Table 3.1). Unfortunately, in all cases and across all ligands tested, only biphenyl **137** was observed, resultant of a biaryl homo-coupling between two equivalents of bromobenzene.

**Table 3.1** First-round screening of the cobalt-manganese REC system



Entry	Ligand	Ligand loading (mol%)	Catalyst loading (mol%)	Manganese (equiv.)	Isolated yield ( <b>137</b> ) (%)
1	$\text{PPh}_3$	10	10	4	25
2	$\text{PPh}_3$	10	10	6	31
3	$\text{PPh}_3$	20	20	4	18
4	$\text{PCy}_3$	10	10	4	28
5 <sup>a</sup>	$\text{PPh}_3$	10	10	4	23
6 <sup>b</sup>	$\text{PPh}_3$	10	10	4	10
7 <sup>c</sup>	$\text{PPh}_4$	10	10	4	21
8 <sup>d</sup>	$\text{PPh}_4$	10	10	4	26

Reaction conditions: 2.5mmol bromobenzene, 2.75 mmol 1-bromo-4-chlorobutane, 3mL DMA, 0.5mL pyridine. <sup>a</sup>DMF substituted for DMA. <sup>b</sup>Reaction temperature lowered to  $20^\circ\text{C}$ . <sup>c</sup>2.2 equiv of 1-bromo-4-chlorobutane used. <sup>d</sup>Two equiv (100  $\mu\text{L}$ ) of trifluoroacetic acid used to activate the manganese powder.

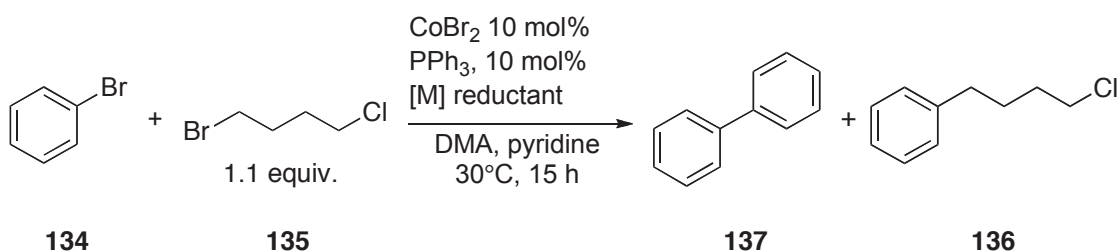
In each case, crude reaction mixtures were analyzed by TLC and  $^1\text{H}$  NMR spectroscopy, which showed incomplete conversion of bromobenzene but no 1-chloro-4-phenylbutane. Tricyclohexylphosphine ( $\text{PCy}_3$ ), which furnished the alkyl-aryl REC products in moderately high yield during the optimization studies of Gosmini and Amatore,<sup>65</sup> also failed to promote the reaction in our hands. This may be, in part, due to the reduced reactivity of our substrate; our simple bromobenzene **134** model does not have *para* electron-withdrawing groups to further activate the carbon-bromide bond.

While we anticipated this reduced activity, the complete lack of REC product, here 4-chloro-1-phenylbutane, suggests other issues with the synthetic design.

### 3.2.4 Metal studies

Deeper study of the cobalt-manganese REC system was required to determine the discrepancy with the literature. Convinced within reasonable certainty of the purity of our substrates, we set out to analyze the effects of those reagents most susceptible to variation in quality, starting with the manganese powder (Table 3.2). Several reductants were evaluated, including the use of alternate metals (Entries 2, 3, neither successful), freshly purchased manganese powder (Entry 4) and highly activated Rieke manganese, prepared in-house by an operationally modified Rieke group procedure<sup>20</sup> (Entry 5).

**Table 3.2** Variations of the reductive metal in the cobalt-manganese REC



Entry	Reductant	Biphenyl (137) (%)	4-chloro-1-phenylbutane (136) (%)
1	Mn	27	N.D.
2 <sup>a</sup>	Al	N.D.	N.D.
3	Zn	N.D.	N.D.
4 <sup>b</sup>	Mn	10	27
5 <sup>c</sup>	Mn	8	56

Reaction conditions: 2.5 mmol bromobenzene, 2.75 mmol 1-bromo-4-chlorobutane, 10 mol% CoBr<sub>2</sub>, 10 mol% PPh<sub>3</sub>, 3 mL DMA, 0.5 mL pyridine. <sup>a</sup>Aluminum foil, finely shredded. <sup>b</sup>New (previously unopened) lot of manganese powder. <sup>c</sup>Rieke manganese.<sup>66</sup> Yields reported are isolated yields

Gratifyingly, 4-chloro-1-phenylbutane **136** was obtained in an increasing yield as the activity of the manganese reductant was increased. GC-MS analysis of the first successful REC reaction (Table 3.2, entry 4) confirmed presence of 1-bromo-4-chlorobutane and no other side products associated with homo-coupling of the alkyl component. A trace impurity was noted, displaying two mass fragments of 134 and 91

m/z, which may be n-butylbenzene **138**, arising from over-reduction of the desired product by insertion into the carbon-chlorine bond. No 4-phenylbutene **139** was detected, suggesting that beta-hydride elimination is slower than reductive elimination within this catalytic cycle.

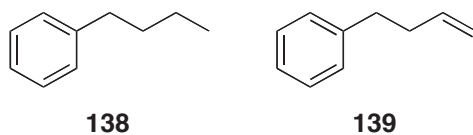
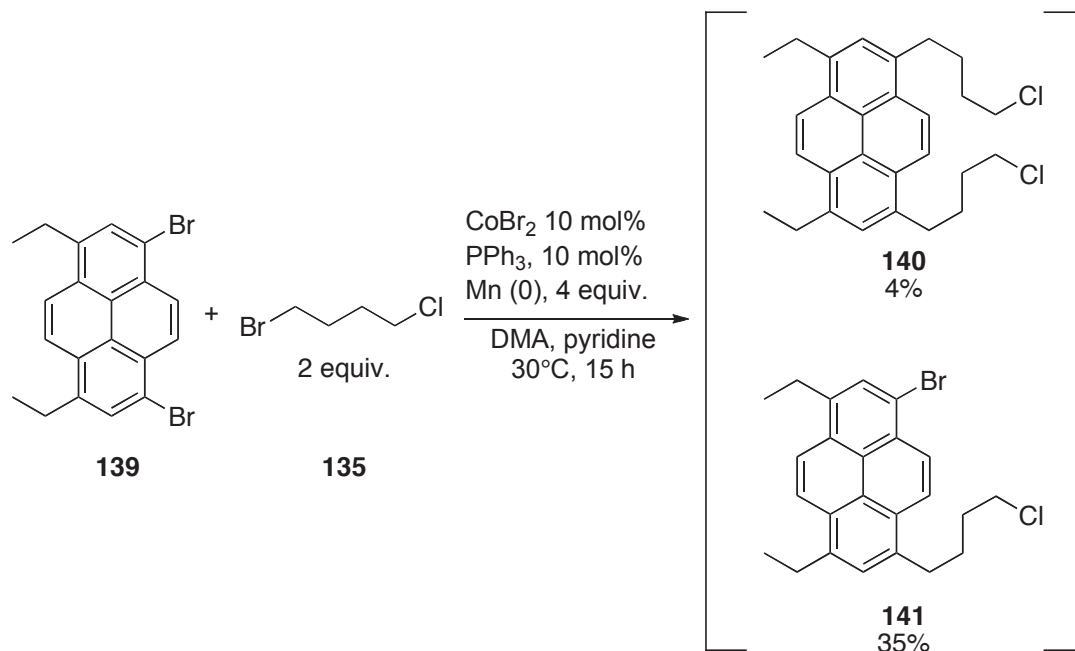


**Figure 3.1** Expected REC reaction side products

Having found a suitable reducing metal, we returned to the optimization trials only to find that the quality of the Rieke manganese powder immediately begins to degrade upon storage. Yields could not be maintained for the re-optimization of ligands and products ratios began to favour biphenyl over 4-chloro-1-phenylbutane.

**Equation 3.3**



Trial reactions using more complex model asphaltene substrates were not reproducible. 1,8-Dibromo-3,6-dimethyl pyrene **139**, synthesized by a colleague,<sup>67</sup> was coupled with 1-bromo-4-chlorobutane to obtain a 9 : 1 ratio of the mono- **140** and bis-

coupled products **141** respectively (Eq. **3.3**). When this same reaction was repeated just a week later, no cross-coupled products were observed.

While we attribute this rapid loss of REC activity to degradation of manganese powder, we have no assignable cause. No appreciable spikes in drybox atmospheric oxygen content occurred while the manganese was directly exposed. Given the inherent variability observed while using the cobalt-manganese REC system under (apparently) controlled conditions, it was our decision to pursue other routes to archipelago tether coupling.

### 3.3 Chloroalkylated island synthesis: $\alpha$ -bromo- $\omega$ -chloroalkane coupling

In addition to developing a viable pathway to tether installation, we simultaneously explored an efficient synthesis of  $\alpha$ -bromo- $\omega$ -chloroalkanes. Initial studies involved the use of 1-bromo-4-chlorobutane **135**, as this compound is commercially available. In the event that a successful REC reaction was established, we would require a range of tether lengths wider than those available commercially (Figure **3.2**) to further expand the catalogue of asphaltene models.

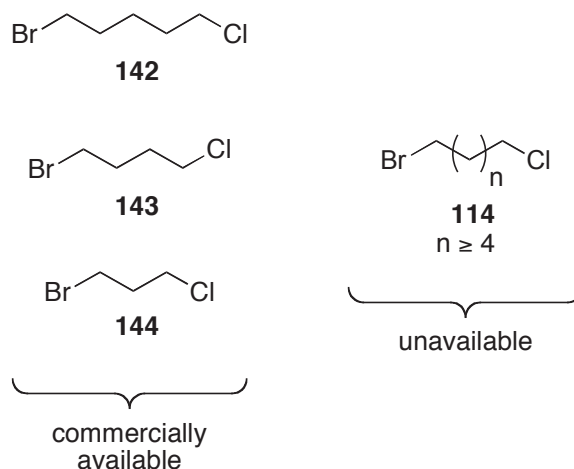
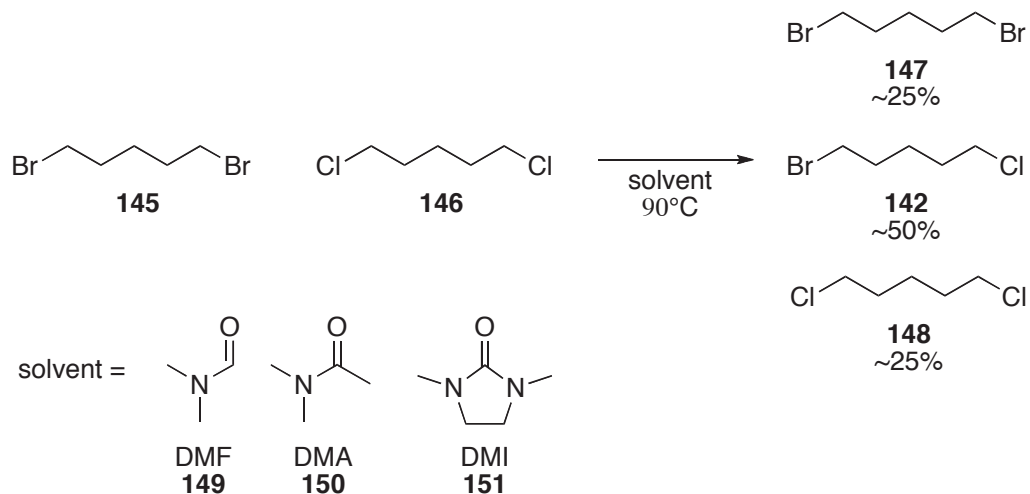


**Figure 3.2** Commercially available  $\alpha$ -bromo- $\omega$ -chloroalkanes

A patent by Takehiki, *et al.*,<sup>68</sup> claims the scalable synthesis of  $\alpha$ -bromo- $\omega$ -chloroalkanes from  $\alpha,\omega$ -dibromoalkanes and  $\alpha,\omega$ -dichloroalkanes in the presence of aprotic, polar solvents such as DMF **149**, DMA **150**, and N/N-dimethylimidazolidinone (DMI) **151** (Eq. **3.3**). It is presumed that the solvent catalysis involves nucleophilic displacement of the halogens to yield a statistical mixture of each di-homohalogenated

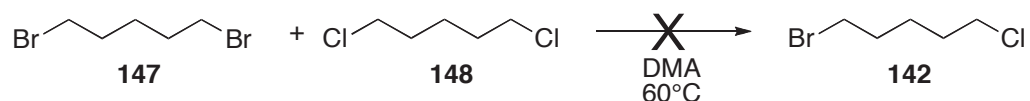
alkane, 33% each, and the heterohalogenated alkane at %66. In our hands, the reaction was performed as described, using DMA, to furnish 1-bromo-5-chloropentane **142** in a 62% following vacuum distillation.

### Equation 3.4

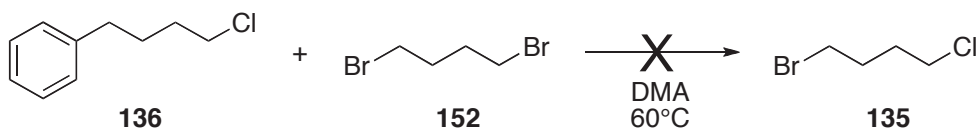


As our REC method was being evaluated in DMA and DMF, additional testing of the above synthesis (Eq. **3.3**) was required to ascertain if a similar nucleophilic exchange would be possible during our intended one-pot procedure. Reaction of the dibromo- **147** and dichloropentanes **148** at 60 °C (Eq. **3.4**), and that of 1-chloro-4-phenylbutane **136** and 1,4-dibromobutane **153** at the same temperature (Eq. **3.5**) both showed no presence of any  $\alpha$ -bromo- $\omega$ -chloroalkanes. From this, we can determine that any degradation of our product is not likely to be caused of solvent-assisted chlorine displacement.

### Equation 3.5



### Equation 3.6

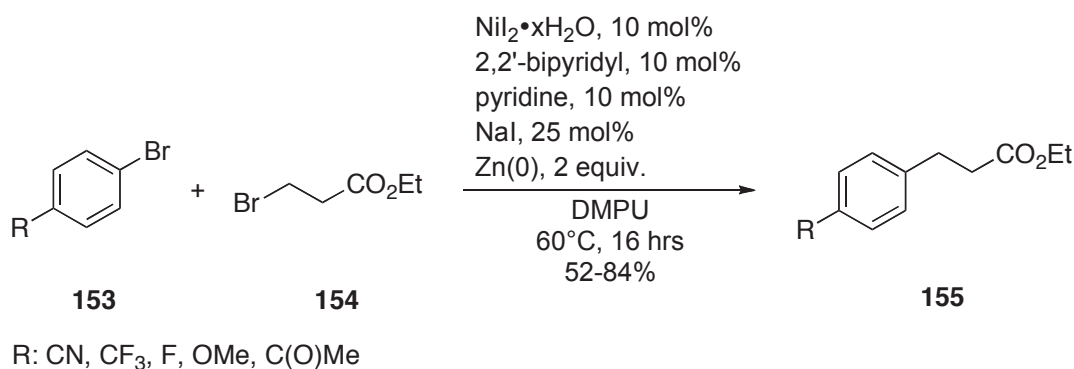


### 3.4 Reductive cross-coupling of haloarenes and bromoalkanes: the nickel-zinc system

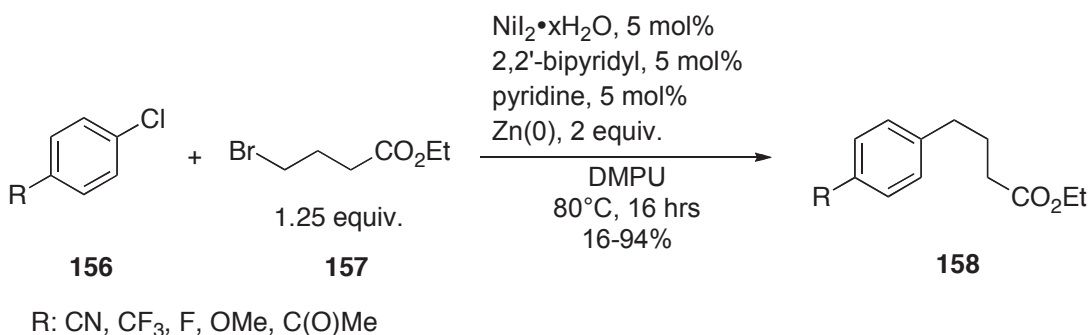
#### 3.4.1 Literature cross-coupling: the Weix nickel-zinc system

Following preliminary investigations of a novel REC method using aryl and alkyl iodides,<sup>69</sup> Weix and coworkers refined an air- and water-stable nickel-zinc REC system to couple alkyl bromides with either aryl bromides (Eq. 3.11) or aryl chlorides (Eq. 3.12).<sup>70</sup>

#### Equation 3.7



#### Equation 3.8

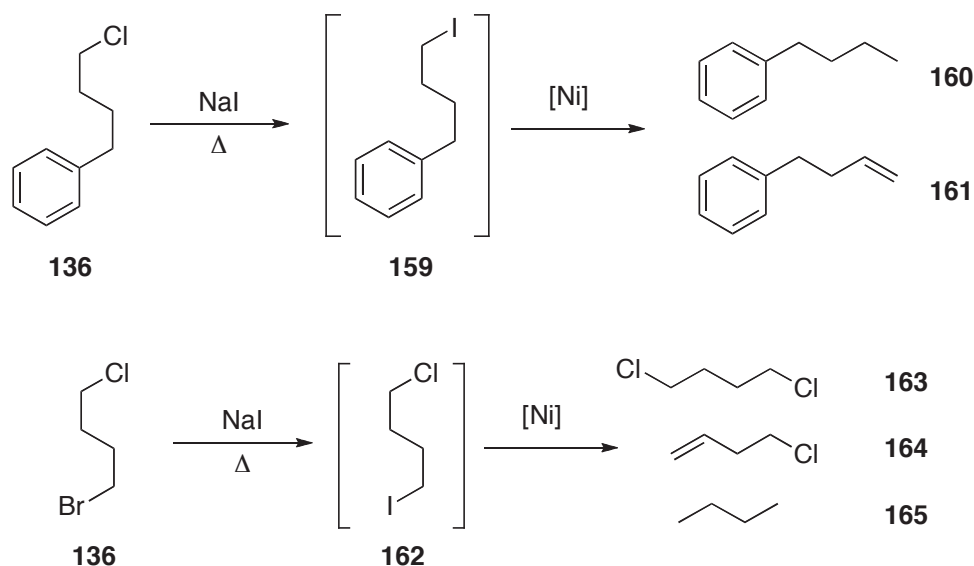


Bearing similarities to the previously studied cobalt-manganese REC system, it was our hope that this nickel-zinc variant would display greater levels of activity and robustness, and an overall decreased sensitivity to reagent quality.

#### 3.4.2 Initial evaluation of the nickel-zinc REC system

Overtly, the nickel-zinc system described by Weix stands out as an exemplary REC method: the catalyst and reductant are less prone to deactivation and

decomposition in the presence of oxygen or water, the product distributions are highly favourable for the cross-REC product, and the reaction boasts a very wide substrate scope. We thus performed initial tests using bromobenzene **134** and 1-bromo-4-chlorobutane **135** as test substrates. To begin, we selected bipy as an appropriate starting ligand, based on the Weix optimization.

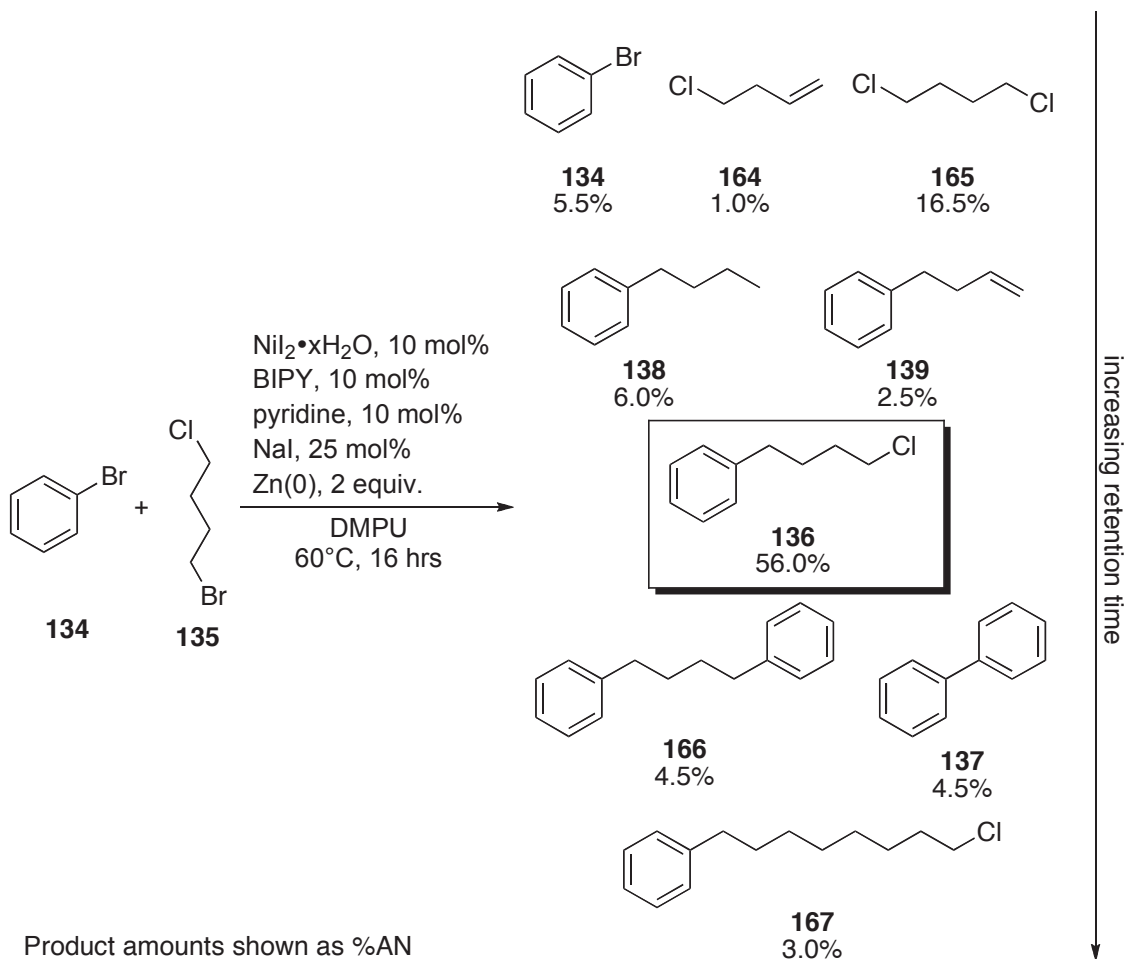


**Scheme 3.9** Potential side products of the nickel-zinc REC system.

Our primary concern, in addition to the wide range of reduction and homo-alkyl coupling side products reported by Weix and coworkers,<sup>70</sup> was the propensity for *in-situ* Finklestein reactions (Scheme 3.9). Optimized literature conditions called for 25 mol% NaI, which has the potential to displace the terminal halides on the REC product and the starting  $\alpha$ -bromo- $\omega$ -chloroalkane. This would likely lead to loss of selectivity in the coupling process.

The reaction mixture (Scheme 3.10) contained 4-chloro-1-phenylbutane **136**, our intended tethered island product in moderate yield, alongside significant number of side products. GC-MS analysis performed on the reaction mixture following removal of metals on a short Fluorisil plug, revealed the following compounds: biphenyl **137**, the result of aryl-aryl homocoupling; 1,4-diphenylbutane **166**, arising from coupling between the desired product **136** and a second equivalent of bromobenzene; 8-chloro-1-phenyloctane **167**, which results from coupling of the desired product with a second equivalent of 1-bromo-4-chlorobutane. Additional off-cycle minor products were noted,

including 4-chlorobutene **165** and 4-phenyl-1-butene **162**, both of which result from  $\beta$ -hydride elimination following insertion into the terminal C-X bond. While many of these products are descendent of our main product, arising from the degradation of our alkyl chloride, the overall amount of these products were low. Considering the ease by which the reaction could be effected, and the moderate yield of our 4-chloro-1-phenylbutane **136** obtained, we considered the reaction a significant advancement over the previous cobalt-mangansese REC system and set forth to optimize the reaction conditions for the coupling of arylbromides and  $\alpha$ -bromo- $\omega$ -chloroalkanes



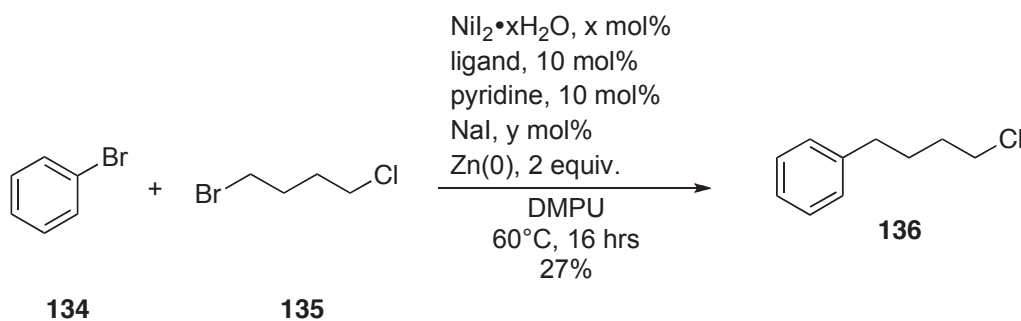
**Scheme 3.10** Initial analysis of the nickel-zinc REC system

### 3.4.3 Optimization of the nickel-zinc REC reaction

Initial screening of reaction conditions included varying the catalyst, ligand, reductant, and sodium iodide content (Table 3.3). Reducing the amount of NaI additive, first to 10 mol% (entry 2) then to zero (entry 3) improved product yields significantly.

Increased catalyst loading showed only a marginal effect on yield (entry 4), as did the use of zinc powder that had been exposed to nominal atmosphere (entry 5). The use of a chelating diphosphine ligand, here dppe (entry 6) greatly inhibited the REC cycle. Using the substituted bipy ligands on-hand, we also attempted the REC reaction with 4,4'-dimethyl-2,2'-bipyridine **168** and 2,2'-di-tert-butyl-2,2'-bipyridine **169**, but both of these ligands showed lower yields than bipy itself.

**Table 3.3** Optimization of the nickel-zinc REC catalyst for 4-chloro-1-phenylbutane



Entry	Ligand	Catalyst loading (mol%)	Sodium iodide (mol %)	Product yield (%)
1	bipy	10	25	51
2	bipy	10	10	65
3	bipy	10	0	71
4	bipy	20	25	55
5 <sup>a</sup>	bipy	10	25	49
6	dppe	10	25	5
7	4,4'-dmbipy	10	25	35
8	4,4'-dtbipy	10	25	26

Reaction conditions: 0.04 mmol ligand, 0.75 mmol bromobenzene, 0.65 mmol 1-bromo-4-chlorobutane, 1.5mmol zinc powder, 3μL pyridine, 3mL DMPU. <sup>a</sup> Aged zinc powder used

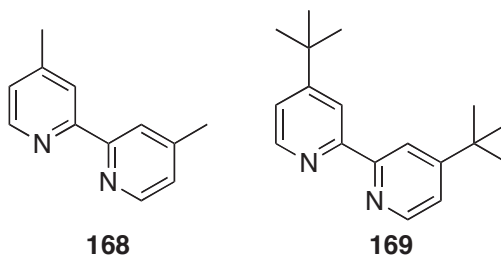


**Figure 3.3** Alternative bipyridine-based ligands 4,4'-dimethyl-2,2'-bipyridine **168** and 4,4'-di-tert-butyl-2,2'-bipyridine **169**

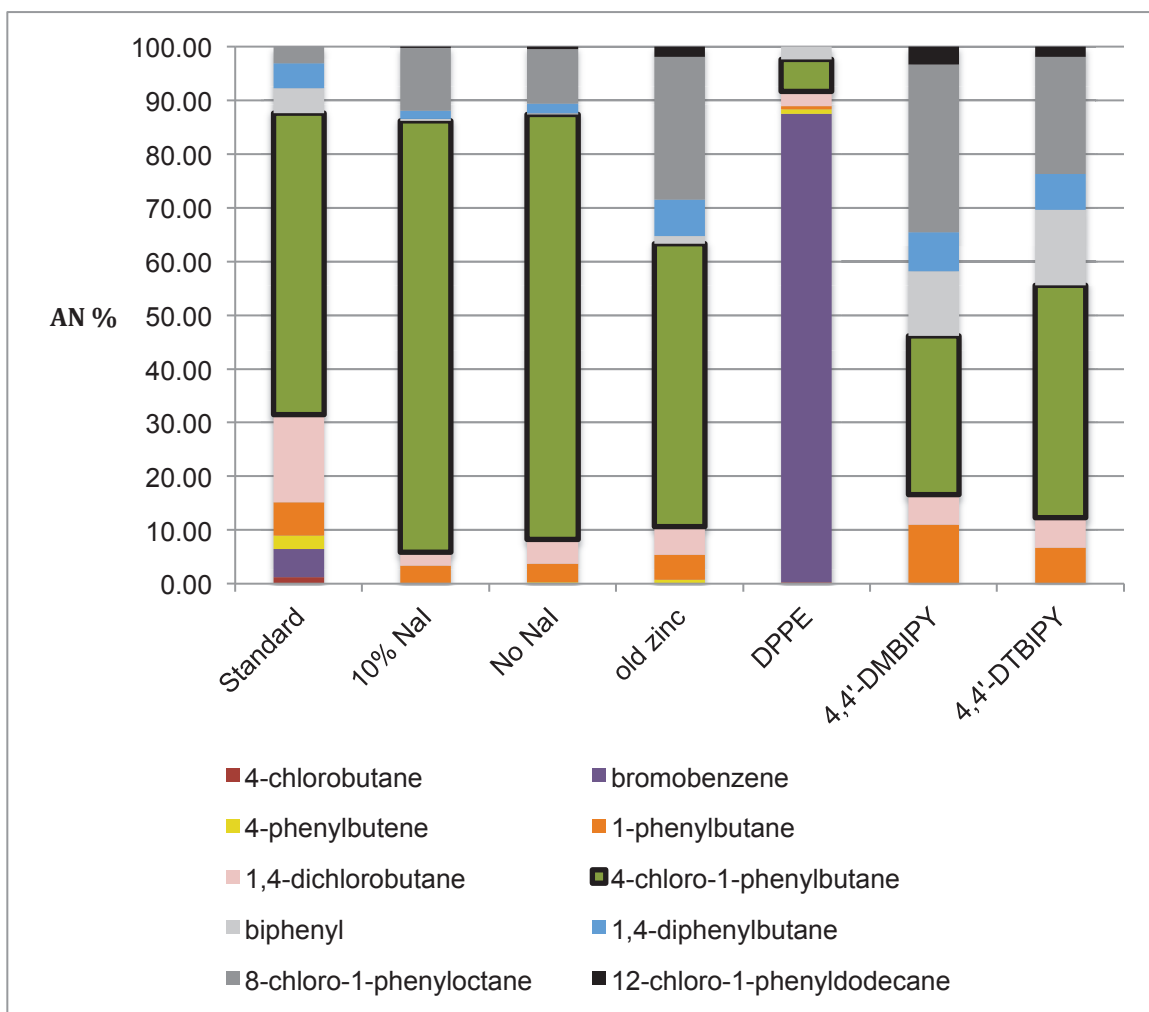


**Figure 3.4** GC-MS analysis of the nickel-zinc REC product distribution as a function of conditions (Table 3.3).

Within the ligand series, we observed an increase in the side products formed by further reaction with the intended coupling product **136**. The use of either dmbipy **168** or 4,4'-dtbipy **169** led to an increase in chain-extension products 8-chloro-1-phenyloctane **167** and 12-chloro-1-phenyldodecane (not pictured). As these two ligands also produce a higher amount of over-reduction product 4-phenylbutane **138**, these alternatives were deemed unsuitable. Phosphorus-based ligands, with dppe as an example, were tested, (entry 6, Table 3.3) and were found to be completely unsuitable for our system.

The diminishing sodium iodide loading led to a slight reduction in the chain extension products and a sizable increase in yield. Our hypothesis proved correct – sodium iodide has a deleterious effect on the nickel-zinc REC when using  $\alpha$ -bromo- $\omega$ -chloroalkanes as coupling partners.

We also attempted the REC reaction in the presence of “aged” zinc powder (Entry 5), of a similar mesh to the newly-purchased lot used for all other nickel-zinc reactions described above, but after long-term exposure to atmospheric moisture and oxygen. While the product yield was unaffected, an increase in 8-chloro-1-phenyloctane **167** production was noted. As such, all subsequent reactions used fresh zinc (40 mesh) stored in a drybox.

#### 3.4.4 Mechanism of the nickel-zinc REC reaction

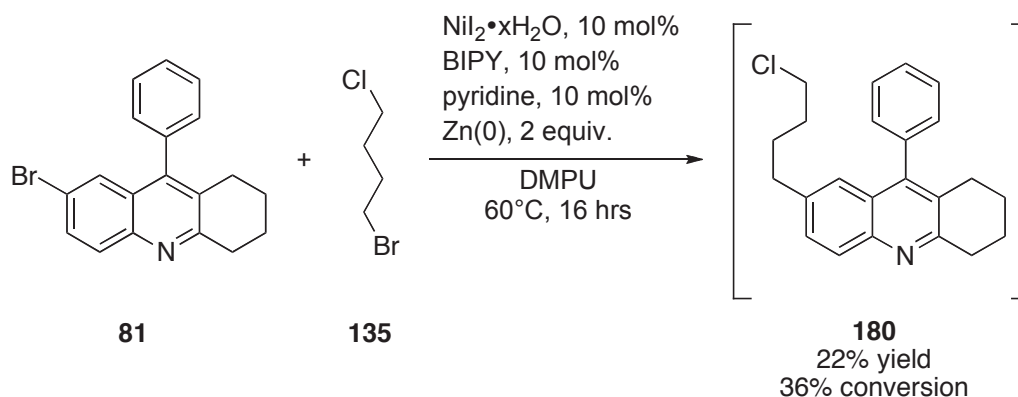
During our work to optimize the system for our needs, Weix and coworkers went on to describe in great detail studies on the nickel-zinc reaction mechanism.<sup>71</sup> In Scheme **3.11** is shown this proposal, adapted to our model substrates.

The initial formation of alkyl radical **174** is proposed to occur by an alternate initiation process. An arylnickel(II) intermediate **178**, formed *via* oxidative addition across the aryl C-Br bond, catalyzes the homolysis of the alkyl C-Br bond. Subsequent reaction of this radical (**174**) and a second nickel(II) adduct would drive the cycle forward to the formation of the disubstituted aryl(alkyl)nickel(III) intermediate **172**, from which the product is formed by reductive elimination, giving Ni(I) intermediate **173**.<sup>70,71</sup>

The key points of the Weix group investigations are as follows: (1) Ni(0), in the presence of bipy, reacts selectively with an aryl iodide over an alkyl iodide; (2) reactions using stoichiometric amounts of the arylnickel(II) intermediate **171** (as expected from oxidative addition) and alkyl iodides form the intended REC product, without the use of reductant; (3) reactions using pre-formed arylnickel(II) and alkylnickel(II) as reactants do not produce the REC product; and finally, (4) that an alkyl radical, whose concentration is directly proportional to the catalyst loading, participates in the reaction.<sup>71</sup>



### Equation 3.9



REC conversions were greatly reduced in the application to our islands, almost by half of that previously observed, and the yields of the tethered island products were low. The reaction time could not be further extended; though this may have brought the reaction closer to completion, further exposure of our product to the reaction conditions would have reduced yields in the formation of chain-extension byproducts **181**. These compounds were observed *via*  $^1\text{H}$  NMR spectroscopy as an increased abundance of alkyl region signals; no comparative GC-MS study could be obtained for these large molecules. Our product was isolated by arduous recrystallization, during which the vast majority of the 7-bromo-9-phenyl-1,2,3,4-tetrahydroacridine **81** starting material was recovered (64%). Despite repeated attempts, the tethered acridine **180** could not be completely isolated from its chain-extension side products **181**. Though low-yielding the reaction was successful in applying a four carbon tether to our phenylquinoline island.

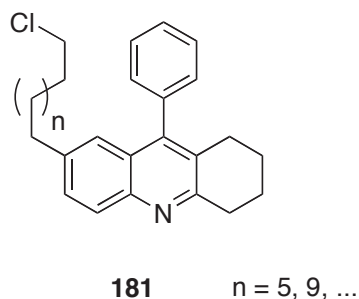
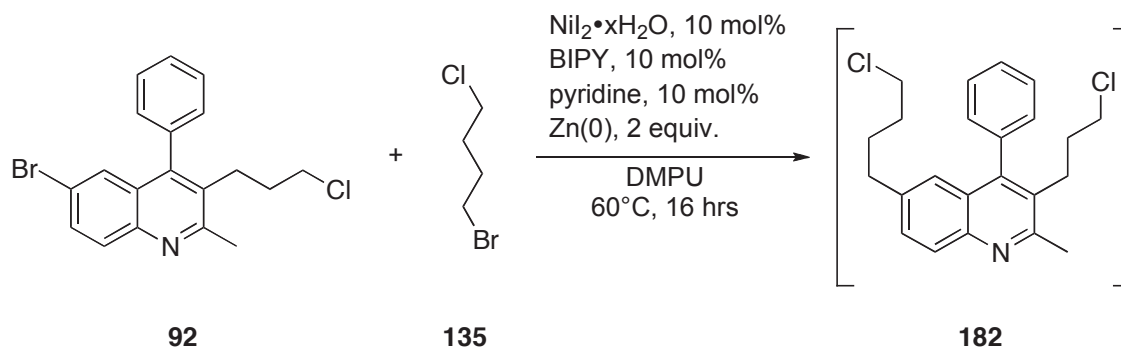


**Figure 3.5** Nitrogenous asphaltene mimic chain-extension products

### Equation 3.10



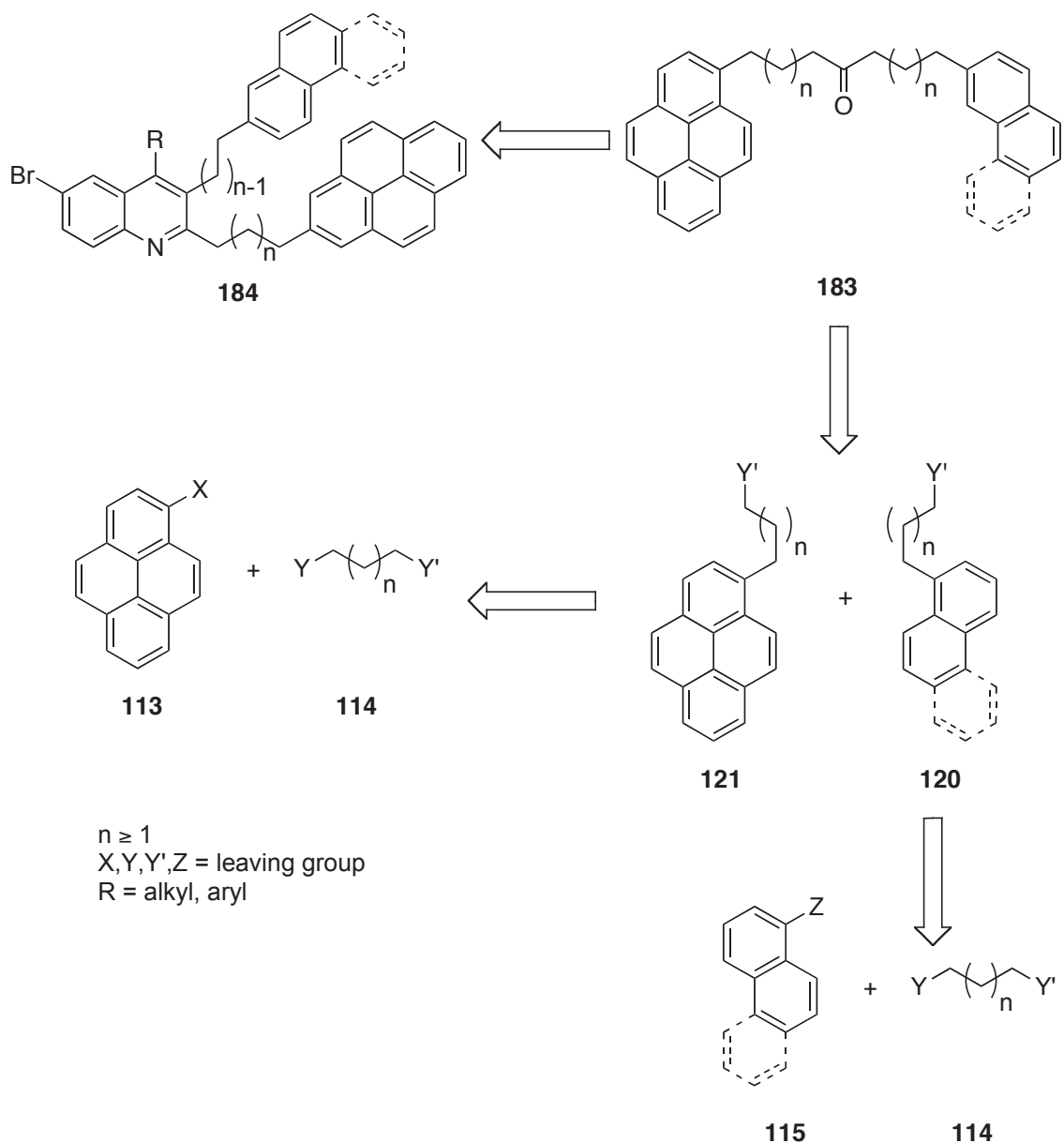
Using 6-bromo-3-(3-chloropropyl)-2-methyl-4-phenylquinoline **92**, selected to generate unsymmetrical, double-tethered islands (Eq. **3.11**). An isolated yield could not be determined for this reaction, as we were unable effectively separate the adduct from its chain-extended isomers (not pictured). Off-cycle chain-extension of the additional alkyl chloride, coupled with the already low conversions observed, reduces the overall crude yield of **182** to less than 15%.

Thus, while the nickel-zinc REC system proved capable of installing  $\alpha$ -bromo- $\omega$ -chloroalkanes on simple aromatic systems, significant rework is required before the reaction can be applied to the synthesis of basic nitrogen polycyclic aromatics.

## 3.5 Synthesis of Nitrogenous Archipelago Cores

### 3.5.1 Introduction

With efforts towards dual REC methods momentarily halted, we turned to a new strategy for tether attachment and archipelago synthesis. In similar vein to earlier discussions (Scheme **3.5**), we envisioned that the  $\omega$ -chloroalkyl intermediates could be used to synthesize long-chain ketone substrates for use in the optimized Wu-Friedländer reaction (Scheme **3.12**). To add an additional point of variability we set out to synthesize  $\omega, \omega'$ -di(aryl)ketones **183**.



**Scheme 3.12** Retrosynthetic plan for the Friedländer synthesis of archipelago model asphaltenes

### 3.5.2 Dialkylketones by carbonylation – Collman's Reagent

Iron carbonyls, particularly iron pentacarbonyl **185**, have been explored as catalysts for carbon-carbon bond formation since it was discovered in 1891, by both Berthelot<sup>72</sup> and Mond.<sup>73</sup> Given its toxicity and volatile liquid state, alternative reactive iron complexes have since been developed. One of the more popular methods is by use of disodium tetracarbonylferrate **186**, which is obtained as a dioxane complex and commonly referred to as Collman's reagent.<sup>74</sup>

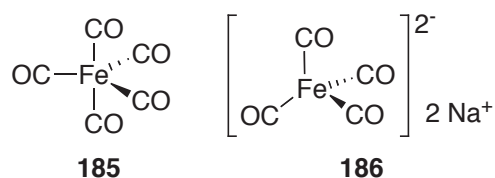
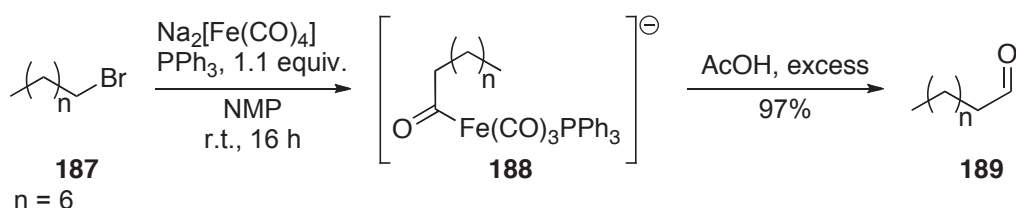


**Figure 3.6** Iron carbonyl complexes

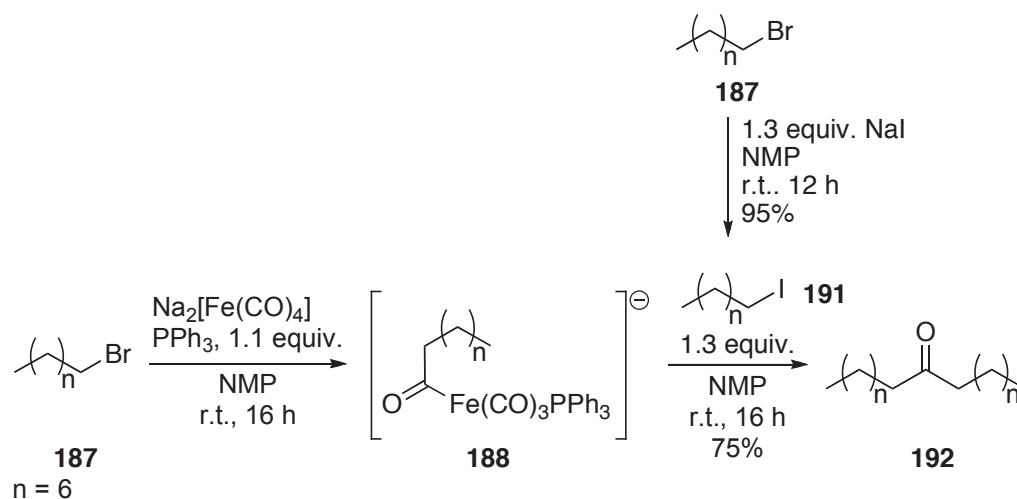
Using the tested literature procedure,<sup>75</sup> we synthesized Collman's reagent **186** on gram scale. As the purity of the reagent could not be determined conventionally, due to its high reactivity, we instead determined purity indirectly, by efficacy. Thus, *n*-bromooctane **187** was cleanly carbonylated to afford nonenal **189** in high yield (Scheme 3.13). From this result, we determined our synthesis of Collman's reagent successful.



**Scheme 3.13** Determination of the purity of Collman's Reagent; synthesis of nonenal

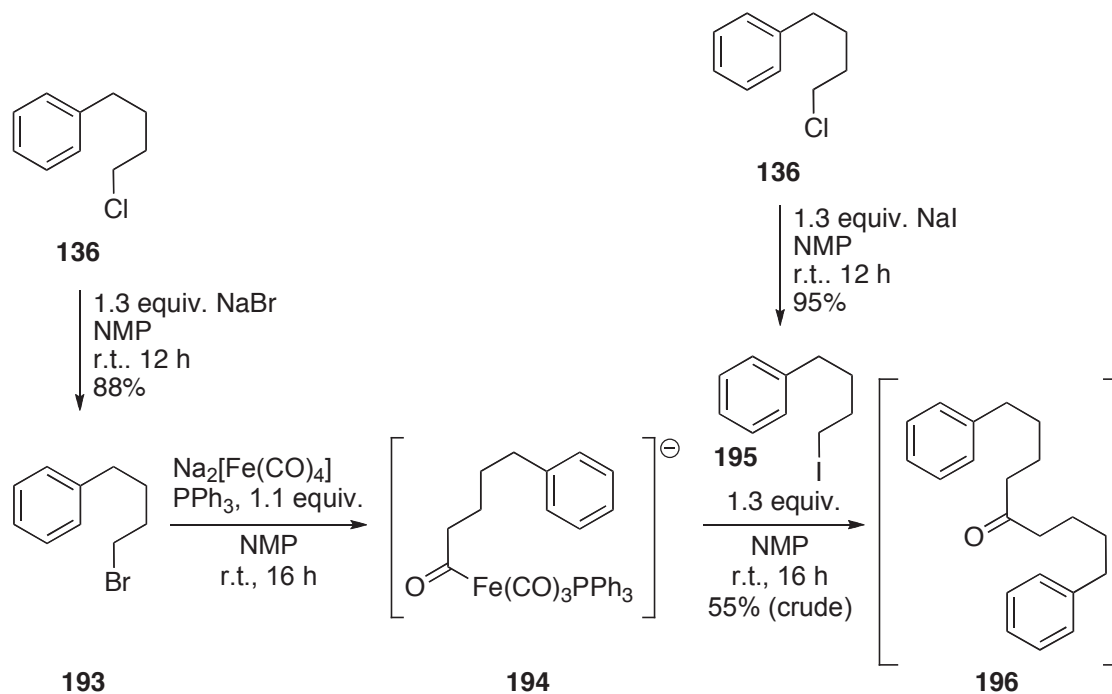
### 3.5.3 Towards the synthesis of symmetrical ketones – simple archipelago synthesis

As a proof of concept, we then set out to synthesize the symmetrical ketone from the intermediate acyliron complex **188**. Anticipating low reactivity of this complex, a Finkelstein reaction was performed on *n*-bromooctane **187** to generate the more reactive iodide **191**. The conversion, effected at room temperature in NMP with excess sodium iodide, was monitored by <sup>1</sup>H NMR spectroscopy. Once complete, the reaction mixture was filtered through Celite and added to complex **188**, which had been concurrently prepared. Yields were slightly diminished, but heptadecan-9-one **192** was successfully synthesized.



**Scheme 3.14** Generic symmetrical ketone synthesis

Encouraged by this result, we attempted a similar synthesis using 4-chloro-1-phenylbutane **136**. As above, a Finklestein reaction was performed on both equivalents of the chloride to generate 4-bromo-1-phenylbutane **193**, for the initial acylation step, and 4-iodo-1-phenylbutane **194**, for the second addition.



**Scheme 3.15** Synthesis of bis-tethered symmetrical ketones

The symmetrical, bis-tethered ketone **196** presented as a fine white powder, which began precipitating from solution almost immediately following the addition of

iodide **195**. Unfortunately, this compound was lost during isolation. Due to time constraints, the synthesis was not repeated.

### **3.6 Conclusions**

Two REC catalyst systems have been evaluated for use as general methods for archipelago tether installation. The first, a cobalt-manganese system, proved too unstable for reproducible applications; the second, however, displayed good applicability, specifically towards the selective coupling with the difficult  $\alpha$ -bromo- $\omega$ -chloroalkanes. Using this second method, we successfully synthesized  $\omega$ -chloro tethered islands. Introductory work towards bis-tethered ketone synthesis has also been explored and shown to be a viable means of ketone synthesis.

## 4 Concluding Remarks

The work conducted herein has described improved methodology for the synthesis of diverse, alkylated quinolines by two refined syntheses, has demonstrated the application of reductive, cross-electrophile coupling to install alkyl tethers on polyaromatic scaffolds, and has outlined preliminary investigations towards the synthesis of symmetrical ketones.

The Hua domino reaction was optimized to gram scale and refined to furnish the 4-methyl-2phenylquinoline products without the necessity of chromatography. Brief substrate exploration determined that alkyl chain extension inhibits this reaction. A further quinoline synthesis, the Wu-Friedländer reaction, was also optimized to gram scale bereft of chromatography. A wide range of ketones was used to provide 4-phenylquinolines of increased diversity, appropriate carbon-hydrogen ratios, and improved solubility. This reaction was adapted to the more appropriate yet problematic 2'-aminoacetophenone **102** substrate. Future research with the Wu-Friedländer should be focused on the adaptation of the synthesis to aldehydes, as well as pre-tethered substrates.

The cobalt-manganese REC reaction was evaluated and found to be too sensitive for our needs. Thus a second REC reaction was employed, using nickel and zinc, to install  $\omega$ -chloro alkyl tethers on both simple aromatics and our Wu-Friedländer 4-phenylquinolines. Further research is required to improve conversion for nitrogenous aromatic substrates. Additional work may be desired to determine conditions appropriate for the synthesis of the chain-extension products.

Work towards the synthesis of symmetrical ketones has shown Collman's reagent to be a suitable means of obtaining compounds with long alkyl tethers. While only initial efforts have been made, one example has been provided for a simple bis-tethered island ketone, suggesting a wide array of these compounds may be attainable. Research into catalytic methodology may further improve this synthesis.

## 5 Experimental Section

### 5.1 General Procedure

All air-sensitive experimental procedures were performed using either standard Schlenk techniques on a vacuum/nitrogen double manifold or in an MBraun Labmaster SP inert atmosphere glovebox under nitrogen at oxygen levels less than 5 parts per millions (ppm), as measured by a Teledyne lead-based fuel cell sensor. All material was transferred to the glovebox sealed, when at high purity under dry, inert conditions, or in open vials covered with Kimwipes; three vacuum-nitrogen cycles were employed within the antechamber to degas all material and ensure maximum dryness. All glassware was oven dried at 150 °C for a minimum of thirty minutes prior to transfer to the glovebox antechamber.

Sealed reactions were carried out in *reaction bombs*, medium-walled cylindrical glass vessels fitted with Kontes Teflon high-vacuum stopcocks and ground glass sidearms.

All reactions were carried out over IKA RTC Basic stir plates. Reactions performed at elevated temperatures were achieved as required by heating heavy mineral oil (20 °C – 90 °C) or heavy silicon oil (20 °C – 300 °C). Glassware employed for Schlenk use was dried either by natural gas flame or for a minimum three hours exposure to a 150 °C oven prior to being assembled and placed under nitrogen while still warm. All stirbars used were Teflon coated unless otherwise stated.

### 5.2 Instrumental Analyses

GC-MS and elemental analysis were conducted by Wayne Moffatt and the staff of the Department of Chemistry Instrumentation Laboratory; GC-MS samples were submitted in 9 mm clear borosilicate glass vials sealed with PTFE/silicon septa, and injected into a Hewlett Packard 5890 MSD with a G1800A GC-MS. An Agilent & JW DB-MS column was used, 25 m x 0.25 mm I.D., 0.25 µm film thickness, and a split liner packed with deactivated glass wool was used for all injections. General GC parameters were as follows: helium gas, split flow, 1.0 mL/min, injector and detector port temperatures both set to 280 °C. The GC oven was programmed to 50 °C for two minutes, then ramped at 10 °C/min to 280°C and held for two minutes. All GC-MS spectral analyses were performed on Chemstation version 1.3.

Samples for CHNS elemental analyses were submitted in clear borosilicate glass vials with polyethylene caps and analyzed using a Carlo Erba EA1108 Elemental Analyzer.

Mass spectrometry was conducted by department technical staff, and all samples were submitted in standard clear borosilicate glass vials with polyethylene caps. Samples were analyzed on an Agilent Technologies 6220 aoTOF spectrometer for high-resolution electrospray ionization, and a Kratos Analytical MS-50 spectrometer for high resolution electron impact.

$^1\text{H}$  and  $^{13}\text{C}$  NMR spectra were obtained using the following spectrometers: Agilent/Varian Inova 300 MHz, Agilent/Varian Inova 400 MHz, Agilent/Varian Mercury 400 MHz (with robotic autosampler) and Agilent/Varian VNMR5 500 MHz dual cold-probe (with robotic autosampler). All NMR chemical shifts are reported in parts per million (ppm,  $\delta$ ) relative to tetramethylsilane.

### 5.3 Chemical Materials Used

All standard solvents were purchased from the Department of Chemistry stores and dried, and distilled, and deoxygenated prior to use using sodium/benzophenone ketyl (tetrahydrofuran, diethyl ether, benzene), potassium/benzophenone ketyl (hexane, pentane), sodium (toluene) or calcium hydride (acetonitrile, dichloromethane), each under nitrogen.

All reagents and specialty solvents were purchased from Sigma-Aldrich, Fluka, Alfa Aesar, Strem, or VWR, and used as received from each supplier unless otherwise noted. Further purification, when required, was accomplished following standard procedures.<sup>31</sup>

Purified solvents and reagents were stored according to sensitivity; air- and/or moisture-sensitive material was stored under inert atmosphere in medium-walled cylindrical glass storage vessels fitted with with Kontes Teflon high-vacuum stopcocks and ground glass sidearms. Light-sensitive materials, when stored in clear vials or jars, were surrounded by sleeve of aluminum foil. Temperature-sensitive materials were stored as required, within at  $-10\text{ }^\circ\text{C}$  in a standard freezer,  $-30\text{ }^\circ\text{C}$  in the glovebox freezer, or at  $-80\text{ }^\circ\text{C}$  in a cryofreezer.

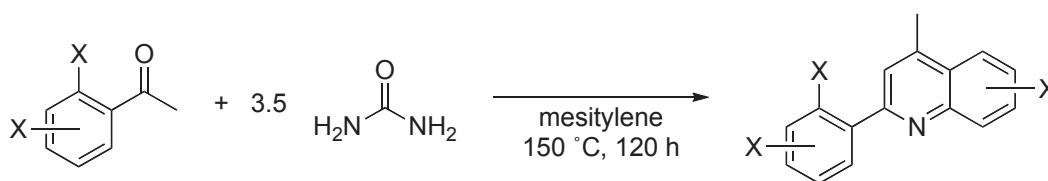
Tetra-*n*-butylammonium tribromide **79**,<sup>52</sup> 1-(2-bromophenyl)propan-1-one **66**,<sup>56</sup> 9-methyl-1,2,3,4-tetrahydroacridine **96**,<sup>76</sup> 1-(2-amino-5-bromophenyl)ethanone **107**,<sup>78</sup> Reike manganese,<sup>66</sup> 1-bromo-5-chloropentane **142**,<sup>68</sup> disodium tetracarboxylferrate

dioxane complex **186**,<sup>75</sup> and nonenal **189**<sup>77</sup> were all prepared according to literature procedures.

## 5.4 Synthetic Procedures

### 5.4.1 General procedure for the condensation of *ortho*-haloacetophenones

The following procedure was used to synthesize halophenyl-4-methylquinolines using the Hua haloacetophenone domino reaction. Specific details for each substrate are listed below under their individual headings.



X = Br, Cl

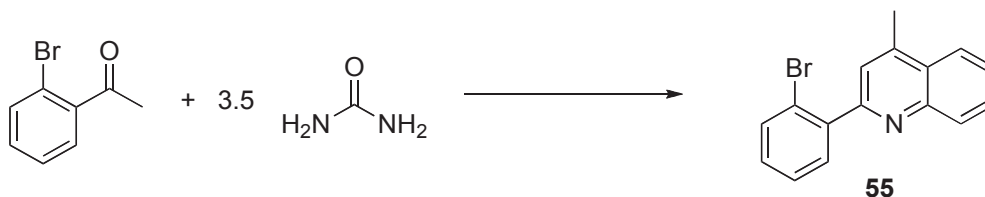
A three-neck, 100 mL round-bottom flask was fitted with a one-inch stir bar and charged with *ortho*-haloacetophenone (0.126 mmol), urea (22.0 g, 0.377 mmol) and mesitylene (28 mL). Each reagent was used as purchased with no additional drying. One of the side ports was sealed with a glass stopper, the other with a thermometer adapter and mercury thermometer, and the central neck was fitted with a Liebig condenser. The flask was set to stir and heated to 150°C over a silicon oil bath.

Reaction progress was monitored by TLC, 5:1 hexanes:ethyl acetate, and was deemed complete after 120 hours. During this time, urea may sublime and collect around the condenser tube; this light solid can be removed back into solution using a glass stir rod. After the flask had cooled to room temperature with vigorous stirring, the mesitylene was decanted off of the tan solid into a 250mL round-bottomed flask. 20mL DCM was added to the three-neck flask and the solids crushed into a fine powder. The flask was allowed to stir for ten minutes before the urea solids were filtered off.

After adding the DCM extract to the reaction liquors, all solvent was removed *via* vacuum on a Schlenk line. Gentle heating over a warm water bath was employed once DCM had been fully removed. Upon drying, an yellow-orange solid precipitated out. The solid was dissolved in a minimal amount of hot isopropanol before cooling to room temperature. To ensure complete crystallization, the solution was cooled to -30°C for

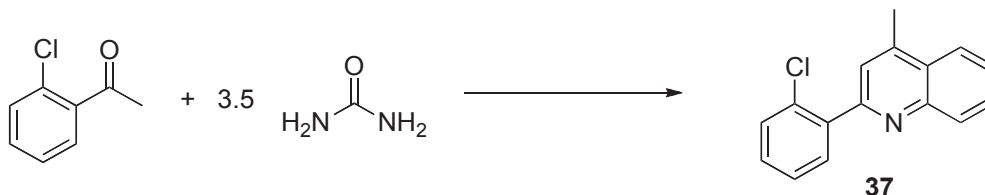
thirty minutes before collecting the crystals by suction. Darkening crystal colour (from yellow to light brown) is a general indicator of increasing entrained *ortho*-haloacetophenone content. Serial recrystallization was required for maximum purity; two recrystallizations were sufficient for general purity.

### 2-(2-bromophenyl)-4-methylquinoline **55**



General procedure 5.4.1 was followed. 2-(2'-bromophenyl)-4-methylquinoline **55** was obtained in 81% yield (30.43 g) and crystallized as short, translucent, pale yellow rods following the second recrystallization in minimal, hot isopropanol. <sup>1</sup>H NMR (500 MHz, CDCl<sub>3</sub>): δ 8.21 (d, *J* = 0.5 Hz, 1H), 8.07 (d, *J* = 0.5 Hz, 1H), 7.77 (ddd, *J* = 8.5, 7.1, 1.6 Hz; 1H), 7.73 (dd, *J* = 8.2, 1.1 Hz; 1H), 7.65 (d, 1.0 Hz), 7.63-7.60 (m, 2H), 7.47 (ddd, *J* = 7.6, 7.5, 1.1 Hz; 1H), 7.32 (ddd, 8.2, 7.3, 1.9 Hz; 1H), 2.79 (s, 3H). <sup>13</sup>C APT NMR (125 MHz, CDCl<sub>3</sub>): δ 158.5 (+), 147.8 (+), 141.9 (+), 133.2 (-), 131.5 (-), 130.3 (-), 129.9 (-), 127.6 (-), 127.2 (+), 126.5 (-), 125.7 (+), 123.7 (-), 123.3 (-), 121.9 (+), 18.9 (+). **ESI-MS** *m/z* calculated for C<sub>12</sub>H<sub>16</sub><sup>79</sup>BrN (M<sup>+</sup>) 297.0153; found: 297.0159. **Elemental analysis** calculated for C<sub>12</sub>H<sub>16</sub>BrN: C, 64.45%; H, 4.06%; N, 4.70%; found: C, 64.60%; H, 4.13%; N, 4.65%

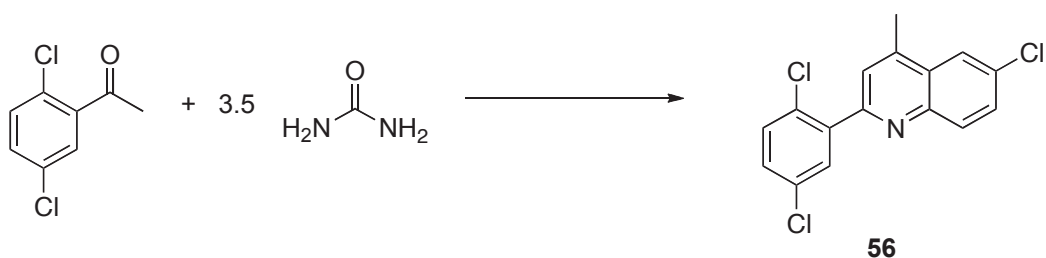
### 2-(2-chlorophenyl)-4-methylquinoline **37**



General procedure 5.4.1 was followed. 2-(2'-chlorophenyl)-4-methylquinoline was obtained in 89% yield (28.45 g) and crystallized as large, bright yellow rods after

recrystallization in minimal, hot isopropanol. **<sup>1</sup>H NMR** (400 MHz, CDCl<sub>3</sub>): δ 8.18 (d, *J* = 6.8 Hz, 1H), 8.05 (d, *J* = 6.9 Hz, 1H), 7.74 (m, 1H), 7.67 (dd, *J* = 6.8, 1.2 Hz, 1H), 7.61 (m, 1H), 7.57 (s, 1H), 7.51 (dd, *J* = 6.8, 1.2 Hz, 1H), 7.38 (m, 1H), 2.74 (s, 3H). **<sup>13</sup>C NMR** (100 MHz, CDCl<sub>3</sub>): δ 127.5, 146.2, 143.7, 139.6, 132.2, 131.4, 130.2, 130.0, 139.9, 127.3, 126.4, 123.5, 123.2, 18.5. **EI-MS** *m/z* calculated for C<sub>16</sub>H<sub>12</sub><sup>35</sup>ClN (M<sup>+</sup>) 253.0658; found: 253.0671 **Elemental analysis** calculated for C<sub>16</sub>H<sub>12</sub>ClN: C, 75.74%; H, 4.77%; N, 5.52%; found C, 75.85%; H, 4.82%; N, 5.39%.

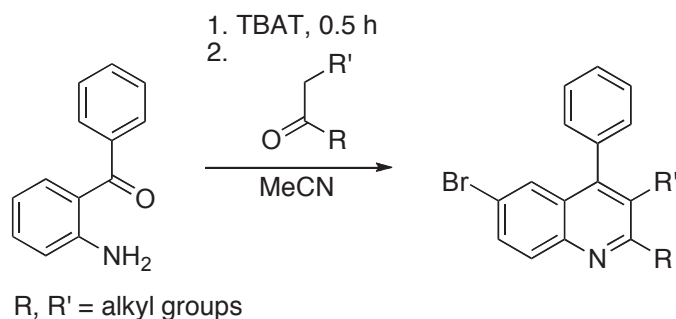
### 6-chloro-2-(2,5-dichlorophenyl)-4-methylquinoline 46



General procedure 5.4.1 was followed. 6-chloro-2-(2',5'-chlorophenyl)-4-methylquinoline was obtained in 86% yield (34.96 g) and is obtained as a pale tan powder following recrystallization in minimal, hot isopropanol. **<sup>1</sup>H NMR** (400 MHz, CDCl<sub>3</sub>): δ 8.10 (d, *J* = 7.0 Hz, 1H), 8.19 (d, *J* = 1.1 Hz, 1H), 7.68 (m, 1H), 7.58 (s, 1H), 7.44 (d, *J* = 7.1 Hz, 1H), 7.35 (dd, *J* = 7.1, 1.1 Hz, 1H), 2.76 (s, 3H). **<sup>13</sup>C NMR** (**<sup>13</sup>C NMR** (100 MHz, CDCl<sub>3</sub>): δ 157.4, 146.6, 143.9, 140.4, 133.6, 133.3, 132.4, 132.2, 132.1, 131.3, 131.1, 130.5, 128.6, 124.3, 123.6. **Elemental analysis** calculated for C<sub>16</sub>H<sub>10</sub>Cl<sub>3</sub>N: C, 59.57%; H, 3.12%; N, 4.34%; found C, 59.66%; H, 3.19%; N, 4.20%.

#### 5.4.2 General procedure for TBAT-catalyzed Wu-Friedländer condensations

The following procedure was used to synthesize 4-phenylquinolines using the Wu-Friedländer reaction. Specific details for each substrate are listed below under their individual headings.



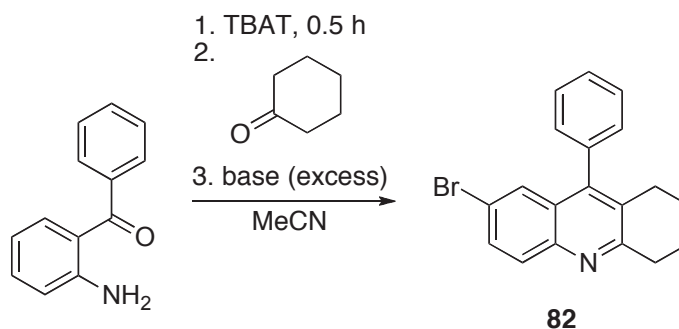
To a 10 mL round-bottom flask equipped with a half-inch stir bar, 2-aminobenzophenone (0.197 g, 0.5 mmol), tetra-*n*-butylammonium tribromide (0.241 g, 0.5mmol), and 4 mL MeCN were added. The flask was sealed with a septum and set to stir for 30 min. Conversion to 5-bromo-2-aminobenzophenone was monitored by TLC and by solution colour change from clear, bright orange to clear, pale yellow. This procedure was used consistently across the entire suite of condensations reported.

The ketone, (0.5 mmol) was dissolved in 1 mL MeCN (or 1 mL DCM, where required by solubility) and added to an addition funnel, which was then capped with a septa and fitted to the round-bottom flask. The ketone solution was added dropwise. An addition rate of 1 drop per second was maintained until the addition was complete, after which the funnel was rinsed with 0.5 mL of MeCN, which was then added directly to the reaction. Ketones of high sensitivity to the acidic reaction conditions were taken up in a 5 mL glass-barreled syringe and fitted into a syringe pump for slow addition, 0.1 – 0.5 mL/min. This modification will be noted when used in subsequent sections.

The solution was allowed to stir between 12 h and 3 d. During this time a precipitate formed, after which the reaction was stirred for an additional 6 hours. When deemed complete by TLC, the reaction mixture was cooled to -10 °C and filtered through a glass frit under a flow of nitrogen from an inverted funnel connected to the nitrogen manifold. The solid was washed with cold MeCN (2x 10 mL) to yield a tan or brownish solid. After drying for 5-10 minutes *via* water aspirator, the solid was removed and dissolved, with stirring, in a mixture of 10 mL DCM and 2 mL water. Once the solids dissolved, the two-phase mixture was added to a separatory funnel and washed with sodium bicarbonate (2 x 10 mL), water (2 x 10 mL), and brine (10 mL), and then dried over magnesium sulfate. Concentration on a rotary evaporator produced fine, pale yellowish powders. The crude quinoline was dissolved in boiling isopropanol, 95% ethanol, or a mixture of the two, then cooled to room temperature for fifteen minutes,

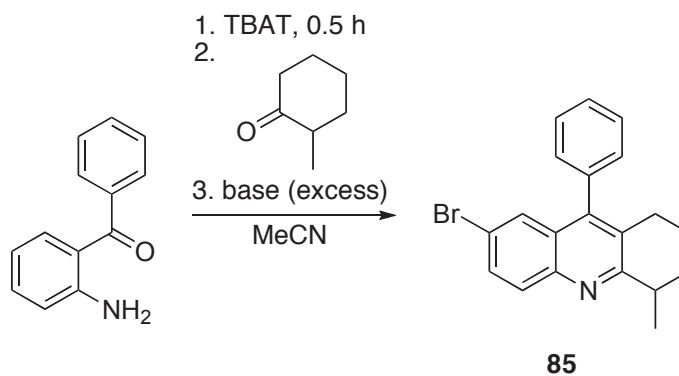
then to -30 °C for no less than one hour. The crystalline solid that deposited was collected by suction filtration and washed with cold isopropanol.

### 7-bromo-9-phenyl-1,2,3,4-tetrahydroacridine 82



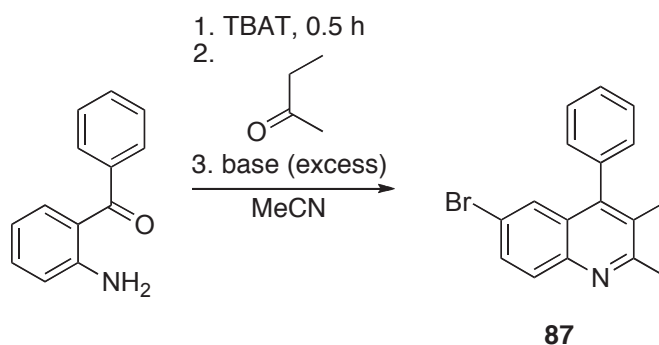
General procedure 5.4.2 was followed. A precipitate formed after ~18 h. The freebase acridine was recrystallized from hot isopropanol to afford short, translucent, pale yellow rods (29.29 g, 86.9%). **<sup>1</sup>H NMR** (500 MHz, CDCl<sub>3</sub>): δ 7.89 (d, *J* = 8.7 Hz, 1H), 7.67 (dd, *J* = 9.0, 2.3 Hz; 1H), 7.49-7.58 (m, 3H), 7.47 (d, 1.9 Hz, 1H), 7.23 (d, 8.8 Hz, 2H), 3.19 (dd, 2.4 Hz, 2H), 2.61 (dd, 2.5 Hz, 2H), 1.94-2.02 (m, 2H), 1.76-1.84 (m, 2H). **<sup>13</sup>C NMR** (100 MHz, CDCl<sub>3</sub>): δ 159.4, 145.7, 144.8, 136.2, 131.8, 130.2, 129.5, 129.1, 128.8, 127.8, 119.5, 34.2, 28.1, 22.9, 22.9. **Elemental analysis:** for C<sub>19</sub>H<sub>16</sub>NBr calculated: C, 67.47%; H, 4.77%; N, 4.14%; Br, 23.62%; found: C, 67.52%; H, 4.82%; N, 4.08%.

### 7-bromo-4-methyl-9-phenyl-1,2,3,4-tetrahydroacridine 85



General procedure 5.4.2 was followed. A precipitate formed after ~12 h. The freebase acridine was recrystallized from hot isopropanol to yield wide, yellow rods (14 mg, 84.0%). **<sup>1</sup>H NMR** (500 MHz, CDCl<sub>3</sub>): δ 7.93 (d, 9.0 Hz, 1H), 7.68 (dd, 9.0, 2.2 Hz; 1H), 7.50-7.59 (m, 3H), 7.47 (d, 2.2 Hz, 1H) 7.18-7.24 (m, 2H), 3.26 (m, 1H), 2.58 (m, 1H), 2.10 (m, 1H), 1.85 (m, 1H), 1.71 (m, 2H), 1.52 (d, 7.0 Hz, 3H). **<sup>13</sup>C APT NMR** (125 MHz, CDCl<sub>3</sub>): δ 163.4 (+), 145.6 (+), 145.1 (+), 136.7 (+), 131.6 (-), 130.6 (-), 129.3 (-), 129.2 (+), 129.1 (-), 128.8 (+), 128.8 (-) 128.0 (-), 127.8 (-), 127.7 (+), 119.4 (+), 37.2 (-), 31.0 (+), 28.7 (+), 21.6 (-), 20.3 (+). **COSY** (500 MHz, CDCl<sub>3</sub>): δ 7.93 ↔ 7.68; 7.68 ↔ 7.93, 7.47; 7.50-7.59 ↔ 7.18-7.24; 7.47 ↔ 7.68; 7.18-7.24 ↔ 7.50-7.59; 3.26 ↔ 1.52; 2.58 ↔ 1.71; 2.10 ↔ 1.85; 1.85 ↔ 2.10; 1.71 ↔ 2.58; 1.52 ↔ 3.26. **HMBC** (500 MHz, CDCl<sub>3</sub>): δ 7.93 ↔ 145.6, 131.6, 127.8; 7.68 ↔ 145.1, 127.7, 119.4; 7.50-7.59 ↔ 136.7, 131.6, 129, 128.8, 128.0; 7.47 ↔ 145.1, 131.6, 119.4; 7.18-7.24 ↔ 129, 128.8; 3.26 ↔ 163.4, 31.0; 2.58 ↔ 163.4, 145.1, 129, 31.0, 20.3; 2.10 ↔ 163.4, 28.7, 21.6; 1.71 ↔ 163.4, 129, 37.2, 21.6; 1.52 ↔ 163.4, 37.2, 31.0. **ESI-MS**: *m/z* calculated for C<sub>20</sub>H<sub>18</sub><sup>79</sup>BrN (M+H)<sup>+</sup> = 352.0701; found C<sub>20</sub>H<sub>18</sub><sup>79</sup>BrN: (M+H)<sup>+</sup> 252.0553.

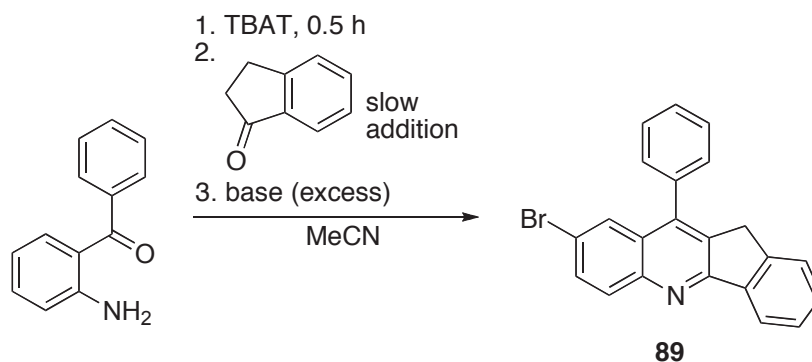
### 6-bromo-2,3-dimethyl-4-phenylquinoline 87



General procedure 5.4.2 was followed. A precipitate formed after ~4 h. The freebase acridine was recrystallized from a hot 50:50 mixture of methanol and ethanol to yield long, thin, bright yellow needles (29.24 g, 94.2%). **<sup>1</sup>H NMR** (500 MHz, CDCl<sub>3</sub>): δ 7.92 (d, *J* = 9.0 Hz, 1H), 7.70 (d, *J* = dd, 8.8, 2.0 Hz, 1H), 7.51-7.60 (m, 3H), 7.48 (d *J* = 2.2 Hz, 1H), 7.23-7.27 (m, 2H), 2.78 (s, 3H), 2.21 (s, 3H). **<sup>13</sup>C APT NMR** (125 MHz, CDCl<sub>3</sub>): δ 159.9 (+) 145.8 (+), 144.2 (+), 137.1 (+), 131.6 (-), 130.4 (-), 129.3 (-), 128.8 (-), 128.6 (+), 128.2 (+), 128.2 (-), 128.1 (-), 119.5, (+), 24.6 (-), 17.3 (-). **COSY** (500 MHz, CDCl<sub>3</sub>): δ 7.92 ↔ 7.70; 7.70 ↔ 7.92, 7.48; 7.51-7.60 ↔ 7.23-7.27; 7.48 ↔ 7.70; 7.23-7.27 ↔

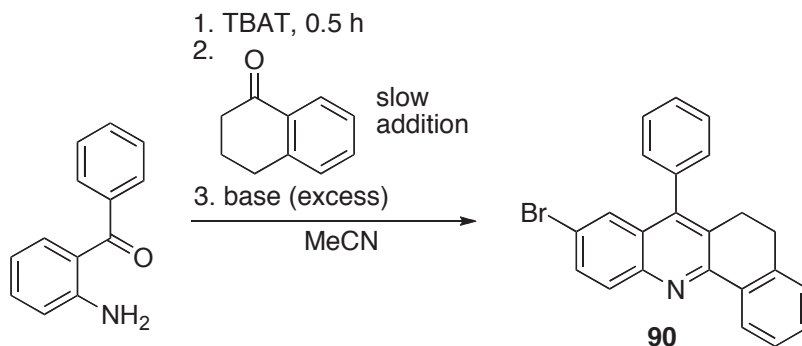
7.51-7.60. **HMBC** (500 MHz, CDCl<sub>3</sub>):  $\delta$ 7.92  $\leftrightarrow$  131.6, 128, 119.5; 7.70  $\leftrightarrow$  144.2, 128, 119.5; 7.51-7.60  $\leftrightarrow$  137.1, 128.8, 128.6, 128; 7.48  $\leftrightarrow$  144.2, 131.6, 119.5; 7.23-7.27  $\leftrightarrow$  145.8, 128; 2.78  $\leftrightarrow$  159.9, 128.2, 119.5; 2.21  $\leftrightarrow$  159.9, 145.8, 119.5. **Elemental analysis** for C<sub>17</sub>H<sub>14</sub>BrN calculated: C, 65.40%; H, 4.52%; N, 4.49%; found: C, 65.42%; H, 4.53%; N, 4.45%.

### 8-bromo-10-phenyl-11H-indeno[1,2-b]quinoline 89



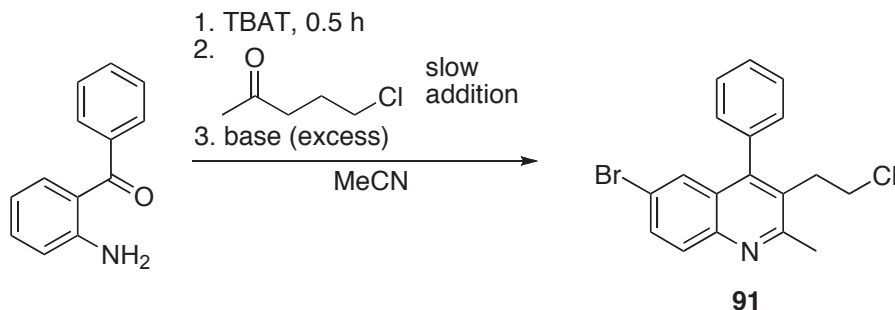
General procedure 5.4.2 was followed, and the ketone was added via syringe pump at a rate of 0.1 ml/h. A precipitate formed  $\sim$ 4 h. The freebase acridine was recrystallized from a hot ethanol to yield short, thin, white rods (32 mg, 88.3%). **<sup>1</sup>H NMR** (500 MHz, CDCl<sub>3</sub>):  $\delta$  8.33 (d,  $J$  = 7.0 Hz, 1H), 8.13 (d,  $J$  = 9.0 Hz, 1H), 7.83 (d,  $J$  = 2.2 Hz, 1H), 7.78 (dd,  $J$  = 9.0, 2.2 Hz, 1H), 7.47-7.65 (m, 8H), 3.87 (s, 2H). **ESI-MS**:  $m/z$  calculated for C<sub>22</sub>H<sub>14</sub><sup>79</sup>BrN (M<sup>+</sup>) = 371.0310 found C<sub>22</sub>H<sub>14</sub><sup>79</sup>BrN (M<sup>+</sup>) 371.0307. **Elemental analysis** for C<sub>22</sub>H<sub>14</sub>NBr calculated: C, 70.98%, H, 3.79%, N, 3.76%, Br, 21.46%; found: C, 71.11%, H, 3.79%, N, 3.79%.

### 9-bromo-7-phenyl-5,6-dihydrobenzo[*c*]acridine 90



General procedure 5.4.2 was followed; the ketone was added *via* syringe pump at a rate of 0.1 ml/h. A precipitate formed after ~7 h. The freebase acridine was recrystallized from a hot ethanol to yield an off-white powder (3.427 g, 89.4%). **<sup>1</sup>H NMR** (500 MHz, CDCl<sub>3</sub>): δ 8.60 (dd, *J* = 7.8, 1.4 Hz; 1H), 8.05 (d, *J* = 8.9, 1H), 7.72 (dd, *J* = 7.9, 2.3 Hz; 1H), 7.51-7.62 (m, 3H), 7.38-7.47 (m, 4H), 7.29-7.33 (m, 2H), 2.88 (m, 4H). **<sup>13</sup>C APT NMR** (125 MHz, CDCl<sub>3</sub>): δ 163.2 (+), 147.0 (+), 145.4 (+), 142.7 (+), 140.6 (+), 135.9 (+), 134.8 (+), 132.1 (-), 130.3 (-), 129.2 (-), 129.0 (-), 128.6 (-), 127.9 (-), 127.6 (-), 127.6 (+), 125.4 (-), 119.8 (+), 35.2 (+). **COSY** (500 MHz, CDCl<sub>3</sub>): δ 8.60 ↔ 6.75; 8.05 ↔ 7.72; 7.72 ↔ 8.05; 7.51-7.62 ↔ 8.60; 7.38-7.47 ↔ 7.38-7.47. **ESI-MS**: *m/z* calculated for C<sub>23</sub>H<sub>16</sub><sup>79</sup>BrN (M+1)<sup>+</sup> = 385.0466; found C<sub>23</sub>H<sub>16</sub><sup>79</sup>BrN (M+1)<sup>+</sup> 385.0461. **Elemental analysis** for C<sub>23</sub>H<sub>16</sub>NBr calculated: C, 71.51%; H, 4.17%; N, 3.63%; found: C, 71.54%; H, 4.23%; N, 3.70%.

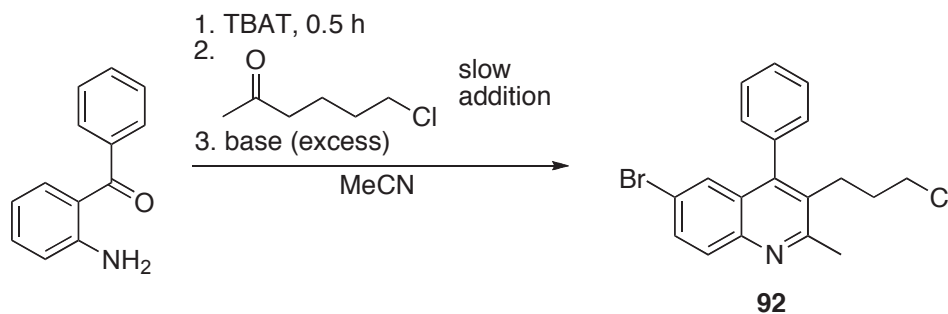
### 6-bromo-3-(2-chloroethyl)-2-methyl-4-phenylquinoline 91



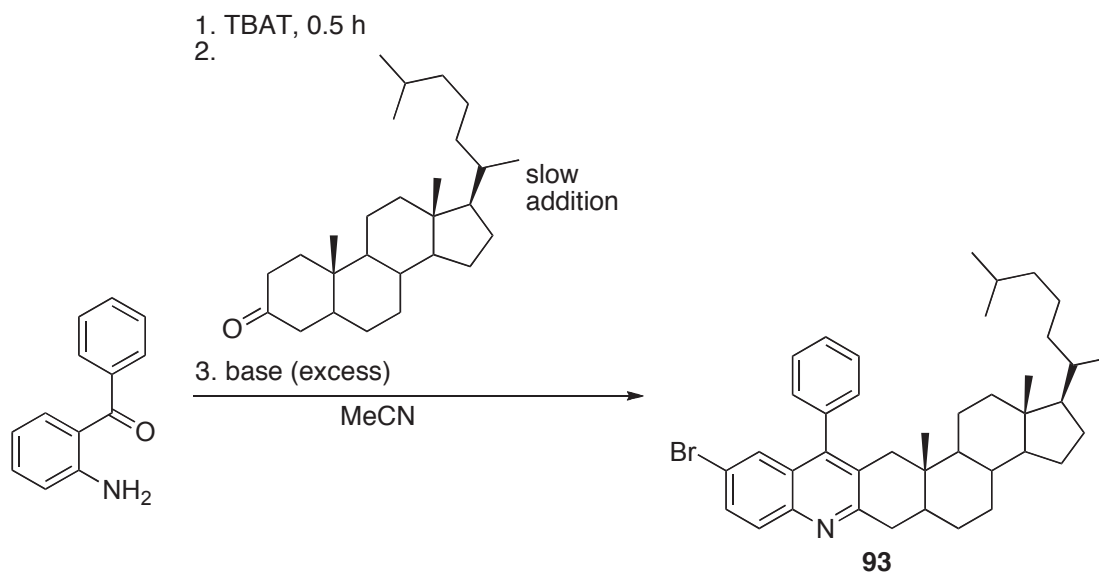
General procedure 5.4.2 was followed; the ketone was added *via* syringe pump at a rate of 0.1 ml/h. A precipitate formed after ~5 h. The freebase acridine was recrystallized from a hot methanol to yield a very fine off-white powder (27 mg, 80.3%). A second recrystallization in ethanol yielded short, shiny white rods. **<sup>1</sup>H NMR** (500 MHz, CDCl<sub>3</sub>): δ 7.93 (d, *J* = 9.0 Hz, 1H), 7.74 (dd, *J* = 8.8, 2.2 Hz; 1H), 7.55-7.62 (m, 3H), 7.41 (d, *J* = 2.2 Hz, 1H), 7.25-7.79 (m, 2H), 3.48 (dd, *J* = 7.9, 8.2 Hz; 2H), 3.12 (dd, *J* = 9.0, 7.9 Hz; 2H), 2.88 (s, 3H). **<sup>13</sup>C APT NMR** (125 MHz, CDCl<sub>3</sub>): δ 159.5 (+), 145.6 (+), 142.9 (+), 132.5 (-), 130.4 (-), 129.1 (-), 128.9 (-), 128.6 (-), 128.4 (-), 128.4 (+), 128.2 (+), 120.2 (+) 42.2 (+), 34.0 (+), 23.8 (-). **COSY** (500 MHz, CDCl<sub>3</sub>): δ 7.93 ↔ 7.74; 7.74 ↔ 7.39, 7.41; 7.55-7.62 ↔ 7.25-7.79; 7.41 ↔ 7.74; 7.25-7.79 ↔ 7.55-7.62; 3.48 ↔ 3.48; 3.12 ↔

3.12. **HMBC** (500 MHz, CDCl<sub>3</sub>): δ 7.93 ↔ 132.5, 128.9; 7.74 ↔ 145.6, 130.4; 7.55-7.62 ↔ 128, 145.6; 7.41 ↔ 142.9, 132.5, 120.2; 7.25-7.79 ↔ 128, 145.6; 3.48 ↔ 128.2, 34.0; 3.12 ↔ 159.5, 145.6, 128.2, 42.2; 2.88 ↔ 159.5, 128.4. **ESI-MS**: *m/z* calculated for C<sub>18</sub>H<sub>17</sub><sup>79</sup>Br<sup>35</sup>CIN (M+2)<sup>+</sup> = 361.0232; found C<sub>18</sub>H<sub>17</sub><sup>79</sup>Br<sup>35</sup>CIN (M+2)<sup>+</sup> 361.0053. **Elemental analysis** for C<sub>18</sub>H<sub>15</sub>NBrCl calculated: C, 59.94%; H, 4.19%; N, 3.88%; found: C, 59.86%; H, 4.25%; N, 3.91%.

### 6-bromo-3-(3-chloropropyl)-2-methyl-4-phenylquinoline 92

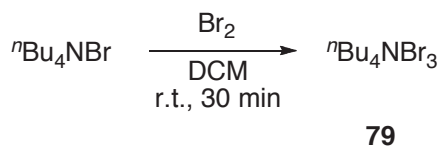


General procedure 5.4.2 was followed; the ketone was added *via* syringe pump at a rate of 0.1 ml/h. A precipitate formed after ~14 h. The freebase acridine was recrystallized from a hot methanol to yield a very fine off-white powder (29.476 g, 79.4%). **<sup>1</sup>H NMR** (500 MHz, CDCl<sub>3</sub>): δ 7.82 (d, *J* = 8.7 Hz, 1H), 7.70 (d, *J* = 8.8 Hz, 1H), 7.52-7.61 (m, 3H), 7.41 (d, *J* = 2.1 Hz, 1H), 7.23-7.28 (m, 2H), 3.43 (dd, *J* = 8.3, 8.0 Hz; 2H), 2.85 (s, 3H), 2.77 (m, 2H), 1.90 (m, 2H). **<sup>13</sup>C APT NMR** (125 MHz, CDCl<sub>3</sub>): δ 159.4 (+), 146.3 (+), 145.7 (+), 136.1 (+), 132.0 (-), 131.9 (+), 130.4 (-), 129.2 (-), 128.8 (-), 128.3 (-), 128.3 (+), 119.7 (+), 45.4 (+), 33.6 (+), 28.3 (+), 24.4 (-). **COSY** (500 MHz, CDCl<sub>3</sub>): δ 7.70 ↔ 7.70; 7.70 ↔ 7.70, 7.41; 7.52-7.61 ↔ 7.23-7.28; 7.41 ↔ 7.70; 7.23-7.28 ↔ 7.52-7.61; 3.43 ↔ 1.90; 2.77 ↔ 1.90; 1.90 ↔ 3.43, 2.77. **HMBC** 500 MHz, CDCl<sub>3</sub>): δ 7.70 ↔ 146.3, 132.0, 128.3, 119.7; 7.70 ↔ 145.7, 128.3, 119.7; 7.52-7.61 ↔ 128.3, 129.2; 7.41 ↔ 146.3, 132.0, 119.7; 7.23-7.28 ↔ 145.7, 128.3; 3.43 ↔ 33.6, 28.3; 2.77 ↔ 159.4, 145.7, 131.9, 45.4, 33.6; 1.90 ↔ 131.9, 45.4, 33.6. **ESI-MS**: *m/z* calculated for C<sub>19</sub>H<sub>19</sub><sup>79</sup>Br<sup>35</sup>CIN (M+2)<sup>+</sup> = 375.0389; found C<sub>19</sub>H<sub>19</sub><sup>79</sup>Br<sup>35</sup>CIN (M+2)<sup>+</sup> 361.0208. **Elemental analysis** for C<sub>19</sub>H<sub>17</sub>NBrCl calculated: C, 60.90%; H, 4.57%; N, 3.74%; found: C, 60.30%; H, 4.52%; N, 3.58%



General procedure 5.4.2 was followed, with the following modification: due to its reduced solubility, cholestanone was dissolved in 1 mL DCM. The ketone was added at a rate of 0.1 mL/min. A precipitate formed after ~12 h. The freebase acridine was recrystallized from a hot ethanol to yield a tan powder (43 mg, 69.5%). **<sup>1</sup>H NMR:** (400 MHz, CDCl<sub>3</sub>): δ 7.92 (d, 8.5 Hz, 1H), 7.67 (dd, 8.4. 1.3 Hz; 1H), 7.57-7.60 (m, 4H), 7.47 (d, 2.2 Hz, 1H) 7.19-7.23 (m, 2H), 3.91 (dd, *J* = 2.3, 1.0 Hz, 1H), 3.19, (dd, *J* = 2.2, 1.9 Hz, 1H), 2.71 (d, *J* = 2.5 Hz, 1H), 2.53 (d, *J* = 2.7 Hz, 1H), 1.93 (d, *J* = 2.4 Hz, 1H), 1.79 (m, 4H), 1.57 (m, 5H), 1.32 (m, 6H), 1.09 (m, 9H), 0.88 (d, *J* = 1.4 Hz, 3H), 0.87 (d, *J* = 1.4 Hz, 6H), 0.76 (s, 3H), 0.64 (s, 3H). **EI-MS:** *m/z* for C<sub>39</sub>H<sub>51</sub><sup>79</sup>BrN (M<sup>+</sup>) = 625.3283; found 625.3285. **Analysis** for C<sub>40</sub>H<sub>52</sub>NBr calculated: C, 76.65%, H, 8.36%, N, 2.23%; found: C, 76.52%, H, 8.42%, N, 2.31%.

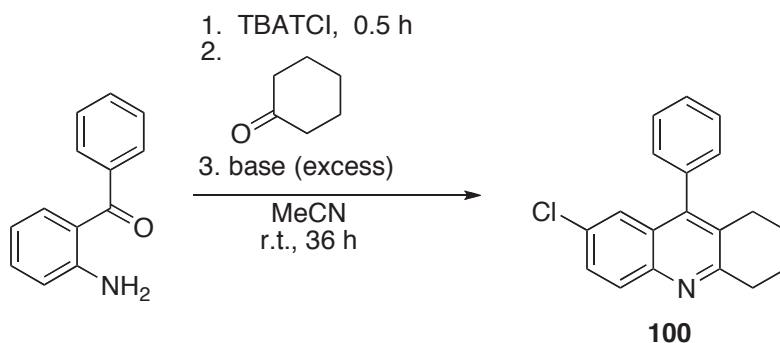
#### Tetra-*n*-butylammonium tribromide **79**



Reaction mixtures from the condensation of 2-aminobenzophenone were filtered, and the solids filtered, as described in Section 2.2.3. The mother liquors were then

added to a separatory funnel and thrice washed with an equivalent volume of 10% NaOH. Aqueous washes were combined and thrice back-extracted with an equivalent volume of pre-dried ethyl acetate. This solution was reduced to approximately 20mL before the careful addition of 20mL distilled diethyl ether. Following crystallization, the solids were filtered and immediately transferred to an appropriate sized, pre-weighed round bottom flask and stirred under high vacuum. After 10 hours the flask was back-filled with argon. A second ten-hour drying cycle applied. This semi-pure solid was then used directly in the synthesis of TBAT<sup>52</sup>. **Elemental analysis** calculated for C<sub>16</sub>H<sub>36</sub>NBr<sub>3</sub>: C, 39.86; H, 7.53%; N, 2.90%; found: C, 39.89%; H, 7.51%; N, 3.02%.

### 7-chloro-9-phenyl-1,2,3,4-tetrahydroacridine 100



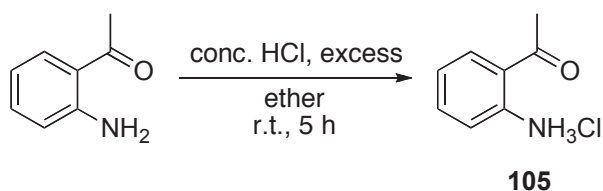
To a 10 mL round-bottom flask equipped with a half-inch stir bar, 2-aminobenzophenone (0.0197 g, 0.1 mmol), tetra-*n*-butyltetrachloroiodate (0.051 g, 0.1 mmol), and 4 mL MeCN were added. The flask was sealed with a septum, wrapped in aluminum foil, and set to stir for 30 min. Conversion to 5-chloro-2-aminobenzophenone was monitored by TLC and by solution colour change from clear, bright pink to clear, pale yellow.

Cyclohexanone, (0.010g, 0.1 mmol) was dissolved in 1 mL MeCN and added to an addition funnel, which was then capped with a septa and fitted to the round-bottom flask. The ketone solution was added dropwise. An addition rate of 1 drop per second was maintained until the addition was complete, after which the funnel was rinsed with 0.5 mL of MeCN, which was then added directly to the reaction.

The solution was allowed to stir for 10 h. During this time the solution darkened to black, and a small amount of precipitate formed; after cooling the reaction to 0 °C the precipitate was filtered on a glass frit and washed with cold MeCN (2x 10 mL) to yield a bright black solid. After drying for 5-10 minutes *via* water aspirator, the solid was

removed and dissolved, with stirring, in a mixture of 10 mL DCM and 2 mL water. Once the solids dissolved, the two-phase mixture was added to a separatory funnel and washed with sodium bicarbonate (2 x 10 mL), water (2 x 10 mL), and brine (10 mL), and then dried over magnesium sulfate. Concentration on a rotary evaporator produced a fine, purple-hued crystalline powder.  $^1\text{H NMR}$ : (400 MHz,  $\text{CDCl}_3$ ):  $\delta$  7.61 (m, 1H), 7.43 (m, 1H), 7.33 (m, 1H), 3.77 (dd,  $J = 2.1, 2.6$  Hz, 2H), 2.65 (dd  $J = 2.3, 2.4$  Hz, 2H), 2.10 (m, 2H), 1.84 (m, 2H).

### 2-aminoacetophenone hydrogen chloride 95



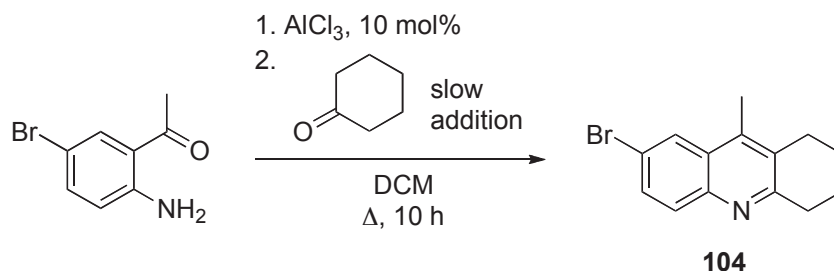
To a 100 mL round-bottomed flask fitted with a one-inch stirbar, 2-aminoacetophenone (0.5 g 3.7 mmol), 15 mL conc. HCl (181.5 mmol) and 50 mL ether were added. The reaction was allowed to stir for 5 hours, after which time the ether layer was subjected to analysis by TLC (5:1 hexanes:ethyl acetate) to confirm reaction completion. Reaction was then cooled to  $-10^\circ\text{C}$  for twenty minutes. Long, translucent white needles crashed out, which were vacuum filtered and washed with cold ether. The crystals were transferred to a pre-weighed 5-dram vial and placed in a drying tube. Pre-drying was effected *via* Schlenk line for 30 minutes before transferring to a high-vacuum line for 2 hours. A final dry weight of 0.613 g (96.9%) was collected, verified by elemental analysis, and stored in a sealed vial in a standard desiccator. **Elemental analysis** calculated for  $\text{C}_8\text{H}_{10}\text{ONCl}$ : C, 55.99; H, 5.87; N, 8.16; found: C, 55.89%; H, 5.81%; N, 8.14%.

### 7-bromo-9-methyl-1,2,3,4-tetrahydroacridine 94



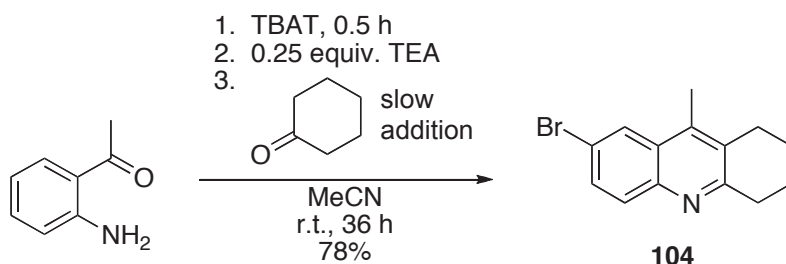
To a 10 mL round-bottomed flask fitted with a half-inch stirbar, 9-methyl-1,2,3,4-tetrahydroacridine (0.050 g, 0.25 mmol) and 5 mL DCM were added. Solution was stirred over a dry ice-ethylene glycol bath, with dry ice added at such a rate to maintain the bath temperature at 15 °C. Bromine (6.5 mL, 0.25 mmol) was carefully dissolved in 2 mL DCM and added to an addition funnel. The funnel was fitted to the round-bottom flask, after which the bromine solution was added dropwise. The reaction was allowed to stir for 12 h. The crude reaction mixture was added to a separatory funnel and washed with sodium bicarbonate (2 x 10 mL), water (2 x 20 mL), and brine (20 mL), and then dried over magnesium sulfate. Concentration on a rotary evaporator produced grey-brown residue, to which hot methanol was added with vigorous stirring. Once the residue was dissolved the solution was allowed to cool at room temperature, which caused precipitation of a grey-yellow powder. The powder was collected by suction filtration and washed with 10 mL cold methanol to afford the bromoacridine product (0.105 g, 76.2%). **<sup>1</sup>H NMR:** (400 MHz, CDCl<sub>3</sub>): δ 8.21 (d, *J* = 8.0 Hz, 1H), 7.54 (d, *J* = 1.9 Hz, 1H), 7.96 (d, *J* = 9.1 Hz, 1H), 3.65 (m, 2H), 3.06 (m, 2H), 2.02 (m, 4H).

#### 5.4.3 Additional syntheses of 7-bromo-9-methyl-1,2,3,4-tetrahydroacridine **104**



A 10 mL round-bottomed flask fitted with a one inch stirbar was transferred inside a glove box, where aluminum trichloride (0.007 g, 0.05 mmol) was added. The flask was sealed and removed to a Schlenk line where 1-(2-amino-5-bromophenyl)ethanone (0.106 g, 0.5 mmol) and 5 mL DCM were added to form a clear, orange solution. The solution was allowed to stir under argon for ten minutes while cyclohexanone (0.049 g,

0.5 mmol) was dissolved in 2 mL DCM. This solution was taken up into a Hamilton syringe, which itself was fitted with a long needle and loaded into a syringe pump. The cyclohexanone solution was added at a rate of 0.2 mL/min. Following the completion of the addition, the solution was allowed to stir under argon for 10 h. An orange-grey precipitate crashed out during this time. The reaction was quenched in ice water, and 10 mL 1 N HCl was carefully added. The resultant biphasic mixture was added to a separatory funnel and washed with sodium bicarbonate (2 x 20 mL), water (2 x 10 mL), and brine (10 mL), and then dried over magnesium sulfate. Concentration on a rotary evaporator produced a yellow-grey powder, to which hot methanol was added until the powder was dissolved. The solution was allowed to cool at room temperature, which caused precipitation of a grey-yellow powder. The powder was collected by suction filtration and washed with 10 mL cold methanol to afford the bromoacridine product (0.104 g, 76.0 %).



To a 10 mL round-bottom flask equipped with a half-inch stir bar, 2'-aminoacetophenone (0.067 g, 0.5 mmol), tetra-*n*-butylammonium tribromide (0.121 g, 0.5 mmol), and 4 mL MeCN were added. A pale yellow precipitate formed immediately following the addition of TBAT. The flask was sealed with a septum and set to stir for 30 min.

Triethylamine (0.013 g, 0.125 mmol) was added to the reaction flask. Cyclohexanone, (0.049 g, 0.5 mmol) was dissolved in 1 mL MeCN and added to an addition funnel, which was then capped with a septa and fitted to the round-bottom flask. The ketone solution was added dropwise at a very slow rate.

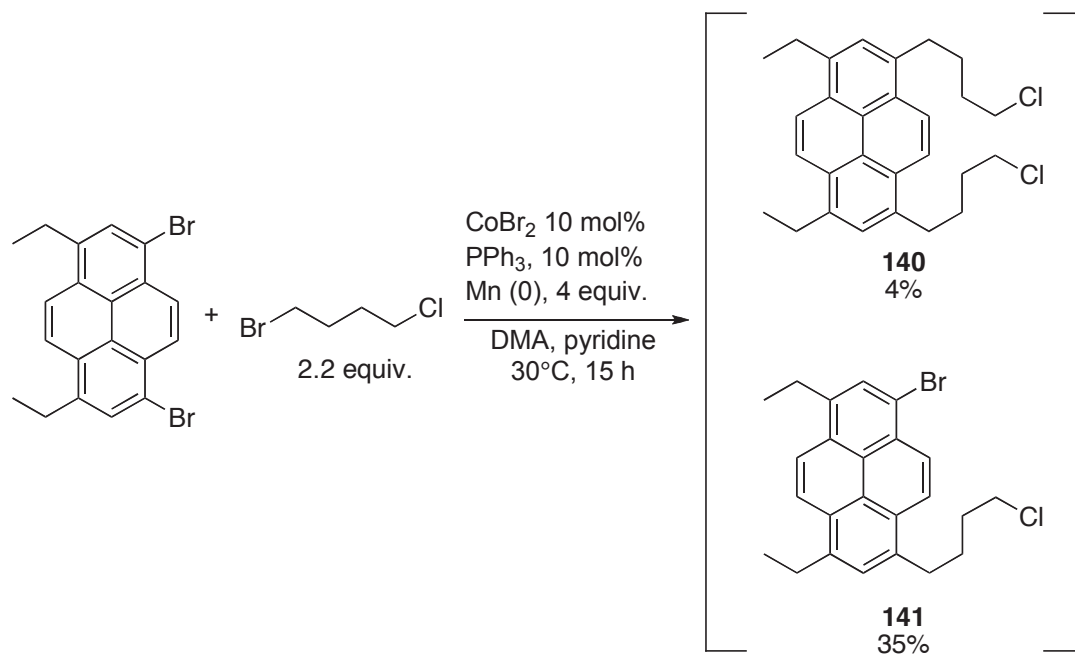
The reaction was allowed to stir 12 h, during which it began to darken to a charcoal colour. All reaction solvents were removed under vacuum, after which 5mL cold acetonitrile was added and the mixture filtered on a glass frit. The grey-green solid was washed with cold MeCN (2x 10 mL). After drying for 5 min the solid was removed and dissolved, with stirring, in a mixture of 10 mL DCM and 2 mL water. The biphasic

mixture was added to a separatory funnel and washed with sodium bicarbonate (2 x 10 mL), water (2 x 10 mL), and brine (10 mL), and then dried over magnesium sulfate. Concentration on a rotary evaporator produced a fine grey powder. The crude bromoacridine was dissolved in boiling methanol cooled to room temperature, then to -30 °C for 2 h. A very fine tan powder crashed out, which was collected by suction filtration and washed with cold methanol to afford the pure product (0.107 g, 78.4%).

#### 5.4.4 *General procedure for cobalt-manganese REC reactions*

In a dry box, cobalt(II) bromide (0.055 g, 0.25 mmol), triphenylphosphine (0.066 g, 0.25 mmol), Rieke manganese (0.550 g, 1 mmol), a bromoarene (2.5 mmol), 1-bromo-4-chlorobutane (0.472 g, 2.75 mmol), pyridine (0.5 mL) and DMA (3 mL) were added to a 25 mL Schlenk flask fitted with a half-inch stirbar. The flask was sealed with a glass stopper, removed to a Schlenk manifold, put under nitrogen, and set to stir for 2 h over a 30 °C oil bath. Following the 15 h reaction period, the now dark solution was allowed to cool to room temperature and was filtered through a Celite plug into a small Erlenmeyer fitted with a half-inch stirbar. The Schlenk flask was rinsed with DCM (2x 10 mL), and each rinse was used to further rinse the Celite plug. Aliquats for GC-MS analysis were subjected to a fluorisil plug and injected directly. Minimal 2N hydrochloric acid was added to the Erlenmeyer and the filtered solution was allowed to stir for 10 minutes until it became a clear, red solution. After this time the solution was added to a separatory funnel and 5-10mL DCM was added. The organic layer was washed with sodium bicarbonate (2x 10mL), water (2x 10mL) and brine (10mL) and dried over magnesium sulfate. Once concentrated on a rotary evaporator, the resultant oil was passed through a short fluorisil pipette to remove any trace metal salts.

### 1,8-bis(4-chlorobutyl)-3,6-diethylpyrene **140**



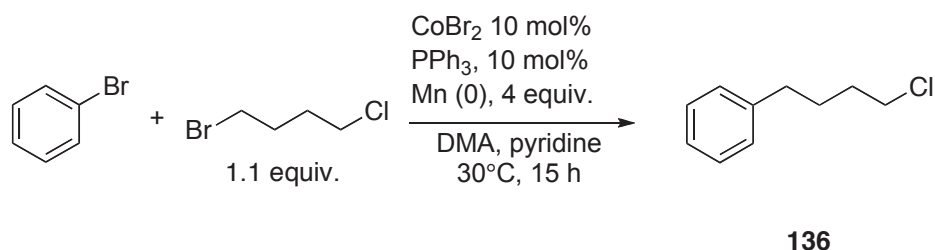
Product was obtained as a crude mixture (0.426 g total) of off-white powder containing traces of the mono-tethered intermediate **141**.  $^1\text{H NMR}$  (400 MHz,  $\text{CDCl}_3$ ):  $\delta$  8.23 (s, 2H), 8.19 (s, 2H), 7.72 (s, 2H), 3.60 (m, 4H), 3.36 (m, 8H), 1.9-2.1 (m, 4H), 1.56 (d,  $J = 4.1$  Hz, 6H), 1.52 (m, 4H)

#### 5.4.5 General procedure for nickel-zinc REC reactions

In a standard four-dram vial, fitted with a half-inch stirbar, nickel(II) iodide hydrate (0.012 g, 0.04 mmol), bipy (0.006 g, 0.04 mmol), zinc powder (0.098 g, 1.5 mmol), bromoarene (0.75 mmol), pyridine (3  $\mu\text{L}$ ) and DMPU (3 mL) were added. The vial was capped and the green-grey solution was heated to  $60^\circ\text{C}$  over a silicon oil bath. A separate solution of 1-bromo-4-chlorobutane (0.161 g, 0.75 mmol) and DMPU (1 mL) was added to a Hamilton glass-barreled syringe, which was then loaded into a syringe pump. The alkylbromide was added at a rate of 0.1 mL/h, and the reaction mixture began to darken with during this addition. Once the addition was complete, the reaction was allowed to heat for an additional 5 h. Following reaction completion, the mixture was

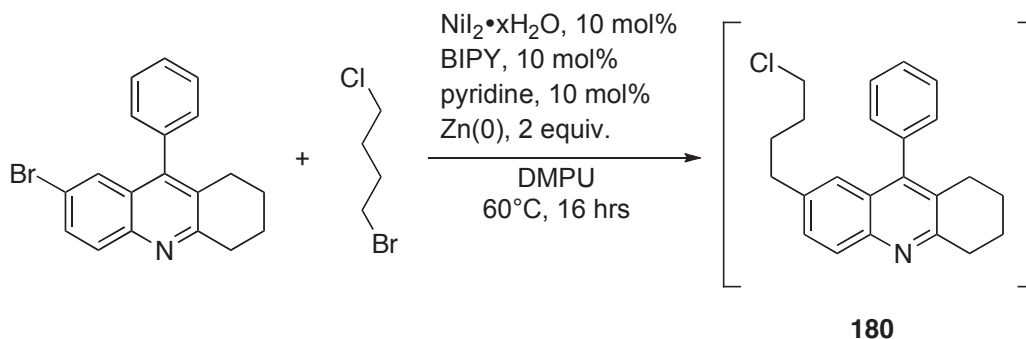
passed through a Celite and Fluorisil plug, which was rinsed with minimal DCM. All solvent was removed on a rotary evaporator to yield a thick, yellow-tan paste. From this crude mixture the unconverted starting material may be removed, using exhaustive serial recrystallization with hot methanol. The crude product mixture thus obtained is a clear, thick oil.

#### 4-chloro-1-phenylbutane 136



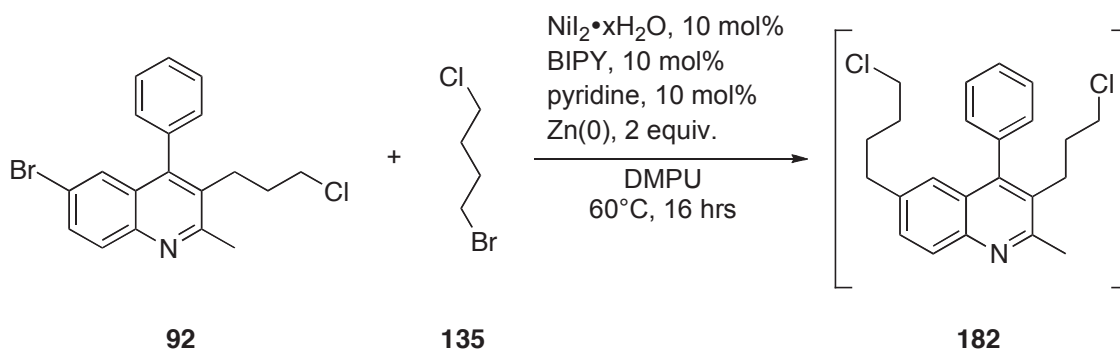
Obtained as a thin, clear oil (0.235 g, 56.1%) following distillation from crude workup mixture at 1 mmHg, 78 °C. **<sup>1</sup>H NMR** (500 MHz, CDCl<sub>3</sub>): δ 7.39 (m, 2H), 7.25 (m, 3H), 3.62 (dd, *J* = 7.5, 7.8 Hz; 2H), 2.73 (t, *J* = 8.0 Hz; 2H), 1.84 (m, 4H). **<sup>13</sup>C APT NMR** (125 MHz, CDCl<sub>3</sub>): δ 141.2 (+), 128.4 (-), 126.3 (-), 44.1 (+), 35.0 (+), 32.3 (+), 29.7 (+). **COSY** (500 MHz, CDCl<sub>3</sub>): δ 7.39 ↔ 7.25; 7.25 ↔ 7.39; 3.62 ↔ 1.84; 2.73 ↔ 1.84; 1.84 ↔ 3.62, 2.73. **HMBC** (500 MHz, CDCl<sub>3</sub>): δ 7.39 ↔ 141.2, 128.4; 7.25 ↔ 126.3, 44.1; 3.62 ↔ 35.0, 32.3; 2.73 ↔ 141.2, 128.4, 32.3, 29.7; 1.84 ↔ 3.62, 2.73 ↔ 141.2, 44.1, 35.0, 32.3, 29.7. **Elemental analysis** calculated for C<sub>10</sub>H<sub>13</sub>Cl: C, 71.21%; H, 7.77%; found: C, 71.20%; H, 7.75%.

#### 7-(4-chlorobutyl)-9-phenyl-1,2,3,4-tetrahydroacridine 180



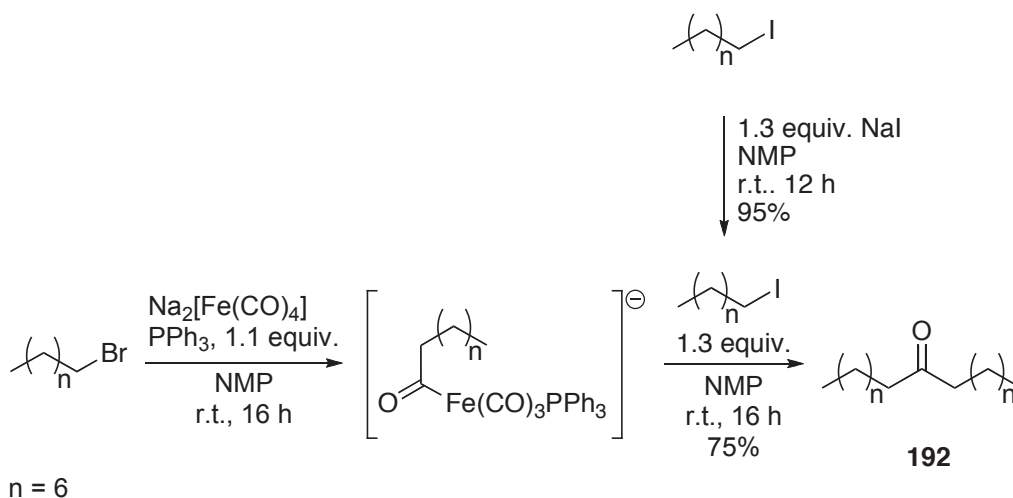
Impure pale yellow oil (0.058 g, 22.1%).  $^1\text{H NMR}$  (400 MHz,  $\text{CDCl}_3$ ):  $\delta$  7.84 (dd,  $J = 8.2$  Hz, 1H), 7.45-7.56 (m, 4H), 7.19-7.24 (m, 3H), 3.18 (dd,  $J = 6.2, 7.0$  Hz, 4H), 2.59 (dd,  $J = 6.3, 6.9$  Hz, 4H), 1.92-2.03 (m, 4H), 1.76-1.82 (m, 4H).

### 6-(4-chlorobutyl)-3-(3-chloropropyl)-2-methyl-4-phenylquinoline 182



Impure product obtained as a viscous tan oil.  $^1\text{H NMR}$  (400 MHz,  $\text{CDCl}_3$ ):  $\delta$  8.04 (d,  $J = 8.3$  Hz, 1H), 7.62 (dd,  $J = 8.2, 6.9$  Hz; 1H), 7.48-7.56 (m, 3H), 7.33 (dd,  $J = 8.2, 6.9$  Hz; 1H), 7.24-7.28 (m, 2H), 3.41 (dd,  $J = 6.3, 8.3$  Hz; 4H), 2.83 (s, 3H), 2.74 (m, 4H), 1.89 (m, 2H), 1.73 (m, 2H).

### Heptadecan-9-one 192



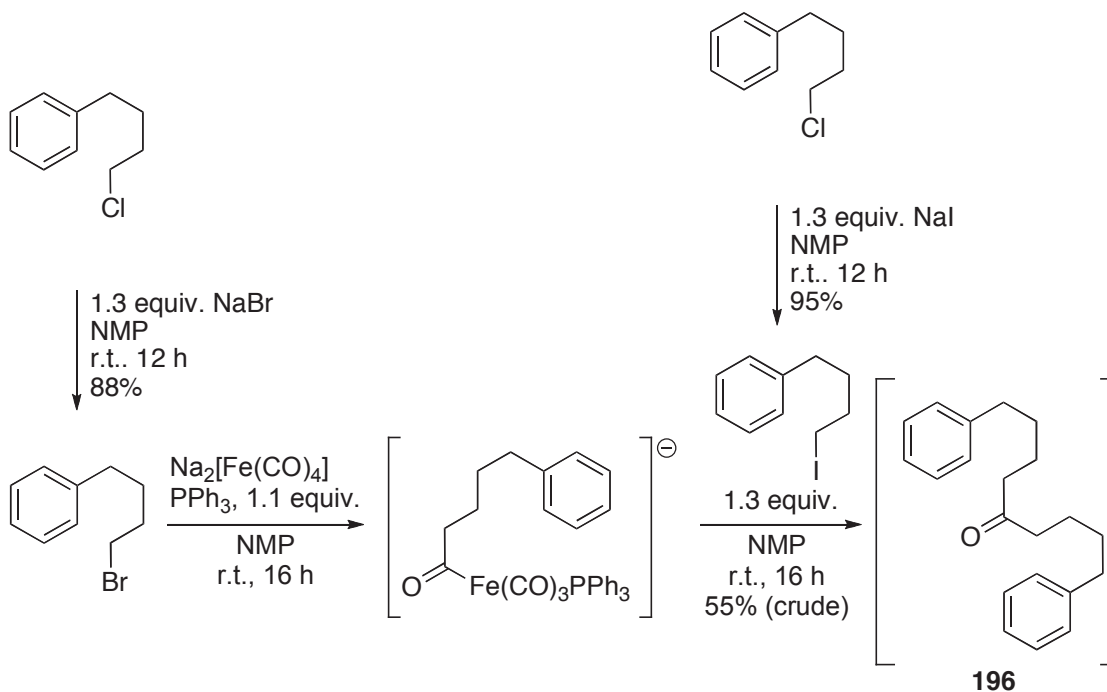
Prior to the reaction proper, iodoctane was prepared. In a drybox, a 5 dram vial was fitted with a flea stirbar and charged with bromooctane (0.251 g, 1.30 mmol), sodium iodide (0.390 g, 2.6 mmol) and THF (5 mL) were added. The solution was allowed to stir overnight; crude  $^1\text{H}$  NMR analysis showed at 30:1 conversion to the iodide based on the individual  $\text{CH}_2\text{X}$  signals.

In a drybox, a 20 mL headspace GC vial was fitted with a half-inch stirbar and charged with Collman's reagent (0.346 g, 1.00 mmol). Great care was taken to minimize exposure of the reagent to light; ambient lighting was turned off and the flask was wrapped in aluminum foil. Triphenylphosphine (0.318 g, 1.20 mmol) and NMP (5 mL) were added to the reagent, creating a dark red solution which was stirred for 2 min. Bromooctane (0.193 g, 1.00 mmol) was added to the vial, which was then crimp capped and set to stir for 24 h.

The iodoctane solution was allowed to sit undisturbed for 30 min, allowing the precipitate fully settle. After this time the iodoctane solution was decanted and added to the main reaction flask, which was re-capped and set to stir for an additional 24 h.

Following the completion of the reaction, the flask was removed from the glovebox. While maintaining an argon pad, the liquids were decanted and transferred to a separatory funnel. Hexanes (20 mL) was added, and the mixture was washed with water (3x 50 mL). The solvents were removed *via* rotary evaporator, after which a pink oil was obtained. This oil was re-dissolved in hexanes (10 mL) and transferred to a 25 mL round-bottomed flask. House air, filtered in-line to remove any impurities, was bubbled through the solution for 6 h during which time precipitate formed. Finally, this solution was filtered and the hexane removed *via* rotary evaporator to yield a thin, pale pink oil ( g, 75.5%). **EI-MS** calculated for  $\text{C}_{17}\text{H}_{34}\text{O}$ : 254.2610; found 254.2630.

## 1,9-diphenylnonan-5-one 196



Prior to the reaction proper, 4-bromo-1-phenylbutane was prepared. In a drybox, a 5 dram vial was fitted with a flea stirbar and charged with 4-chloro-1-phenylbutane (0.25 g, 1.49 mmol), sodium bromide (0.306 g, 3 mmol) and THF (5 mL) were added. The solution was allowed to stir overnight.

In a drybox, a 20 mL headspace GC vial was fitted with a half-inch stirbar and charged with Collman's reagent (0.519 g, 1.50 mmol). Great care was taken to minimize exposure of the reagent to light; ambient lighting was turned off and the flask was wrapped in aluminum foil. Triphenylphosphine (0.445 g, 1.70 mmol) and NMP (5 mL) were added to the reagent, creating a dark red solution which was stirred for 2 min. The 4-bromo-1-phenylbutane solution was decanted and added to the reaction vial, which was then crimp capped and set to stir for 24 h. Concurrently, 4-iodo-1-phenylbutane was prepared in the same manner as the bromide, using sodium iodide (0.446 g, 3 mmol) and an additional 1.49 mmol of 4-chloro-1-phenylbutane. The solutions was allowed to stir overnight.

The 4-iodo-1-phenylbutane solution was allowed to sit undisturbed for 30 min, allowing the precipitate fully settle. After this time the solution was decanted and added to the main reaction flask, which was re-capped and set to stir for an additional 24 h. Following this period a very fine, lustrous white solid had precipitated out of solution; this

product was filtered on a glass frit, rinsed with minimal hexanes, and then removed from the dry box. In a 50 mL round-bottomed flask was added the crude product and 25 mL hexanes, after which time house air was bubbled through the solution for 5 h. This final crude product was then collected on a glass frit. After this point, the product was lost.

## Notes and references.

1. Akbarzadeh, K.; Hammami, A.; Kharrat, A.; Zhang, D.; Allenson, S.; Creek, J.; Kabir, S.; Jamaluddin, A.; Marshall, A. G.; Rodgers, R. P.; Mullins, O. C.; Solbakken, T. *Oilfield Review*, **2007**, Summer ed., 22-43
2. Marsh, R.; Parks, K.; Crowfoot, C. Eds.; *Alberta's Energy Reserves 2012 and Supply/Demand Outlook for 2013-2022*, Energy Resources Conservation Board: Calgary, **2012**.
3. Glass, D.J., ed. *Lexicon of Canadian Stratigraphy, Vol. 4*, Western Canada. Canadian Society of Petroleum Geologists; Calgary, **1997**.
4. *Bitumen*, (2015, April 14) Retrieved from <http://www.unitedgoldencompany.info/asphalt-bitumen.html>
5. Strausz, O. P.; Lown, E. M. *The Chemistry of the Alberta Oil Sands, Bitumens and Heavy Oils*; Alberta Energy Research Institute: Calgary, **2003**.
6. Boussingault, J. B. *Ann. Chim. Phys.* **1837**, 141-151
7. Mitchell, D. L.; Peight, J. G. *Fuel*, **1973**, 149-152
8. *Asphaltenes*, (2015, April 14) Retrieved from <http://www.albertatechfutures.ca/RDSupport/BioandIndustrialTechnologies/IndustrialSensorsTechnologies/NearInfraRedAsphalteneAnalyzer.aspx>
9. Marcusson, J. Z. *Angew. Chem.* **1919**, 113-115.
10. Goual, L.; *Crude Oil Emulsions – Composition, Stability and Characterization*, Abdul-Raouf, M. E. S , ed; InTech: Rijeka, **2012**; Chapter 2, pp 28-42.
11. a) Pelet, R., Behar, F., Monin, J. C. *Org. Geochem.* **1986**, 481-498 b) Trejo, F., Centeno, G., Ancheyta, J. *Fuel*, **2004**, 83, 2169-2175
12. Barré, L. Simon, S. Palermo, T. *Langmuir*, **2008**, 3709-3717.
13. a) Strausz, O. P., *Can. Inst. Min. Metall.* **1977**, 171-176. b) Ancheyta, J., Betancourt, G., Centeno, G., Marroquín, G., Alonso, F., Garciafigueroa, E. *Energy Fuels*, **2002**, 1438-1443 c) Ancheyta, J., Betancourt, G., Centeno, G., Marroquín, G., Castañeda, L. C., Alonso, F., Muñoz, J. A., Gómez, Ma. T., Rayo, P. *Appl. Catal. A.* **2002**, 159-170
14. Mullins, O.C., Sheu, E.Y., Hammami, A., Marshall, A.G. *Asphaltenes, Heavy Oils, and Petroleomics*; Springer-Verlag: New York, **2007**.
15. Groenzin, H., Mullins, O. C. *Energy Fuels*, **2000**, 14, 677-684
16. Strausz, O. P., Safarik, I., Lown, E. M., Morales-Izquierdo, A. *Energy Fuels*, **2008**, 1156-1166.

17. Murgich, J., Abanero, J. A., Strausz, O. P. *Energy Fuels*, **1994**, 8, 536-544
18. Murgich, J. *Mol. Simul.*, **2003**, 29, 451-461
19. Schulze, M.; Tykwinski, R. R., manuscript in preparation.
20. a) Aske, N.; Kallevik, H.; Johnsen, E. E.; Sjöblom, J. *Energy Fuels*, **2002**, 1287-1295. b) Morgan, T. J.; Alvarez-Rodriguez, P.; George, A.; Herod, A. A.; Kandioyti, R. *Energy Fuels*, **2010**, 3977-3989.
21. Gray, M. R. *Upgrading of Oilsands Bitumen and Heavy Oil*. University of Alberta Press; Edmonton. Publication forthcoming.
22. Sheu, E. Y. *Energy Fuels* **2002**, 74-82.
23. Gray, M. R.; Tykwinski, R. R.; Stryker, J. M.; Tan, X. *Energy Fuels*, **2011**, 3125-3134.
24. a) Førdedal, H., Schildberg, Y., Sjöblom, J., Volle, J. *Colloids. Surf. A.: Phys. Chem. Eng. Aspects*, **1996**, 33-47. b) McLean, J. D., Kilpatrick, P. K. *J. Colloids. Interface Sci.*, **1997**, 242-250.
25. a) Yan, Z.; Elliot, J. A. W.; Masliyah, J. H. *J. Colloids. Interface Sci.*, **1999**, 329-337. b) Zhang, L. Y.; Breen, P.; Xu, Z.; Masliyah J. H. *Energy Fuels*, **2007**, 274-285.
26. a) Murgich, J. Merino-Garcia, D., Andersen, S. I., Manuel del Rio, J., Galeana, C. L. *Langmuir*, **2002**, 9080-9086. b) Khvostichenko, D. S., Andersen, S. I. *Energy Fuels*, **2008**, 3096-2103.
27. Tan, X.; Fenniri, H.; Gray, M. R. *Energy Fuels*, **2008**, 715-720.
28. Sabbah, H.; Morrow, A. L.; Pomerantz, A. E.; Mullins, O. C.; Tan, X.; Gray, M. R.; Azyat, K.; Tykwinski, R. R.; Zare, R. N. *Energy Fuels*, **2010**, 3589-3594.
29. Cardozo, S. D.; Schulze, M.; Tykwinski, R. R.; Gray, M. R. *Energy Fuels*, **2015**, 1494-1502.
30. Cavaleiro, J.A.S.; Smith, K. M. *Rev. Port. Quim.*, **1989**, 29-41
31. Heidt, T. *Synthesis of Archipelago Model Asphaltenes with a Benzo[b]anthraquinoline Core*. M.Sc. Thesis, University of Alberta, Edmonton, Canada.
32. Scherer, A.; Hampel, F.; Gray, M. R.; Stryker, J. M.; Tykwinski, R. R. *J. Phys. Org. Chem.* **2012**, 597-606.
33. Tomlin, K. R. *Manuscript in preparation*. M.Sc. Thesis, University of Alberta, Edmonton, Canada.
34. Scott, D.; Stryker, J. M. Unpublished results

35. Alajarin, R.; Burgos, C.; Six-Membered Heterocycles: Quinoline and Isoquinoline. In *Modern Heterocyclic Chemistry*; Alvarez-Bullia, J., Vaquero, J. J., Barluenga, 36. Runge, F. F. *Ann. Physik.*, **1834**, 65-78
37. Dewar, J. *Chem. News.* **1871**, 23, 38
38. Koenigs, W. *Ber. Dtsch. Chem. Ges.* **1879**, 453-454
39. Baeyer, A. *Ber. Dtsch. Chem. Ges.* **1879**, 1320-1323
40. Meyers, R. A. ed.; *Encyclopedia of Physical Science and Technology, Third Edition – Organic Chemistry*. University of Michigan Academic Press: Michigan, **2002**. 477 – 493
41. Joule, J.A.; Mills, K.; *Heterocyclic Chemistry, 4<sup>th</sup> Ed.*, Blackwell Science Ltd.: Oxford, 2011
42. Qi, C.; Zheng, Q.; Hua, R. *Tetrahedron* **2009**, 1316–1320.
43. Bernhard, A. M.; Peitz, D.; Elsener, M.; Wokaun, A.; Krocher, O. *Appl. Cat. B. Enviro.* **2012**, 129-137.
44. Koebel, M.; Strutz, E. O. *Ind. Eng. Chem Res.* **2003**, 2093-2100
45. Wang, S.; Morrow, G. W.; Swenton, J. S. *J. Am. Chem. Soc.* **1989**, 5364-5371
46. Fisher, O.; Rudolph, C.; *Ber. Dtsch. Chem. Ges.* **1882**, 1500-1505
47. Friedländer, P. *Ber. Dtsch. Chem. Ges.*, **1882**, 2572-2575
48. a) Streckowski, L.; Czarny, A.; Lee, H. *J. Fluorine Chem.* **2000**, 104, 281-284. b) Desbois, N.; Chezal, J.-M.; Fauvelle, F.; Debouzy, J.-C.; Lartigue, C.; Gueiffier, A.; Blache, Y.; Moreau, E.; Madelmont, J.-C.; Chavignon, O.; Teulade, J.-C. *Heterocycles.* **2005**, 1121-1137. c) Chackal, S.; Houssin, R.; Henichart, J.-P. *J. Org. Chem.* **2002**, 3502-3505. d) Tamura, Y.; Tsugoshi, T.; Mohri, S.-i.; Kita, Y. *J. Org. Chem.* **1985**, 1542-1545. e) Perzyna, A.; Klupsch, F.; Houssin, R.; Pommery, N.; Lemoine, A.; Henichart, J.-P. *Bioorg. Med. Chem. Lett.* **2004**, 2363-2365.
49. a) Dormer, P. G.; Eng, K. K.; Farr, R. N.; Humphrey, G. R. McWilliams, J. C.; Reider, P. J.; Sager, J. W.; Volante, R. P. *J. Org. Chem.* **2003**, 467-468. b) Yasuda, N.; Hsiao, Y.; Jensen, M. S.; Rivera, N. R.; Yang, C.; Wells, K. M.; Yau, J.; Palucki, M.; Tan, L.; Dormer, P. G.; Volante, R. P.; Hughes, D. L.; Reider, P. J. *J. Org. Chem.* **2004**, 1959-1966. c) Tamura, Y.; Tsugoshi, T.; Mohri, S.-i.; Kita, Y. *J. Org. Chem.* **1985**, 50, 1542. d) Ma, H.; Jen, A. K.-Y.; Wu, J.; Wu, X.; Liu, S.; Shu, C.-F.; Dalton, L. R.; Marder, S. R.; Thayumanavan, S. *Chem. Mater.* **1999**, 2218-2225. e) Yu, J.; DePue, J.; Kronenthal, D. *Tetrahedron Lett.* **2004**,

7247-7250.

50. a) Lindstrom, S. *Acta Chem. Scand.* **1995**, 361-363. b) Chelucci, G.; Orru, G. *Tetrahedron Lett.* **2005**, 3493-3496. c) Walz, A. J.; Sundberg, R. J. *Synlett* **2001**, 75-76. d) Gelin, F.; Thummel, R. P. *J. Org. Chem.* **1992**, 3780-3783.
51. Wu, L-Q; Wang, X.; Ma, W-W.; Yan, F-L. *J. Chin. Chem. Soc.*, **2010**, 616-621
52. Tidwell, J. H.; Buchwald, S. L.; *J. Am. Chem. Soc.* **1994**, 11797-11810
53. Armarego, W.L.F.; Chai, C.L.L. *The Purification of Laboratory Chemicals, 5<sup>th</sup> ed.* Elsevier Science: Cornwall. 2003.
54. Marco-Contelles, J.; Pérez-Mayoral, E.; Samadi, A.; Carreiras, M. do C.; Soriano, E. *Chem. Rev.* **2009**, 2652-2671
55. a) Everson, D.A.; Buonomo, J.A.; Weix, D.J. *Synlett.*, **2014**, 233-238. b) Sherry, B.D.; Fürstner, A. *Acc. Chem. Res.*, **2008**, 1500-1511.
56. Cataldo, F. *Eur. Polym. J.* **1996**, 1297-1302
57. a) Hallett, J. P.; Welton, T. *Chem. Rev.* **2011**, 3508. b) Martins, M. A. P.; Frizzo, C. P.; Moreira, D. N.; Zanatta, N.; Bonacorso, H. G. *Chem. Rev.*, **2008**, 2015-2050.
58. Palimkar, S. S.; Siddiqui, S. A.; Daniel, T.; Lahoti, R. J.; Srinivasan, K. V. *J. Org. Chem.*, **2003**, 9371-9378.
59. a) Miyaura, N.; Suzuki, A. *Chem. Rev.* **1995**, 2457–2483 b) Lyons, T.W.; Sanford, M.S. *Chem. Rev.* **2010**, 1147–1169 c) Tietze, L.F.; Ila, H.; Bell, H.P. *Chem. Rev.* **2004**, 3453–3516
60. a) Rosen, B.M.; Quasdorf, K.W.; Wilson, D.A.; Zhang, N.; Resmerita, A-M. Garg, N.K.; Percec, V. *Chem. Rev.* **2011**, 1346–1416. b) Lyons, T.W.; Sanford, M.S. *Chem. Rev.*, **2010**, 1147-1169. c) Liebscher, L.; Liebscher, J. *Chem. Rev.*, **2007**, 133-173.
61. a) Bauer, I; Knölker, H-J. *Chem. Rev.* **2015**, 3170-3387. b) Gopalaiah, K. *Chem. Rev.* **2013**, 3248-3296. c) Sun, C-L; Li, B-J; Shi, Z-J. *Chem. Rev.* **2011**, 1293-1314.
62. a) Cahiez, G.; Moyeux, A. *Chem. Rev.*, **2010**, 1435–1462. b) Pellissier, H.; Clavier, H. *Chem. Rev.*, **2014**, 2775–2823.
63. a) Knappe, C.E.I; Grupe, S.; Gärtner, D.; Corpet, M.; Gosmini, C.; von Wangelin, A.J. *Chem. Eur. J.*, **2014**, 6828-6842. b) Molander, G.A; Traister, K.M.; O'Neill, B.T. *J. Org. Chem.*, **2014**, 5771-5780. c) Cherney, A.H.; Reisman, S.E. *J. Am. Chem. Soc.*, **2014**, 14365-14368.

64. Amatore, M.; Gosmini, C. *Angew. Chem. Int. Ed.*, **2008**, 2089-2092.
65. Amatore, M.; Gosmini, C. *Chem. Eur. J.*, **2010**, 5848-5852.
66. Kim, S.-H. *The Preparation of highly active manganese and its applications in organic synthesis*. Ph. D. thesis, University of Nebraska, Lincoln, United States of America<sup>3</sup>.
67. Diner, C. E. *Manuscript in preparation*. Ph. D Thesis, University of Alberta, Edmonton, Canada.
68. Takehiko, F.; Suzuki, H.; Kinya, O. **2001**. *Preparation of alpha-bromo,omega-chloroalkanes*. EP 0 824 094 B1
69. Everson, D. A.; Shrestha, R.; Weix, D. J. *J. Am. Chem. Soc.* **2010**, 920-921.
70. Everson, D.A.; Jones, B. A.; Weix, D.J. *J. Am. Chem. Soc.*, **2012**, 6146-6159.
71. a) Biswas, S.; Weix, D.J. *J. Am. Chem. Soc.*, **2013**, 16192-16197. b) Everson, D.A.; Weix, D.J. *J. Org. Chem.*, **2014**, 4793-4798. c) Weix, D.J. *Acc. Chem. Res.*, **2015**, 1767-1775.
72. Berthelot, M. C. R. *Hebd. Séances Acad. Sci.* **1891**, 1343-1349.
73. Mond, L.; Quinke, F. *J. Chem. Soc.* **1891**, 604-607.
74. a) Collman, J. P. *Acc. Chem. Res.*, 1975, **8**, 342-347 b) Collman, J. P.; Finke, R. G.; Cawse, J. N.; Brauman, J. I. *J. Am. Chem. Soc.*, **1977**, 99, 2515-2526.
75. Finke, R. G.; Sorrell, T. N. *Org. Syn.* **1979**, 102
76. Senechal-David, K.; Hemeryck, A.; Tancrez, N.; Toupet, N.; Williams, A. G.; | Ledoux, I.; Zyss, J.; Boucekkine, A.; Guegan, J. P.; le Bozec, H. Maury, O. *J. Am. Chem. Soc.*, **2006**, 12243-12255.
77. Cooke, M. P. *J. Am. Chem. Soc.*, **1970**, 6080-6082
78. Wang, S.; Morrow, G. W.; Swenton, J. S. *J. Org. Chem.* **1989**, 5364-5371